Discovery of bacteria producing a novel cycloisomaltotetraose and identification of novel enzymes involved in cycloisomaltotetraose production and metabolism pathway

（新規シクロイソマルトテトラオースを生産する微生物の発見と
シクロイソマルトテトラオース生成・代謝経路に関与する新規酵素の同定）

北海道大学　大学院農学院

藤田章弘

Contents

Abbreviations

Chapter 1 **1**
General introduction

Chapter 2 **10**
Enzymatic synthesis of a cyclic tetrasaccharide, cycloisomaltotetraose, and its crystal structure

Introduction **10**

Materials and Methods **10**
Saccharides 10
Preparation of a marker for isomaltooligosaccharides 10
Enzymes 11
Screening of enzymes derived from bacteria isolated from the soil 11
TLC analysis 12
Identification of bacterial genera using 16S rDNA analysis 13
Preparation of CI4 using a culture supernatant of *Agreia* sp. D1110 13
HPLC and LC-MS analysis 15
NMR measurements 16
Comparison of the culture supernatant from two strains in the CI4 producing reaction 16
Preparation of crystalline powder of CI4 using culture supernatant of *M. trichothecenolyticum* D2006 16
X-ray crystallographic analysis 18
Digestibility test 18

Results **19**
Screening of bacterial strains producing an unknown oligosaccharide 19
Identification of genera of D1110 and D2006 strains 21
Structural analysis of the oligosaccharide 23
(a) Preparation of the oligosaccharide produced using the salt precipitation fraction of the culture supernatant of *Agreia* sp. D1110 and its purification 23
(b) LC-MS analysis 23
(c) NMR analyses 24

Comparison of sugar composition in CI4-producing reactions using the culture supernatants from two strains 35
X-ray diffraction experiment of the single CI4 crystal 37
(a) Preparation of CI4 crystals 37
(b) Crystal structure analysis of CI4 41
Digestibility test 46

Discussion **47**

Chapter 3 **49**
Purification and characterization of cycloisomaltotetraose-forming enzymes from *Agreia* sp. D1110 and *Microbacterium trichothecenolyticum* D2006

Introduction **49**

Materials and Methods **49**
Saccharides 49
Enzymes 50
TLC analysis 50
Culture of *Agreia* sp. D1110 and enzyme purification 50
Culture of *M. trichothecenolyticum* D2006 and enzyme purification 51
CI4-forming activity 52
Dependency of CI4 production on protein concentration and reaction time 53
Effects of pH on the activity of the CI4-forming enzymes 53
Effects of temperature on the activity of the CI4-forming enzymes 53
Effects of pH on the stability of the CI4-forming enzymes 54
Effects of temperature on the stability of the CI4-forming enzymes 54
Effects of metal ions on the activity of the CI4-forming enzymes 55
Determination of protein concentration 55
SDS-PAGE analysis 55
N-terminal amino acid sequence analysis 55
Analysis of products in the reaction using the CI4-forming enzymes and various substrates 56
Coupling reaction between CI4 and acceptor molecules 56
Reaction time dependency of the amount of CI4 in 8, 24, 48 or 72 h-reactions 57
Preparation of starch-derived substrates 57
Production of CI4 from starch-derived substrates 57
Methylation analysis 58

Results **59**
Purification of the CI4-forming enzymes from *Agreia* sp. D1110 and *M. trichothecenolyticum* D2006 59
Dependency of CI4 production on protein concentration and reaction time 62
Enzymatic properties of the CI4Tases from two strains 64
Analysis of products in the reaction using the CI4Tases and various substrates 68
Coupling reaction catalyzed by AgCI4Tase and MtCI4Tase 73
Reaction time dependency of the amount of CI4 in 8, 24, 48 or 72 h-reactions 75
Production of CI4 from starch-derived substrates 78

Discussion **81**

Chapter 4 **85**
Sequence analysis of the CI4Tases using draft genome sequence analyses and model for CI4-production and metabolism

Introduction **85**

Materials and Methods **85**
Saccharides 85
Draft genome sequence analysis, assembly and prediction 85
Cloning of ORF9038 and ORF5328 86
Expression of ORF9038(-pep) and ORF5328(-pep) 88
Enzyme reaction to analyze the abilities of the recombinant enzymes to produce CI4 88
Preparation of the CI4Tase mutants 89
Constructing expression vectors for ORF9042-derived protein and ORF9041-derived protein 90
Expression of recombinant ORF9042-derived protein and ORF9041-derived protein 90
Purification of ORF9042-derived protein and ORF9041-derived protein 91
Enzyme reaction to analyze the activities of ORF9042-derived protein 91
Enzyme reaction to analyze the activities of ORF9041-derived protein 91
The reaction using purified ORF9042-derived protein and each substrate 92
Determination of protein concentration 92
SDS-PAGE 92

Multiple alignments 93
Analyses of identity of amino acid residues 93
BLASTP search 93

Results **95**
Sequence analysis of the gene encoding the CI4Tases 95
Recombinant expression of ORF9038 and ORF5328 in *E. coli* 97
Domain architecture of the CI4Tases 99
Comparison of amino acid sequences between the CI4Tases and the CITases 101
Analysis of the ability of mutant enzymes to produce CI4 106
A gene cluster including the CI4Tase genes 109
Sequence characteristics of proteins encoded in the gene clusters 113
Recombinant expression of ORF9041 and ORF9042 and their purification 120
Analysis of enzymatic activity of ORF9042-derived protein and ORF9041-derived protein 123
The reaction using purified ORF9042-derived protein and each substrate 125
BLASTP search 127

Discussion **132**

Chapter 5 **137**
General conclusions

References **142**

Acknowledgements **151**

Abbreviations

Oligosaccharides

CDs	cyclodextrins
CI4	cycloisomaltotetraose
CIs	cycloisomaltooligosaccharides
CMM	cyclobis-(1→6)-maltosyl
CNN	cyclobis-(1→6)-nigerosyl

Enzymes

CGTase	cyclomaltodextrin glucanotransferase
CI4Hase	cycloisomaltotetraose hydrolase
CI4Tase	cycloisomaltotetraose glucanotransferase
CITase	cycloisomaltooligosaccharide glucanotransferase

Others

ABC	ATP-binding cassette
DEPT	distortionless enhancement by polarization transfer
DNA	deoxyribonucleic acid
DP	degree of polymerization
EDTA	ethylenediaminetetraacetic acid
HPLC	high performance liquid chromatography
LC-MS	liquid chromatography-mass spectrometry
NMR	nuclear magnetic resonance
PCR	polymerase chain reaction
SDS-PAGE	sodium dodecyl sulfate-polyacrylamide gel electrophoresis
TLC	thin-layer chromatography

Chapter 1 General introduction

Starch is a mixture of two kinds of polysaccharides, amylose and amylopectin (Robyt, 2008). Amylose is composed of (1→4)-linked α-D-glucosyl residues. Amylopectin is a polysaccharide composed of main chains of amylose and branches of an α-(1→6)-glucosidic linkage. So far, numerous studies on enzymes acting on starch have been performed, and these enzymes are systematically categorized into families based on the amino acid sequences in a database carbohydrate active enzymes (CAZy, http://www.cazy.org/) (Drula *et al*., 2022). In CAZy, the enzymes are categorized into 5 classes, glycoside hydrolases, glycosyltransferases, polysaccharide lyases, carbohydrate esterases and auxiliary activities. Non-catalytic modular structures, which bind to carbohydrates, are categorized in carbohydrate-binding modules (CBMs). The glycoside hydrolases, catalyzing hydrolysis and/or rearrangement of glycosidic bonds, are categorized into 173 families, so-called "glycoside hydrolase family (GH)" (Accessed June 25th, 2022).

Several GHs enzymes are industrially used to produce oligosaccharides from starch. α-Amylase (EC 3.2.1.1) is an enzyme to hydrolyze α-(1→4)-glucosidic linkages in starch in *endo*-manner and is used to produce liquefied starch and maltooligosaccharides in industry (Manners, 1963). β-Amylase (EC 3.2.1.2) hydrolyzes starch in *exo*-manner to produce maltose (Glc(α1-4)Glc) (Adachi *et al*., 1998). Glucoamylase (EC 3.2.1.3) acts on starch in *exo*-manner and produces β-D-glucose (Weill *et al*., 1954). α-Glucosidase (EC 3.2.1.20) mainly acts on oligosaccharides in *exo*-manner, cleaves an α-(1→4)-glucosidic linkage on the non-reducing ends of the substrates and catalyzes two types of reactions, hydrolysis and intermolecular transglycosylation (Chiba *et al*., 1983; Kita *et al*., 1991). In the hydrolysis reaction, α-D-glucose is produced (Chiba *et al*., 1983; Kita *et al*., 1991). In the intermolecular transglycosylation reaction, a covalent linkage between α-D-glucosyl residues on the non-reducing ends is cleaved and a new one between the glucosyl residue and a hydroxy group in other molecules can be

created. The intermolecular transglycosylation of α-glucosidase is industrially used to prepare isomaltooligosaccharides containing isomaltose (Glc(α1-6)Glc, IG2) from maltooligosaccharides (Duan *et al*., 1995; McCleary *et al*., 1989). Several enzymes produce carbohydrates with high degree of polymerization (DP) in intermolecular transglycosylation reaction. Dextran dextrinase (EC 2.4.1.2, DDase) from *Gluconobacter oxydans* (former name; *Acetobacter capsulatus*) ATCC11894 and *G. oxydans* (former name; *A. viscosus*) ATCC 11895 cleaves the non-reducing terminal α-(1→4)-glucosidic linkages in dextrin and form α-(1→6)-glucosidic linkages to the non-reducing ends of another dextrin molecule (Shimwell, 1947). The reaction occurs continuously, enabling the synthesis of dextran, α-(1→6)-glucan, from dextrin (Yamamoto *et al*., 1992; Yamamoto *et al*., 1993a, 1993b). From liquefied starch, two enzymes from *Paenibacillus alginolyticus,* 6-α-glucosyltransferase (EC 2.4.1.24, 6GT) and α-amylase, produce isomaltodextrin containing α-(1→3)-, α-(1→4)- and α-(1→6)-glucosidic linkages and branch structures (Tsusaki *et al*., 2009, 2012).

Several enzymes produce cyclic oligosaccharides by catalyzing intramolecular transglycosylation (cyclization) reactions. Cyclomaltodextrin glucanotransferase (EC 2.4.1.19, CGTase) produces cyclodextrins (CDs, DP is 6, 7 or 8) from starch (Kato & Horikoshi, 1986; Kitahata *et al*., 1974; S. Kobayashi *et al*., 1978). CDs are capable of forming inclusion complexes with small hydrophobic compounds and have been used for solubilization of water insoluble compounds and for volatilization control of volatile compounds (Rawat & Jain, 2004). cyclo-[-6Glcα1-3Glcα1-]$_2$ (CNN, Figure 1-1(a)) (Aga, Higashiyama, *et al*., 2002; Aga, Maruta, *et al*., 2002; Nishimoto *et al*., 2002, 2004) and cyclo-[-6Glcα1-4Glcα1-]$_2$ (CMM, Figure 1-1(b)) (Kohno *et al*., 2018; Mori *et al*., 2008, 2011; Mukai *et al*., 2005, 2006) are also known as cyclic oligosaccharides which are enzymatically prepared using starch as starting material. 6GT acts on partially hydrolyzed starch and catalyzes the intermolecular α-(1→6)-transglucosylation. 3-α-Isomaltosyltransferase (EC 2.4.1.387, IMT) acts on the substrates prepared by 6GT and

catalyzes the intermolecular α-(1→3)-transglycosylation of IG2 units to α-(1→6)-glucosyl residue at the non-reducing ends of the α-glucan. IMT further catalyzes the intramolecular α-(1→3)-transglycosylation to produce CNN from the α-glucan having 3-*O*-α-isomaltosyl-6-α-D-glucosyl residue at the non-reducing ends (Aga, Higashiyama, *et al*., 2002; Aga, Maruta, *et al*., 2002; Kim *et al*., 2004; Tagami *et al*., 2016). CMM is synthesized by 6-α-maltosyltransferase (EC 3.2.1.-, 6MT) derived from *Arthrobacter globiformis* M6 acting on maltooligosaccharides. In this reaction, 6MT catalyzes the intermolecular α-(1→6)-transglycosylation of maltose units, and intramolecular α-(1→6)-transglycosylation to form CMM from the α-glucan harboring an α-(1→6)-maltosyl residue at the non-reducing ends (Kohno *et al*., 2018; Mori *et al*., 2008, 2011; Mukai *et al*., 2006).

It has been reported that the organisms producing the cyclic oligosaccharides also possess enzymes that degrade them. *Kribbella flavida* NBRC 14399 possess 1,3-α-isomaltosidase (EC 3.2.1.204) which hydrolyzes an α-(1→3)-glucosidic linkage in CNN to produce 3-*O*-α-isomaltosyl-isomaltose (Tagami *et al*., 2016), subsequently hydrolyzes an α-(1→3)-glucosidic linkage in the tetrasaccharide to produce IG2. *A. globiformis* M6 possesses CMM hydrolase (EC 3.2.1.-, CMMase) hydrolyzing CMM to produce 6-*O*-α-maltosyl-maltose (Kohno *et al*., 2018). These enzymes are involved in metabolic pathways of these cyclic oligosaccharides in their producing bacteria. *K. flavida* NBRC14399 has two gene clusters involved in CNN production and metabolism (Tagami *et al*., 2016). The bacteria extracellularly produce CNN from starch using IMT encoded by *Kfla_4052* and 6GT encoded by *Kfla_4051*. The produced CNN is imported into the cells via ABC transporter encoded by *Kfla_1894-1899*. The imported CNN is degraded by 1,3-α-isomaltosidase encoded by *Kfla_1895* and GH15-like protein encoded by *Kfla_1896*. Gene clusters involved in CNN production and metabolism are also reported in *Listeria monocytogenes* (Light *et al*., 2016). Notably, starch is a carbon source that can be readily assimilated by other bacteria. The biological significance of this pathway is to

produce carbon sources, CNN in this case, that cannot be assimilated by other bacteria. A similar pathway has been reported for CMM (Kohno *et al*., 2018), suggesting that various bacteria have similar cyclic oligosaccharide production and metabolism system. As described above, much research has been performed on starch-related enzymes, and a great deal of knowledge has been accumulated in both academic and industrial fields. Using the knowledge, various kinds of oligosaccharides are industrially produced from starch.

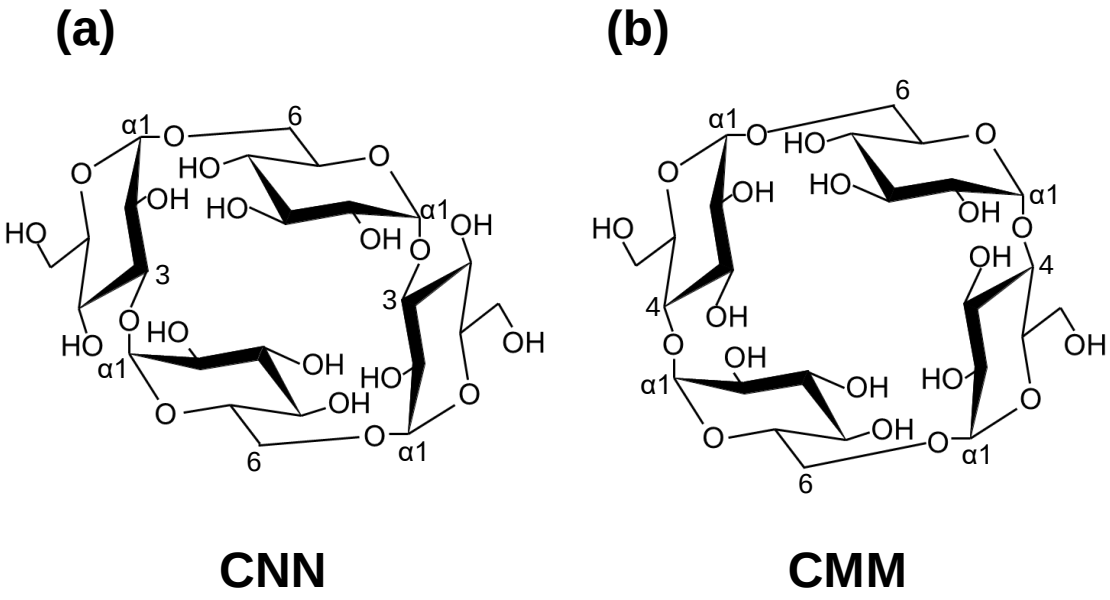

Figure 1-1 Structural formulas of cyclic tetrasaccharides.

(a) CNN, (b) CMM.

Besides starch-related enzymes, dextran-related enzymes have been researched. Dextranase (EC 3.2.1.11) (Elvira *et al*., 2005) acts on dextran in an *endo*-type manner and produce isomaltooligosaccharides. Glucodextranase (EC 3.2.1.70) (Sawai *et al*., 1976), isomalto-dextranase (EC 3.2.1.94) (Sawai *et al*., 1974) and dextran 1,6-α-isomaltotriosidase (EC 3.2.1.95) (Mizuno *et al*., 1996) act on the non-reducing ends of dextran to produce glucose (Glc), IG2 and isomaltotriose (IG3), respectively. Furthermore, cycloisomaltooligosaccharide glucanotransferase (EC 2.4.1.248, CITase) is also known to produce cycloisomaltooligosaccharides (CIs) from dextran. CITases from *Bacillus circulans* T-3040 (CITase-T-3040), *B. circulans* U-155 (CITase-U-155) and *Paenibacillus* sp. 598K (CITase-598K) have been obtained so far (Funane *et al*., 2007; M. Kobayashi *et al*., 1995; Oguma *et al*., 1994, 2014; R. Suzuki *et al*., 2012). These enzymes synthesize CIs of wide range of DP from 7 to 17 (Funane *et al*., 2008; R. Suzuki *et al*., 2012) with cycloisomaltooctaose (CI8), CI8 and CI7 as the main product of CITase-T-3040, CITase-U-155 and CITase-598K, respectively (Oguma *et al*., 1994, 2014; R. Suzuki *et al*., 2012). CIs have been reported to possess valuable properties. CIs, with its high-water solubility and inclusion ability, can be used to stabilize dyes such as Victoria Blue (Funane *et al*., 2007; Oguma, 1997). The CIs' potential to inhibit the formation of biofilm of *Streptococcus mutans* can be exploited for an anti-caries effect (M. Kobayashi *et al*., 1995). It is stated that these properties depend on the DP of the CIs, and it will be industrially relevant to be able to control the DP of the CI produced. The mechanisms determining the DP of the products have been studied to address this issue. Three-dimensional structural analysis revealed that CITase-T-3040, CITase-598K and CITase-U-155 are composed of a Glyco_hydro_66 domain which shows $(\beta/\alpha)_8$-barrel structure and contains an active center, and two Carbohydrate Binding Module family 35 domains (CBM35-1 domain and CBM35-2 domain) (Table 1-1) (N. Suzuki *et al*., 2014). The CBM35-1 domain in CITase-T-3040 is inserted between the 7th β-strand and the 7th α-helix of the Glyco_hydro_66 domain.

The CBM35-2 domain is in C-terminal region. Dextranases in GH66 have no CBM35-1 domain inserted in Glyco_hydro_66 domain (Table 1-1). The inserted CBM35-1 domain is reported to be necessary for predominant production of CI8 in CITase-T-3040 (N. Suzuki *et al*., 2014). On CITase-T-3040, ligand-binding structure with isomaltooctaose (IG8) have been reported and amino acid residues involved in the formation of the subsite from −1 to −8 are known (N. Suzuki *et al*., 2014).

Table 1-1 Domain architecture of the CITases and the Dextranases in GH66.

Organism	EC number	Domain(s)	Genbank accession number
Bacillus circulans T-3040	2.4.1.248	Glyco_hydro_66 CBM35-1[1] CBM35-2[2]	BAA09604.1
Bacillus circulans U-155	2.4.1.248	Glyco_hydro_66 CBM35-1 CBM35-2	BAA13595.1
Paenibacillus sp. 598K	2.4.1.248	Glyco_hydro_66 CBM35-1 CBM35-2	BAL21555.1
Paenibacillus sp. Dex2000	2.4.1.248 3.2.1.11	Glyco_hydro_66 SLH[3] SLH SLH CBM35-1 CBM35-1	AEX15594.1
Paenibacillus sp. 598K	3.2.1.11	Glyco_hydro_66	BBB44432.1
Paenibacillus sp. Dex40-8	3.2.1.11	Glyco_hydro_66 CBM_4_9	AAQ91294.1
Paenibacillus sp. Dex50-2	3.2.1.11	Glyco_hydro_66	AAQ91296.1
Paenibacillus sp. Dex50-2	3.2.1.11	Glyco_hydro_66	AAQ91298.1
Paenibacillus sp. Dex70-1B	3.2.1.11	Glyco_hydro_66	AAQ91301.1
Paenibacillus sp. Dex70-34	3.2.1.11	Glyco_hydro_66	AAQ91303.1
Pseudothermotoga lettingae TMO	3.2.1.11	Glyco_hydro_66	ABV33789.1
Streptococcus criceti ATCC19642	3.2.1.11	Glyco_hydro_66	BAG16274.1
Streptococcus criceti E49	3.2.1.11	Glyco_hydro_66	BAE93687.1
Streptococcus downei NCTC11391	3.2.1.11	Glyco_hydro_66	BAB78732.1
Streptococcus mutans ATCC25175	3.2.1.11	Glyco_hydro_66	AEB70967.1
Streptococcus ratti ATCC19645	3.2.1.11	Glyco_hydro_66	BAD12421.1
Streptococcus salivarius M-33	3.2.1.11	Glyco_hydro_66	BAA06127.1
Streptococcus sobrinus	3.2.1.11	Glyco_hydro_66	AAA21772.1
Thermoanaerobacter pseudethanolicus ATCC33223	3.2.1.11	Glyco_hydro_66	ABY93933.1
Bacteroides thetaiomicron VPI-5482	3.2.1.11	Glyco_hydro_66	AAO78193.1

The dextranases and CITases categorized as characterized enzymes were extracted from GH66 in CAZy. Domain architectures of dextranases and AEX15594.1 were annotated using Pfam (Mistry *et al*., 2021). Domain architectures of CITases are shown on the basis of the previous report (N. Suzuki *et al*., 2014). CBM35-1[1], Carbohydrate Binding Module family 35 domain inserted in Glyco_hydro_66 domain; CBM35-2[2], Carbohydrate Binding Module family 35 domain in the C-terminal region; SLH[3], S-Layer Homology domain.

Enzymes that act on dextran to produce oligosaccharides have been reported less frequently than those that act on starch, resulting in few variations of oligosaccharides linked by α-(1→6)-linkages. Acquisition of new dextran-related enzymes expands technology of oligosaccharide production. Therefore, in this study, novel enzymes to produce novel oligosaccharides from dextran were searched. This dissertation describes the discovery and structural determination of a new CI, cycloisomaltotetraose (CI4, cyclo-[-6Glcα1-]$_4$) produced by bacteria isolated from soil, discovery of CI4-forming enzymes, function of the enzymes and a pathway for CI4 production and metabolism in CI4-producing bacteria.

Chapter 2

Enzymatic synthesis of a cyclic tetrasaccharide, cycloisomaltotetraose, and its crystal structure

Introduction

This chapter describes isolation of bacterial strains from soil, screening experiments to discover CI4, structural determination of CI4 using liquid chromatography-mass spectrometry (LC-MS) and nuclear magnetic resonance (NMR), crystallization of CI4 and its X-ray diffraction experiment.

Materials and Methods

Saccharides

D-Glucose and gellan gum were purchased from Fujifilm Wako Pure Chemical (Tokyo, Japan). Dextran T10 (average molecular weight: 10,000) was purchased from Seikagaku (Tokyo, Japan). Dextran T40 (average molecular weight: 40,000) and dextran T70 (average molecular weight: 70,000) were purchased from Tokyo Chemical Industry (Tokyo, Japan)..

Preparation of a marker for isomaltooligosaccharides

Reaction mixture (300 mL) containing 10% (w/v) dextran T40, 1.0 M H_2SO_4 (Fujifilm Wako Pure Chemical) was heated at 100°C for 60 min. By adding saturated solution of $Ba(OH)_2$, reaction mixture was adjusted to pH 7.0. The mixture was centrifuged at 23,800 ×*g* for 10 min to remove precipitated $BaSO_4$. Three times the volume of absolute ethanol was added, and the mixture was centrifuged at 23,800 ×*g* for 10 min. The supernatant was used as the marker for isomaltooligosaccharides.

Enzymes

α-Glucosidase from *Aspergillus niger* and dextranase from *Chaetomium erraticum* were purchased from Amano Enzyme (Nagoya, Japan). Glucoamylase from *A. niger* was obtained from Nagase Chemtex (Kyoto, Japan). Lysozyme was purchased from Fujifilm Wako Pure Chemical. The activity of α-glucosidase was measured as follows: Reaction mixture (1.0 mL) containing 41 mM methyl α-D-glucoside (Fujifilm Wako Pure Chemical), 16 mM sodium acetate buffer (pH 5.0) and 20% (v/v) enzyme solution was incubated at 40℃ for 60 min. After boiling the mixture for 5 min, the solution was cooled in cold water. Using Glucose CII Test Wako kit (Fujifilm Wako Pure Chemical), the amount of Glc was measured. One U of the activity was defined as the amount of enzyme producing 1.0 μg Glc for 60 min. The activity of glucoamylase was assayed as follows: Reaction mixture (1.0 mL) containing 15 mg/mL soluble starch (Fujifilm Wako Pure Chemical), 15 mM sodium acetate buffer (pH 4.5) and 7.7% (v/v) enzyme solution was incubated at 40℃ for 20 min. NaOH solution (1.0 M, 0.10 mL) was added to the solution to stop the reaction. After incubating the solution at room temperature, 0.10 mL of 1.0 M HCl solution was added to the solution for neutralization. The amount of Glc was measured as described above. One U of the activity was defined as the amount of enzyme producing 1.0 mg Glc for 60 min. The enzymes used in a digestibility test are as follows: α-Amylase derived from *Bacillus licheniformis* was purchased from Novozymes (Bagsværd, Denmark). Protease derived from *B. licheniformis* and amyloglucosidase (glucoamylase) from *A. niger* were purchased from Sigma-Aldrich (St. Louis, MO, United States).

Screening of enzymes derived from bacteria isolated from the soil

One small spoonful of the soil was suspended in 10 mL of saline, and 100 μL of the suspended saline was then added to 10 mL of new saline. The suspension (100 μL) was seeded onto solid medium containing 0.15% (w/v) dextran T70, 0.10% (w/v) K_2HPO_4, 0.10% (w/v)

$MgSO_4 \cdot 7H_2O$, 0.10% (w/v) NaCl, 0.20% (w/v) $(NH_4)_2SO_4$, 0.0010% (w/v) $FeSO_4 \cdot 7H_2O$, 0.0010% (w/v) $MnSO_4 \cdot 7H_2O$, 0.00010% (w/v) $ZnSO4 \cdot 7H_2O$ and 2.0% (w/v) gellan gum (pH 6.8). After culturing at 27°C for 3 d, the colonies grew on the plates were inoculated on new solid medium of the same composition. The isolated bacteria were inoculated in 3.0 mL of liquid medium containing 1.5% (w/v) dextran T70, 0.50% (w/v) hipolypepton (Fujifilm Wako Pure Chemical), 0.10% (w/v) dried yeast extract SH (Fujifilm Wako Pure Chemical), 0.10% (w/v) K_2HPO_4, 0.060% (w/v) $NaH_2PO_4 \cdot 2H_2O$, 0.050% (w/v) $MgSO_4 \cdot 7H_2O$, 0.0010% (w/v) $FeSO_4 \cdot 7H_2O$, 0.0010% (w/v) $MnSO_4 \cdot 5H_2O$ and 0.30% (w/v) $CaCO_3$ (pH 6.8) and incubated in test tubes at 240 rpm and 27°C for 3 d. To the culture solution, 0.20 mg/mL lysozyme and 0.10% (v/v) Triton X-100 were added, and the solution was shaken at 27°C and 240 rpm for 1 h. The solutions containing both the lysed cells and the culture supernatant were used as the crude enzyme solution. Reaction mixture (200 μL) containing 50% (v/v) crude enzyme solution, 10 mg/mL dextran T10, 0.0060% (w/v) hinokitiol (Osaka Organic Chemical Industry; Osaka, Japan) and 50 mM sodium acetate buffer (pH 6.0) were incubated at 40°C for 16 h. The reaction mixtures were analyzed using thin-layer chromatography (TLC).

TLC analysis

The reaction mixtures (1.3 μL) were spotted on a silica gel plate 60 F_{254} (Merck KGaA; Darmstadt, Germany). As a developing solvent, acetonitrile: water: 1-propanol: ethyl acetate = 85: 70: 50: 20 (AWPE) was used. All TLC plates were developed twice using the same developing solvent. Sugar spots were detected by spraying 20% (v/v) sulfuric acid in methanol solution and incubating the plates at 120°C for 5 min. The Rf value was calculated by measuring the relative distance traveled by each compound with respect to the mobile phase.

Identification of bacterial genera using 16S rDNA analysis

Two bacterial strains, D1110 and D2006, were cultured on the solid medium shown in "Screening of enzymes derived from bacteria isolated from the soil" section. A colony of each strain was dissolved in MightyPrep reagent for DNA purchased from Takara Bio (Shiga, Japan). The dissolved solution was heated at 95℃ for 10 min and centrifuged at 23,800 ×*g* for 2 min to prepare lysates containing genomic DNA. Reaction mixtures (20 μL) containing 0.30 μM forward primer (5′-AGAGTTTGATCATGGCTCAG-3′), 0.30 μM reverse primer (5′-TACGGTTACCTTGTTACGACTT-3′), 52% (v/v) PrimeSTAR Max premix solution purchased from Takara Bio, 10% (v/v) lysates were applied to PCR to amplify 16S rDNA. The amplified PCR fragments were purified using ethanol precipitation. DNA sequence of the fragments was analyzed using following primers: Primer 1 (5′-CGTATTACCGCGGCTGCTGG-3′), Primer 2 (5′-CAGGATTAGATACCCTGGTAG-3′), Primer 3 (5′-CTACCAGGGTATCTAATCC-3′) and Primer 4 (5′-AGCTGACGACAGCCATGCAGC-3′). DNA sequencing was performed by Eurofins Genomics K.K. (Tokyo, Japan). The determined 16S rDNA sequences from two strains were used as query sequences to search homologous ones derived from each type strain bacteria in EzTaxon (Chun *et al*., 2007).

Preparation of CI4 using a culture supernatant of *Agreia* sp. D1110

Agreia sp. D1110 was incubated with reciprocal shaking at 27°C for 3 d in 50 mL of liquid medium described in "Screening of enzymes derived from bacteria isolated from soil" section. Culture supernatant of *Agreia* sp. D1110 was collected by centrifugation and solid ammonium sulfate was added to 80% saturation to precipitate the protein. The precipitates were collected by centrifugation at 23,800 ×*g* for 10 min, dissolved in 20 mM Tris-HCl (pH 7.5), and dialyzed against 20 mM Tris-HCl buffer (pH 7.5). The dialysate was heated at 80°C for 30 min to

inactivate contaminating enzymes and centrifuged at 23,800 ×*g* for 10 min. In a preliminary experiment, the heated dialysate possessed activity to produce CI4. The dialysate (40 mL) was used as a crude enzyme solution. Reaction mixture (1.0 L) containing 0.39% (v/v) crude enzyme solution, 10 mg/mL dextran T70 and 50 mM sodium acetate buffer (pH 6.0) was incubated at 40°C for 20 h and then boiled for 10 min to stop the reaction. The reaction mixture was condensed to 100 mL using a rotary evaporator and 200 mL of ethanol was added to precipitate polysaccharides. After centrifugation at 23,800 ×*g* for 20 min, precipitated polysaccharide was removed. The supernatant was condensed to 25 mL using the evaporator and filtered through a 10 kDa cut-off membrane (Amicon Ultra, Merck Millipore; Burlington, MA, United States) to remove polysaccharides remained. The sample was analyzed by HPLC using two-tandemly connected MCI GEL CK04SS columns under the conditions described in a "HPLC and LC-MS analysis" section. After adjusting the pH of the sample to 5.0 with 1.0 M HCl, α-glucosidase (1.0 U/mL) and glucoamylase (10 U/mL) were added to the solution and incubated at 50°C for 4 d to hydrolyze remained dextran and isomaltooligosaccharides to Glc. By adding 6.0 M NaOH, the solution was adjusted to pH 12.0 and boiled for 2 h, decolored using an activated carbon (Futamura Chemical; Nagoya, Japan) and desalted using a cation exchanger resin SK-1B (Mitsubishi Chemical), an anion exchanger resin WA30 (Mitsubishi Chemical) and an anion exchange resin Amberlite IRA-411 (Organo; Tokyo, Japan). The solution of purified oligosaccharide (Figure 2-2(c)) was stored at 4°C until it is solidified. Purity of the purified oligosaccharides was determined by HPLC using two-tandemly connected MCI GEL CK04SS columns under the same conditions as described in "HPLC and LC-MS analysis" section. The oligosaccharide was dried and solidified using centrifugal concentration. The solidified oligosaccharide was weighed to determine yield. For NMR analysis, the oligosaccharide was dissolved in D_2O.

HPLC and LC-MS analysis

The amount of saccharides in each sample were determined by HPLC. Prior to analysis, samples were filtered using a Millex®-LG (0.2 μm, Merck Millipore) and deionized using a micro acilyzer G0 (Asahi Chemical; Tokyo, Japan) and a neosepta cartridge AC110-04 (Astom; Tokyo, Japan). Samples were analyzed using HPLC (Prominence, Shimadzu; Kyoto, Japan) coupled to a refractive index detector (Shimadzu). Detection of all HPLC analyses in this dissertation was done using the refractive index detector. The concentration of each sugar was calculated by multiplying the peak area percentage (%) of each sugar by the concentration of total sugar in the sample. Two-tandemly connected MCI GEL CK04SS columns (10 mm i.d. × 200 mm; Mitsubishi Chemical; Tokyo, Japan) were used in the HPLC analysis at a flow rate of 0.40 mL/min, using water as a solvent at 80°C. The molecular mass of the products was determined by LC-MS analysis using LCMS-IT-TOF (Shimadzu), in which LC conditions were the same as described above. In MS analysis, electrospray ionization (ESI) method was used to ionize the products. ESI conditions were as follows: Curved desolvation line temperature and heat block temperature were 200℃. Conditions in the detection of positive ion mode and negative ion mode were followings; measuring *m/z* was from 500 to 800, event time is 500 msec and ion accumulation time was 10 msec.

A YMC-Pack ODS-AQ-303 column (4.6 mm i.d. × 250 mm) purchased from YMC (Kyoto, Japan) was used to compare sugar composition in the reaction product using the crude enzyme solution from *Agreia* sp. D1110 and *M. trichothecenolyticum* D2006. In this experiments, the column temperature was set at 40℃ and a flow rate of the mobile phase with water was 0.5 mL/min.

NMR measurements

The sample containing 5.0% (w/v) oligosaccharide in D_2O was applied to NMR measurements. All NMR spectral data of ^{1}H-NMR, ^{13}C-NMR, DEPT135°, ^{1}H-^{1}H correlation spectroscopy (^{1}H-^{1}H COSY), heteronuclear single quantum correlation (HSQC) and heteronuclear multiple bond correlation (HMBC) were recorded at 25°C using a Brucker 700 MHz spectrometer (^{1}H 700.33 MHz, ^{13}C 176.12 MHz: Brucker; Billerica, MS, United States) equipped with a 5 mm CPTCI 1H-13C/15N/D Z-GRD Z44908/0021 probe. The chemical shifts were expressed in ppm downfield from the signal of TMSP-d_4, which was used as an external standard.

Comparison of the culture supernatant from two strains in the CI4 producing reaction

Agreia sp. D1110 and *M. trichothecenolyticum* D2006 were respectively incubated with reciprocal shaking at 27°C for 48 h in 50 mL of the liquid medium described in the section of "Screening of enzymes derived from bacteria isolated from the soil". Each culture broth was centrifuged at 23,800 ×*g* for 10 min. The culture supernatant (40 mL) of each strain was diluted by a factor from 1 to 273 times using 50 mM sodium acetate buffer (pH 6.0). The diluted culture supernatants were used as an enzyme to produce CI4. The reaction mixtures containing 10 mg/mL dextran T10, 25% (v/v) the diluted culture supernatants and 50 mM sodium acetate buffer (pH 6.0) were incubated at 40°C for 24 h. The sugar composition of each reaction mixture was analyzed by HPLC using the YMC-Pack ODS-AQ-303 column as described in "HPLC and LC-MS analysis" section.

Preparation of crystalline powder of CI4 using culture supernatant of *M. trichothecenolyticum* D2006

M. trichothecenolyticum D2006 was incubated with reciprocal shaking at 27°C for 48 h in the

liquid medium (total volume 4 L) described in the section of "Screening of enzymes derived from bacteria isolated from the soil". The culture broth was centrifuged, and the supernatant was used for the enzymatic reaction. A reaction mixture (20 L) containing 5.0 mg/mL dextran T70, 10 mM sodium acetate buffer (pH 6.0), 1.0 mM $CaCl_2$, 0.0030% (w/v) hinokitiol and 2.5% (v/v) of the centrifuged supernatant was incubated at 35°C for 16 h. CI4 was collected by ultrafiltration with the ultrafiltration (UF) membrane, microza SEP-1013 (Asahi Kasei; Tokyo, Japan) as permeate (17.5 L). To the retentate, 17.5 L of buffer solution containing 10 mM sodium acetate buffer (pH 6.0), 1.0 mM $CaCl_2$ and 0.0030% (w/v) hinokitiol was added to be 20 L in total, and another 16-h reaction was restarted. The reaction / separation set was done three times in total. Concentration of each oligosaccharide in the reaction mixture and the recovered solution were determined as follows: Total sugar concentration in each samples were measured using anthrone-sulfate methods (Moris, 1948). It was distributed to each oligosaccharide based on the peak area percentage (%) of each sugar. HPLC analyses were performed under the condition described in "HPLC and LC-MS analysis" section. The CI4-containing solution (17.5 L) was treated with 1.0 U/mL dextranase (40℃, 16 h), and the solution was adjusted pH 12.0 using 6.0 M sodium hydroxide solution and boiled for 4 h. The solution was neutralized using the SK-1B resin, decolorized using the activated carbon and filtered using a diatomite (Hayashi Kasei; Osaka, Japan) and desalted using SK-1B, WA30 and IRA-411 resins. The solution was condensed to Brix 53% using the rotary evaporator at 60℃ and incubated at room temperature for 2 h to obtain a slurry containing CI4 crystal. The slurry was separated to a CI4 crystal (Lot 1) and a solution containing CI4 using a glass filter. The solution containing CI4 was re-condensed at 60℃ and incubated at room temperature for 2 h to obtain a new slurry. These separation steps were performed 3 times to obtain 3 lots of CI4 crystal. The water content of the CI4 crystal Lot 1 was analyzed using a Karl Fischer titrator AQV-2200 (Hiranuma Sangyo; Mito, Japan). The purity of the CI4 crystals (Lot1, 2 and 3) was

determined by HPLC analysis using two-tandemly connected MCI GEL CK04SS columns under the same conditions described in "HPLC and LC-MS analysis" section. The yield of the CI4 crystals (Lot 1, 2 and 3) were determined by measuring the weights of the obtained CI4 crystals (Lot1, 2 and 3). The CI4 crystal Lot 3 was re-dissolved, condensed to Brix 48% at 60℃ using the rotary evaporator and incubated at room temperature for 3 d to obtain single CI4 crystals which were used for X-ray crystallographic analysis.

X-ray crystallographic analysis

X-ray crystal structure data of single CI4 crystals were recorded using RIGAKU VariMax with Saturn 724 (Rigaku; Tokyo, Japan). Details of the X-ray data collection, data reduction, structure solution, and crystallographic refinement are described in the deposited file to The Cambridge Crystallographic Data Centre (CCDC, Deposition Number 2003643). Visualization of an asymmetric unit and detecting hydrogen bonds were performed using Mercury (Bruno *et al*., 2002; Macrae *et al*., 2006, 2008, 2020). Pymol ver 2.1.0 was used to perform fitting of two independent CI4 molecules and calculation of torsion angles and distance between oxygen atoms in the CI4 molecules. The definition of each torsion angle was shown in the footnotes of Table 2-8.

Digestibility test

Based on AOAC2001.03 test methods (AOAC international, 2016), digestibility of CI4 were analyzed. The oligosaccharides were digested using α-amylase, protease and amyloglucosidase, and residual oligosaccharides were precipitated using the aqueous ethanol and measured using HPLC on the basis AOAC official methods of analysis (AOAC international, 2016).

Results

Screening of bacterial strains producing an unknown oligosaccharide

Approximately 2,000 soil-derived bacterial colonies were isolated on plates containing 0.15% (w/v) dextran as a sole carbon source. Those bacteria were cultured in a liquid medium, and cells were disrupted by lysozyme directly added to the culture broth. The resultant suspension, mixture of disrupted cells, their lysate and the supernatant, was used as crude enzyme solution. Dextran (10 mg/mL) was reacted with the crude enzyme solutions and the reaction products were analyzed by TLC. The crude enzyme solutions derived from strains D1110 and D2006 produced an unknown oligosaccharide with Rf values of 0.70 on TLC (Figure 2-1). The Rf value was obviously different from those of IG3 (Rf value = 0.75) and isomaltotetraose (IG4, Rf value = 0.67).

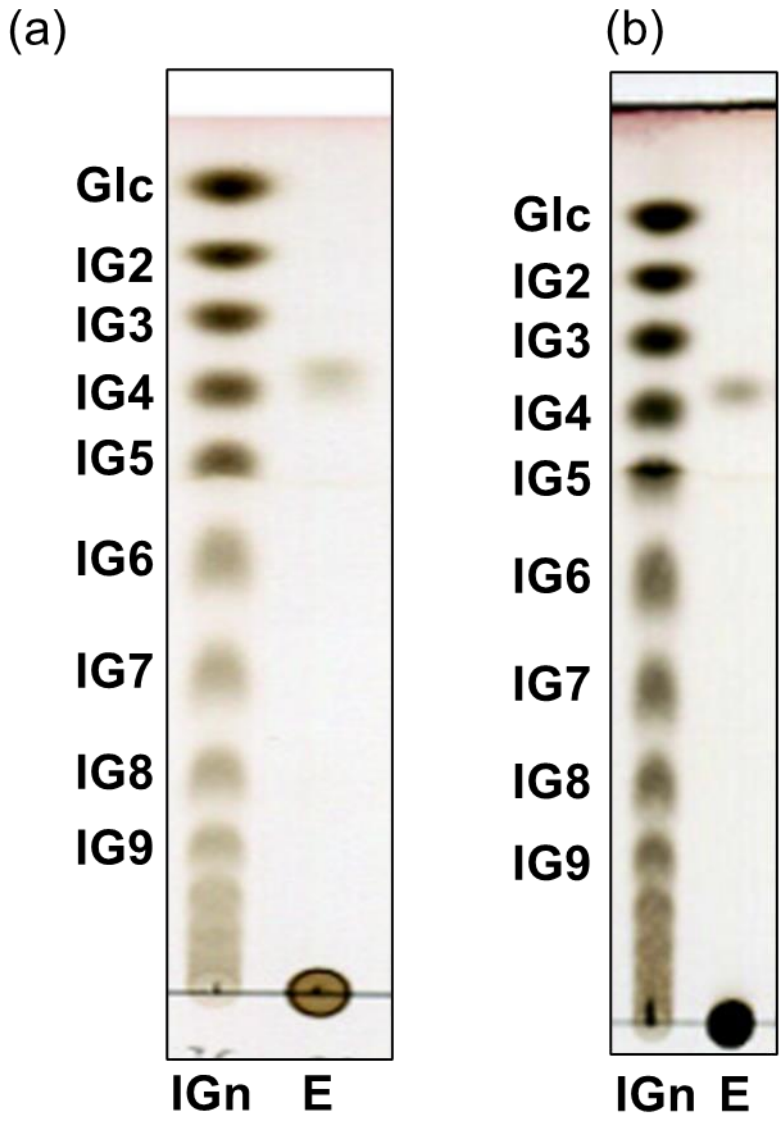

Figure 2-1 The oligosaccharides produced from dextran using crude enzyme solutions of D1110 and D2006 strains.

(a) D1110 strain, (b) D2006 strain. The crude enzyme solutions were a mixture of disrupted cells, cell lysate and culture supernatant. Lane E, reaction product; lane IGn, isomaltooligosaccharide standards. IG9, isomaltononaose; IG8, isomaltooctaose; IG7, isomaltoheptaose; IG6, isomaltohexaose, IG5, isomaltopentaose; IG4, isomaltotetraose; IG3, isomaltotriose; IG2, isomaltose; Glc, glucose.

Identification of genera of D1110 and D2006 strains

Table 2-1 shows a result of EzTaxon search using the 16S rDNA sequence of D1110 and D2006 as a query sequence. Identity of 16S rDNA sequence derived from D1110 on one from *Agreia pratensis* and *Agreia bicolorata* was 98.3% and 98.2%, respectively. No strain from other genera showed such high identity. Identity of 16S rDNA sequence derived from D2006 on *Microbacterium trichothecenolyticum* was 99.2%. Based on these results, D1110 and D2006 strains were identified as *Agreia* sp. and *Microbacterium trichothecenolyticum*, respectively. Two genera, *Agreia* and *Microbacterium*, are categorized in a same family, *Microbacteriaceae* (Parte *et al*., 2020).

Table 2-1(a) EzTaxon search using the 16S rDNA sequence of D1110 strain.

Taxon name	Strain name	Accession	Identity (%)	Diff/Total nt
Agreia pratensis	VKM Ac-2510(T)[1]	jgi.1118336	98.3	24/1443
Agreia bicolorata	VKM Ac-1804(T)	JYFC01000015	98.2	26/1443
Subtercola boreus	K300(T)	AF224722	97.2	39/1434
Leifsonia antarctica	SPC-20(T)	AM931710	97.2	40/1445
Herbiconiux ginsengi	CGMCC 4,3491(T)	jgi.1076294	97.1	42/1446

(T)[1] Type strain.

Table 2-1(b) Results of EzTaxon search using the 16S rDNA sequence of D2006 strain.

Taxon name	Strain name	Accession	Identity (%)	Diff/Total nt
Microbacterium trichothecenolyticum	DSM8608(T)[1]	JYJA01000006	99.2	12/1444
Microbacterium hibisci	THG-T2.14(T)	KX456190	98.5	22/1424
Microbacterium jejuense	THG-C31(T)	JX997974	98.4	23/1422
Microbacterium yannicii	G72(T)	FN547412	98.3	24/1444
Microbacterium testaceum	DSM20166(T)	X77445	98.2	26/1444

(T)[1] Type strain.

Structural analysis of the oligosaccharide

(a) Preparation of the oligosaccharide produced using the salt precipitation fraction of the culture supernatant of *Agreia* sp. D1110 and its purification

Using the heated salt precipitation fraction of the culture supernatant of *Agreia* sp. D1110, the oligosaccharide was produced from dextran, and purified through removal of remaining polysaccharide by ethanol precipitation and ultrafiltration, followed by enzyme digestion of linear saccharides and alkaline treatment as described in "Preparation of CI4 using culture supernatant of *Agreia* sp. D1110" section (Figure 2-2, Table 2-2). In the preparation after removal of dextran, the unknown oligosaccharide was predominant, while dextran and IG4 were observed (Figure 2-2(a)). The oligosaccharide remained after α-glucosidase and glucoamylase digestion while dextran and IG4 were completely degraded into Glc (Figure 2-2(b)). The oligosaccharide remained even after the following alkaline treatment, while the Glc disappeared completely (Figure 2-2(c), Table 2-2). These results suggested that the oligosaccharide was not a linear oligosaccharide. Through the steps, the purified oligosaccharide occupied 99.1% of saccharides in the preparation on the RI detection basis on HPLC. This sample was used for further structural analyses.

(b) LC-MS analysis

LC-MS analysis of the oligosaccharides obtained by the method described in "Preparation of CI4 using culture supernatant of *Agreia* sp. D1110" was performed. Ions with *m*/*z* of 671 (sodium ion adducted form) and of 647 (deprotonated form) were detected in positive ion mode and negative ion mode, respectively (Figure 2-3). These *m*/*z* values suggest that a molecular weight of the product is 648.

(c) NMR analyses

Chemical structure of the oligosaccharide (Figure 2-2(c)) was determined using ^{13}C-NMR (Figure 2-4), DEPT135° (Figure 2-5), ^{1}H-NMR (Figure 2-6), ^{1}H-^{1}H COSY (Figure 2-7), HSQC (Figure 2-8) and HMBC (Figure 2-9). Assignment of all carbons and protons are summarized in Table 2-3. The ^{13}C-NMR spectrum of the oligosaccharide exhibited 6 carbon signals (Figure 2-4). The DEPT135° spectrum indicated that a 67.4 ppm signal was methylene carbon, which is C-6 carbon (Table 2-3(a)). ^{1}H-NMR (Figure 2-6) showed only one doublet splitting signal at 5.13 ppm, which is a hydrogen atom bonded to C1 anomeric carbon. A coupling constant of $J_{1,2}$ = 3.9 Hz for this doublet peak (Figure 2-6) indicates the α-glucosidic linkage. The 99.5 ppm signal correlated with this hydrogen atom in HSQC is that of anomeric carbon (Figure 2-8). Other proton and carbon peaks were assigned using the results of ^{1}H-^{1}H COSY, HSQC and HMBC. The coupling constants shown in Table 2-3(b) suggest that the oligosaccharide should be solely composed of glucopyranosyl residues. Cross-peaks between C-1 and Ha-6, C-1 and Hb-6 and H-1 and C-6 were observed in HMBC analysis (Figure 2-9). These results suggest that the oligosaccharide is composed of α-(1→6)-glucosidic linkages. Combined with the mass spectrometry results, the structure of the oligosaccharide was determined to be cyclo-[-6Glcα1-]$_4$ (Figure 2-10). This tetrasaccharide was named cycloisomaltotetraose (CI4).

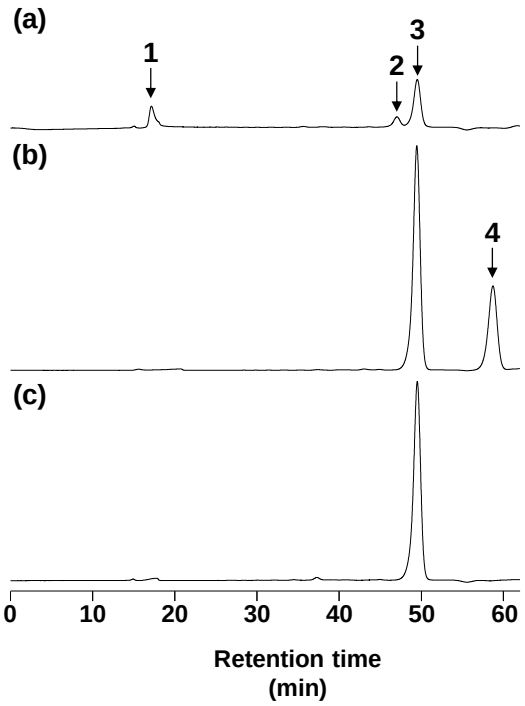

Figure 2-2 HPLC analysis of the oligosaccharides obtained by the action of enzyme solution prepared from culture supernatant on dextran.

Refractive indexes monitored in HPLC are shown. The analyzed oligosaccharide samples were as follows. (a) The oligosaccharides produced using enzyme partially purified from the culture supernatant of *Agreia* sp. D1110, and mostly purified by ethanol precipitation and ultrafiltration with a 10 kDa cut-off membrane. (b) After α-glucosidase and glucoamylase digestion of (a). (c) After alkaline treatment, desalnization and decolorization of (b). (a) and (c) are vertically 5 times magnified. Peak 1, polysaccharide; Peak 2, IG4; Peak 3, unknown oligosaccharide; Peak 4, Glc.

Table 2-2 Sugar composition of each purified sample.

Step	IGn[1] (DP>12)	IGn (DP 5-12)	IG4	Unknown oligosaccharide	Glc[2]	Others
Enzymatic reaction product after ultrafiltration	28.9	6.70	11.8	52.6	N.D.[3]	N.D.
After α-glucosidase and glucoamylase digestion	N.D.	N.D.	N.D.	67.3	30.8	1.90
After alkaline treatment, desalnization and decolorization	N.D.	N.D.	N.D.	99.1	N.D.	0.898

IGn[1], Isomaltooligosaccharides; Glc[2], D-glucose; N.D.[3], Not detected.

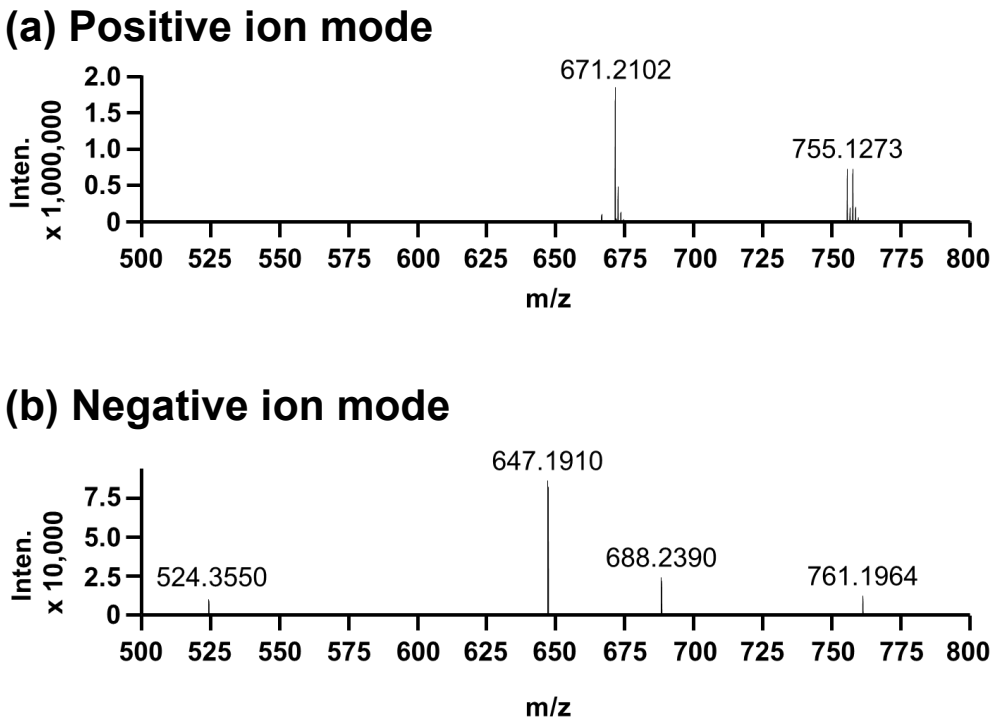

Figure 2-3 Mass spectra of the purified oligosaccharide.

(a) Mass spectrum of positive ion mode. (b) Mass spectrum of negative ion mode.

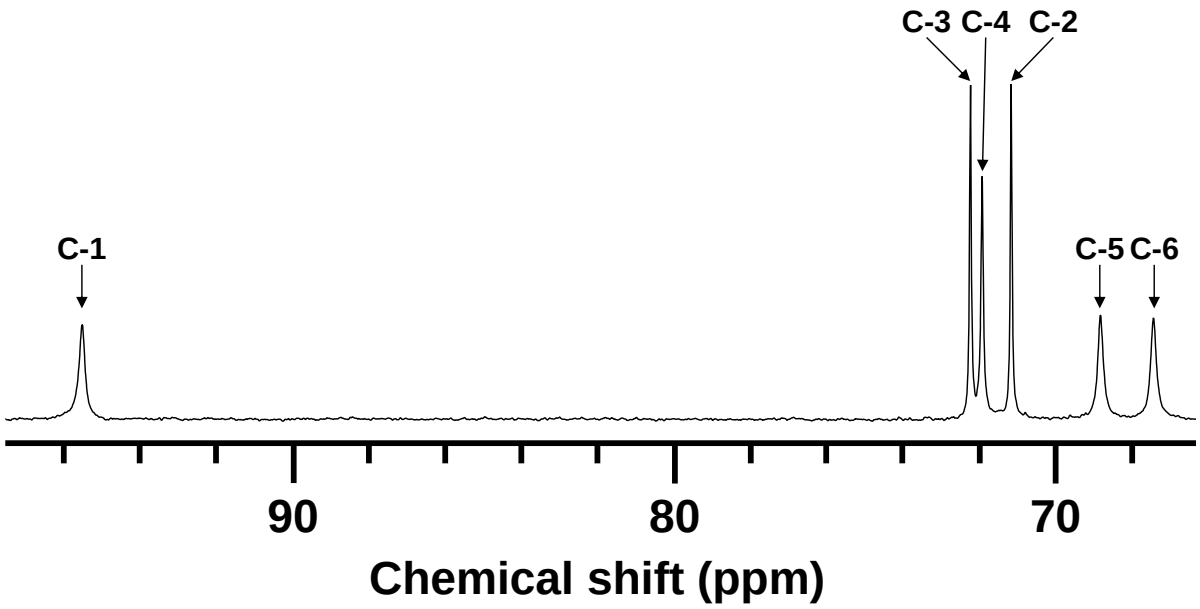

Figure 2-4 ^{13}C-NMR spectrum of the purified oligosaccharide.

Selected parts of the ^{13}C-NMR spectrum of the purified oligosaccharide.

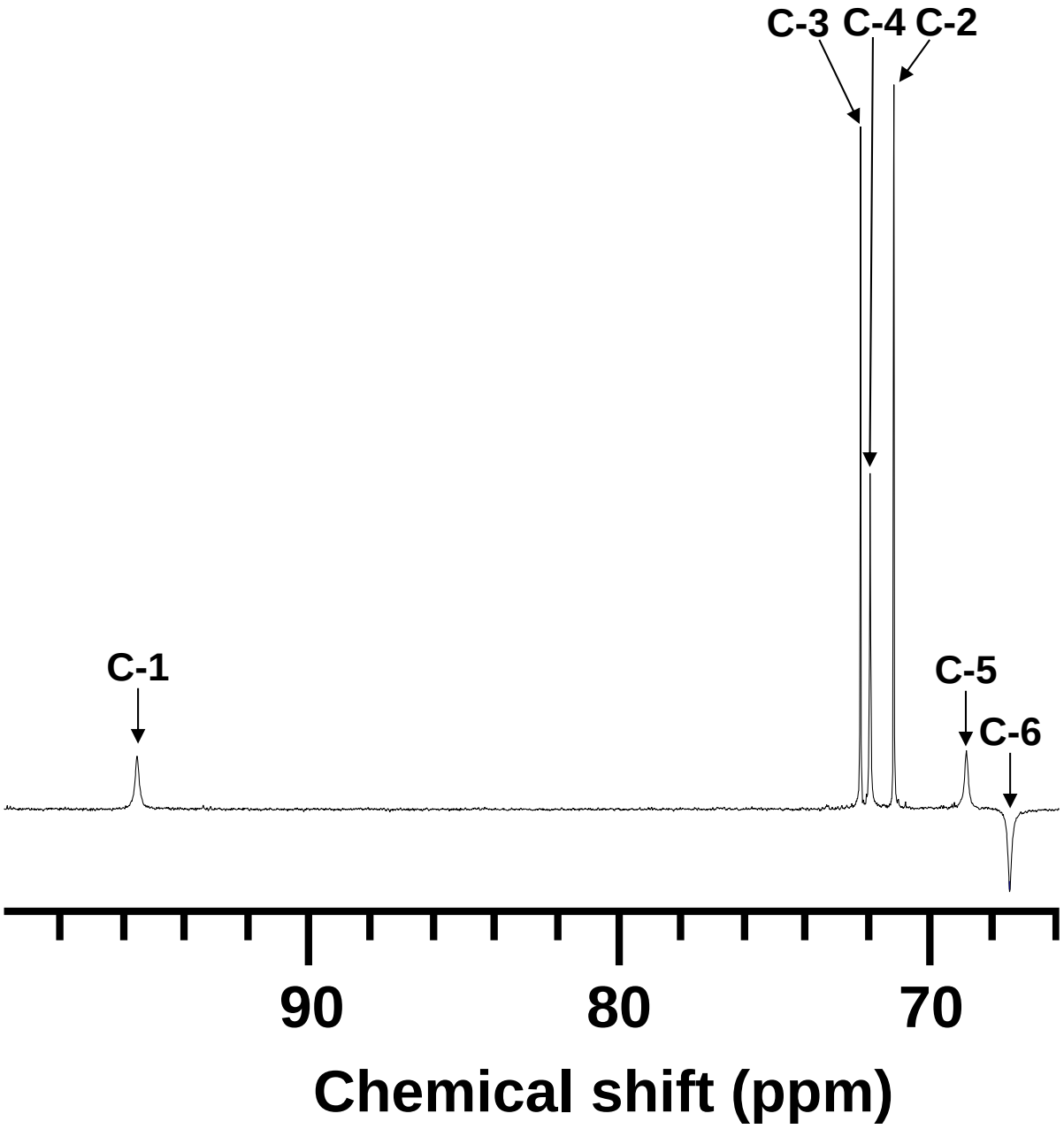

Figure 2-5 DEPT135° spectrum of the purified oligosaccharide.

Selected parts of the DEPT135° spectrum of the purified oligosaccharide.

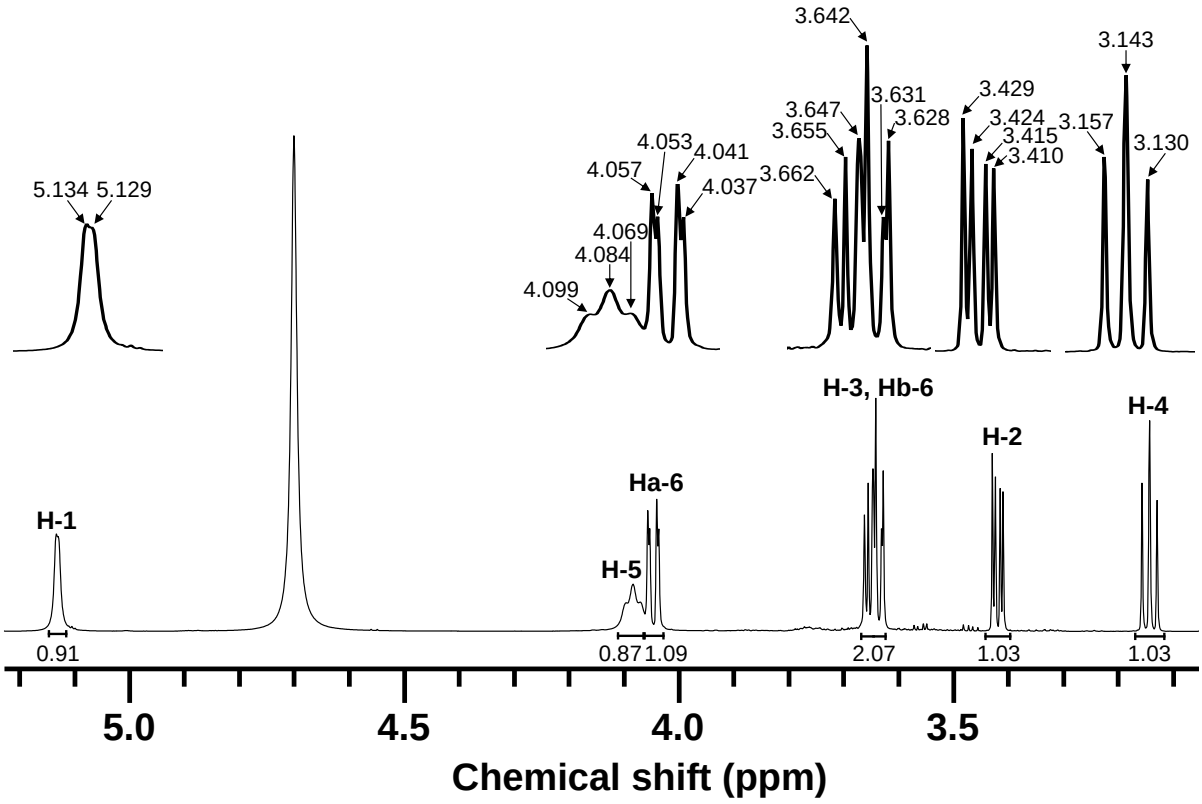

Figure 2-6 ^{1}H-NMR spectrum of the purified oligosaccharide.

Structure of the purified oligosaccharide was analyzed with ^{1}H-NMR. Each peak was assigned using the results of ^{1}H-^{1}H COSY. The numbers under each peak are integration values.

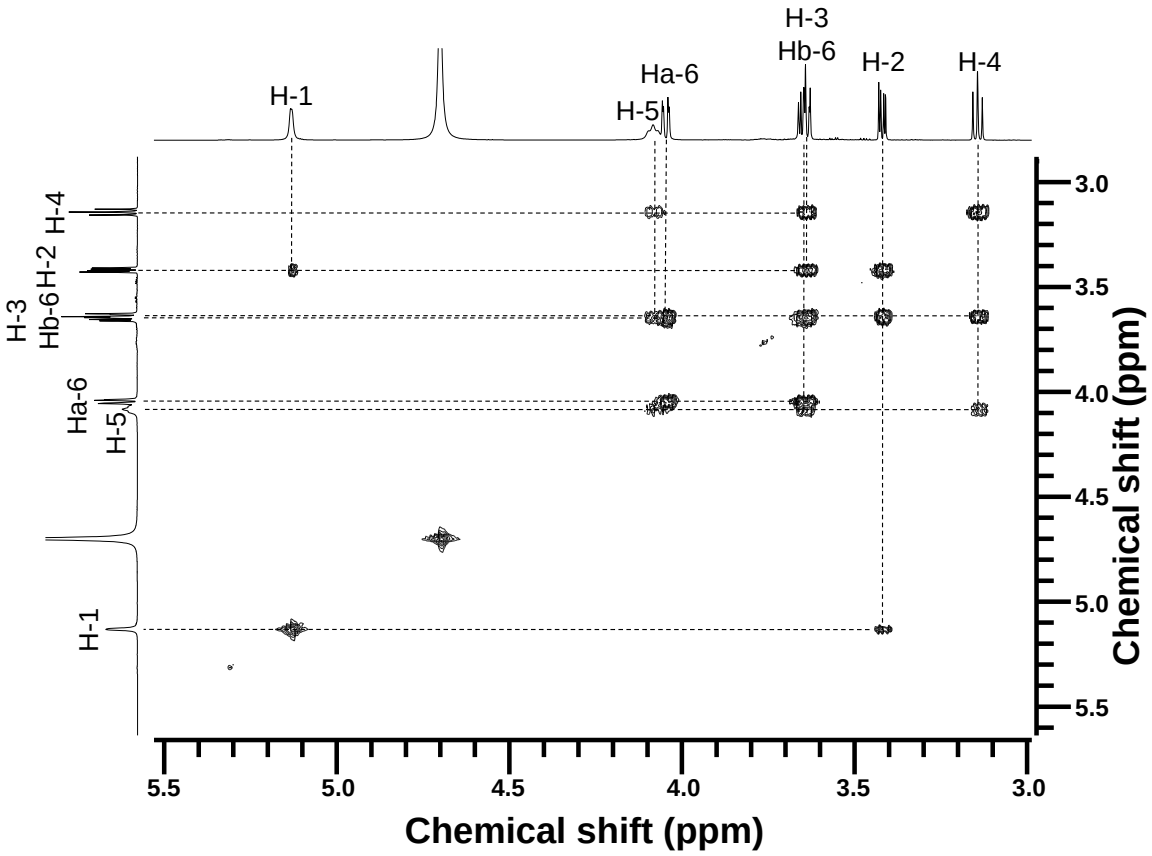

Figure 2-7 ^{1}H-^{1}H COSY spectrum of the purified oligosaccharide.

From H-1, each proton peak was assigned using cross-peak in ^{1}H-^{1}H COSY.

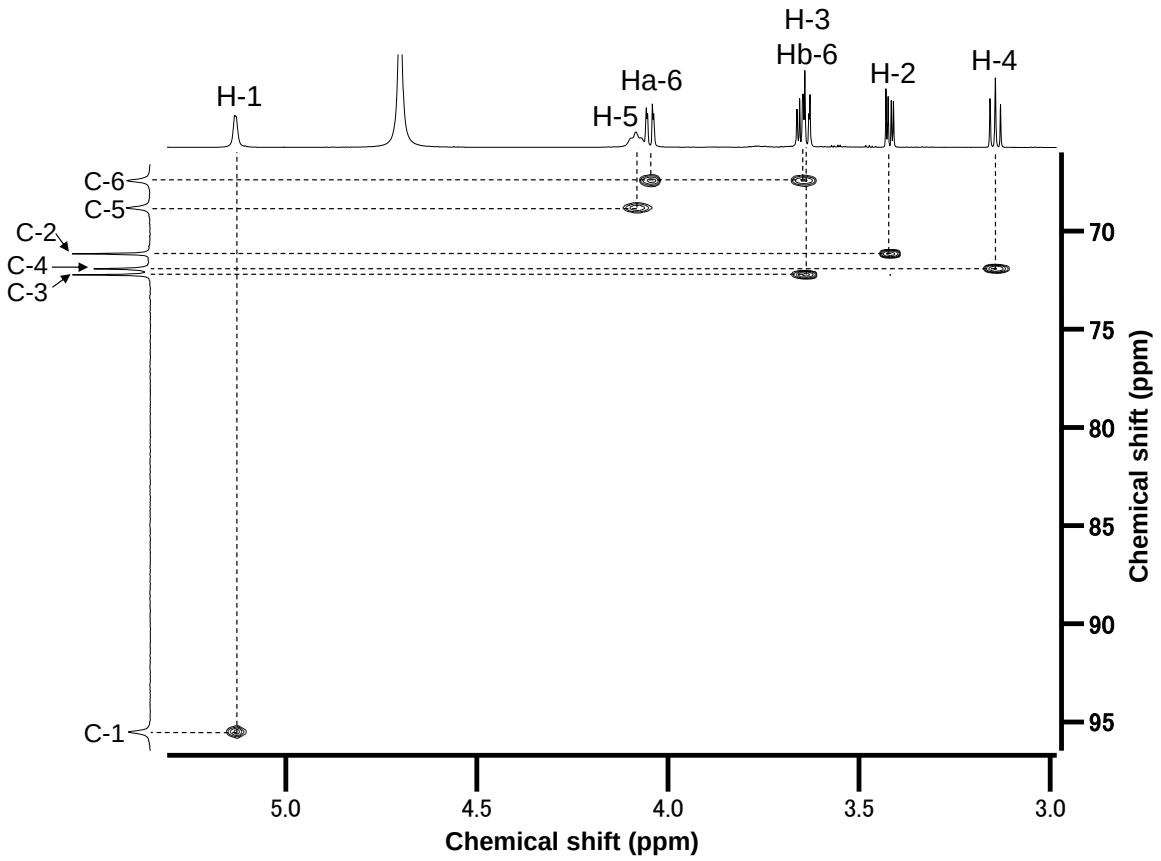

Figure 2-8 HSQC spectrum of the purified oligosaccharide.

Using assigned proton peaks, each carbon peak was assigned in HSQC analysis.

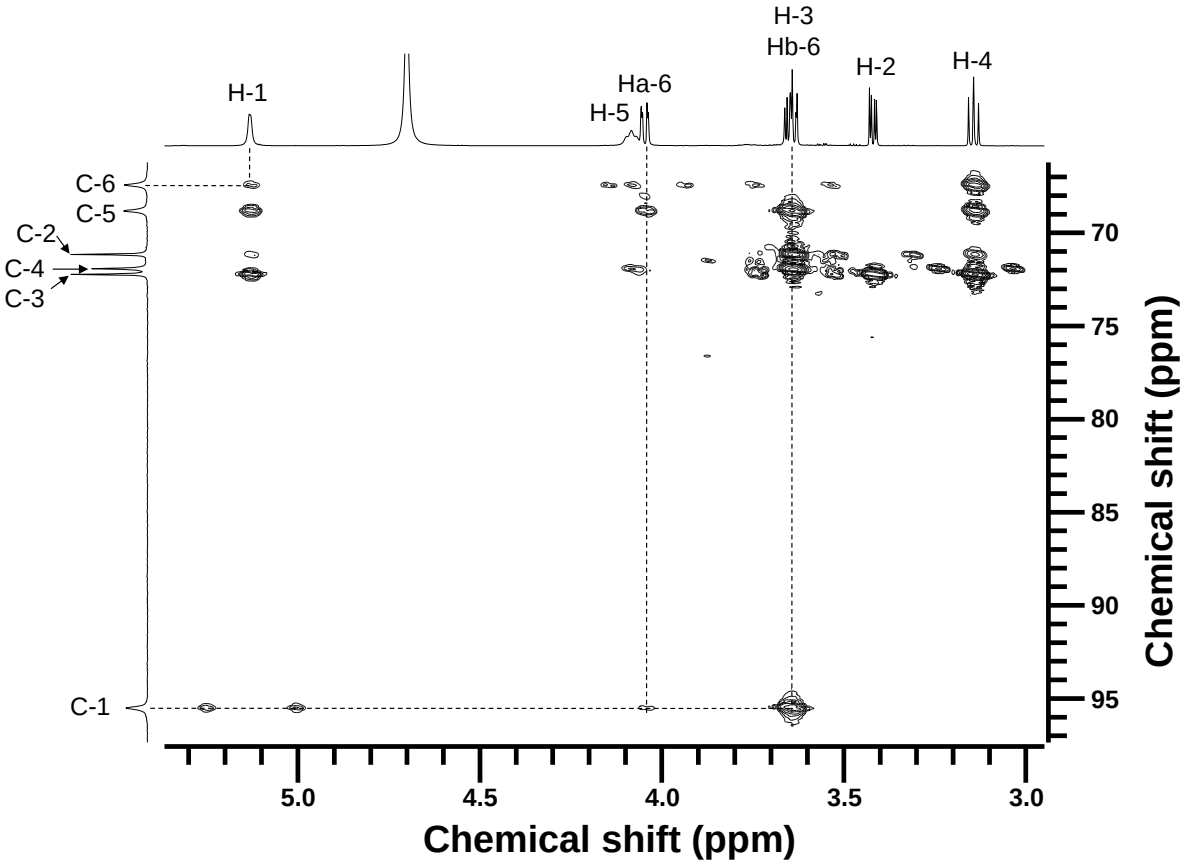

Figure 2-9 HMBC spectrum of the purified oligosaccharide.

Cross-peaks between H-1 and C-6, between Ha-6 and C-1 and between Hb-6 and C-1 were shown in the spectrum.

Table 2-3 (a) ^{13}C-NMR data of the purified oligosaccharide.

Chemical shift (ppm)	Assignment
95.5	C-1
72.2	C-3
71.9	C-4
71.2	C-2
68.8	C-5
67.4	C-6

^{13}C-NMR spectrum was recorded in D_2O at 25°C. Chemical shifts were expressed in ppm downfield from the signal of TMSP-d_4, which was used as an external standard.

Table 2-3 (b) ^{1}H-NMR data of the purified oligosaccharide.

Chemical shift (ppm)	Coupling constant (Hz)	Coupling	Assignment
5.13	3.9	d	H-1
4.08	-	m	H-5
4.05	11.3, 2.6	dd	Ha-6
3.64	9.5	t	H-3
3.64	10.7	t	Hb-6
3.42	9.9, 3.8	dd	H-2
3.14	9.5	t	H-4

^{1}H-NMR spectrum was recorded in D_2O at 25°C. The chemical shifts were expressed in ppm downfield from the signal of TMSP-d_4, which was used as an external standard.

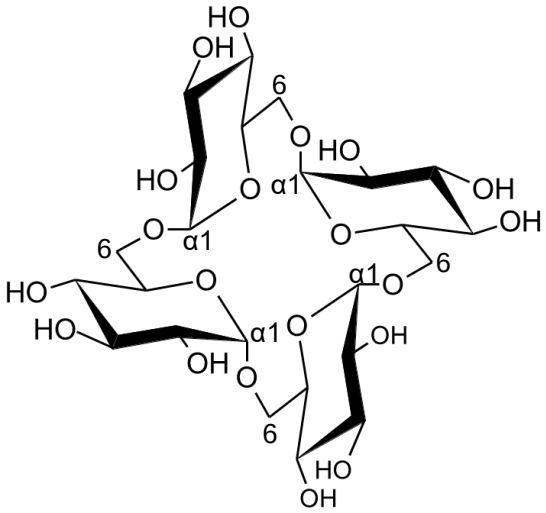

CI4

Figure 2-10 Chemical structure of CI4.

Comparison of sugar composition in CI4-producing reactions using the culture supernatants from two strains

Sugar composition in CI4-producing reactions using the culture supernatants from two strains, *Agreia* sp. D1110 and *M. trichothecenolyticum* D2006, was compared to reveal which culture supernatants are suitable for CI4 production. The culture supernatants of D1110 and D2006 diluted 1-273 folds were used as enzyme solution to react with 10 mg/mL dextran for 48 h, and saccharides in the reaction mixture were quantified by HPLC (Figure 2-11). The conversion from dextran to CI4 was dependent on the amount of the supernatant added to the reaction mixture for both culture supernatants. In both culture supernatants, the highest CI4 production ratio was obtained when the supernatant solutions were used without dilution. However, with the culture supernatant from *Agreia* sp. D1110, IG4 was produced 30.6% of CI4, while it was 5.69% with culture supernatant from D2006 (Table 2-4). Therefore, the culture supernatant of *M. trichothecenolyticum* D2006, showing lower IG4-producing activity, was used for the reaction to prepare the CI4 crystal.

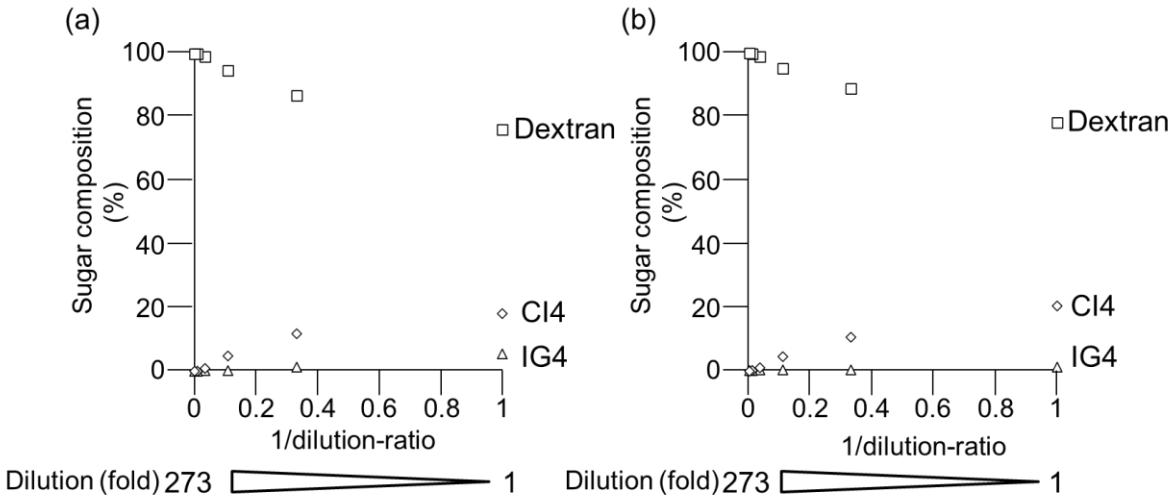

Figure 2-11 Comparison of sugar composition in the reaction product.

Culture supernatants were diluted 1-273 folds and used as enzyme. Sugar compositions in the 47-h reactions were analyzed by HPLC using the YMC-Pack ODS-AQ303 column . (a) *Agreia* sp. D1110. (b) *M. trichothecenolyticum* D2006.

Table 2-4 Sugar composition in each reaction.

Strain	Dilution ratio of the culture supernatants (fold)	Sugar composition (%)				IG4/CI4 (%)
		Dextran	IG4	CI4	Others	
Agreia sp. D1110	1	75.8	5.53	18.1	0.564	30.6
	3	86.5	1.32	11.8	0.356	11.2
	9	94.4	0.386	4.90	0.305	7.88
	27	98.6	0.197	0.870	0.293	22.6
	81	99.6	0.168	N.D.[1]	0.273	-
	273	99.6	0.117	N.D.	0.297	-
M. trichothecenolyticum D2006	1	77.7	1.16	20.4	0.702	5.69
	3	88.4	0.384	10.5	0.638	3.66
	9	94.8	0.327	4.55	0.326	7.19
	27	98.5	0.322	0.943	0.250	34.1
	81	99.4	0.159	0.164	0.300	97.0
	273	99.5	0.160	N.D.	0.306	-

N.D.[1]: Not detected.

X-ray diffraction experiment of the single CI4 crystal

(a) Preparation of CI4 crystals

CI4 was produced from dextran T70 (100 g, 20 L, 5 g/L) by a reaction using culture supernatant (4 L) of *M. trichothecenolyticum* D2006. During the reaction, CI4 was recovered with ultrafiltration as permeate, and the retentate containing the enzymes and dextran T70 was further reacted after adding the reaction buffer till the original volume (20 L). The reaction and separation were repeated three times as shown in Figure 2-12. The amount of dextran T70 in the reaction mixture in each step, produced CI4 and recovered CI4 are shown in Table 2-5 and Figure 2-12. In three cycles, 34 g of CI4 was produced from 100 g dextran T70, and 32 g of CI4 was recovered using the separation (Table 2-5). The CI4 production ratio in the first reaction was 22%, which was similar to the yield (20%) from 10 g/L dextran shown above (Table 2-4). The CI4 production ratio for the three reaction/separation sets was 34%, about 1.6 times higher than the batch reaction yield.

From the ultrafiltration permeate, CI4 crystal was prepared. Linear isomaltooligosaccharides were degraded by dextranase (Figure 2-13(a)), and the produced IG2 and Glc were degraded and removed by alkaline treatment and decolorization (Figure 2-13(b)). The desalinized sample was regarded as purified CI4 (Figure 2-13(c)). CI4 was crystalized at room temperature and separated from the solution containing CI4. The separated solution was re-crystalized. The crystallization/separation set was performed 3 times, and 3 lots of CI4 crystalline powders (Lot 1, 8.6 g, purity 99.5%, water content 13.9%; Lot 2, 6.3 g, purity 98.7%; Lot 3, 1.2 g, purity 98.1%) were obtained. The purity of each crystal was determined by HPLC analysis (Figure 2-14(a)-(c))**.**

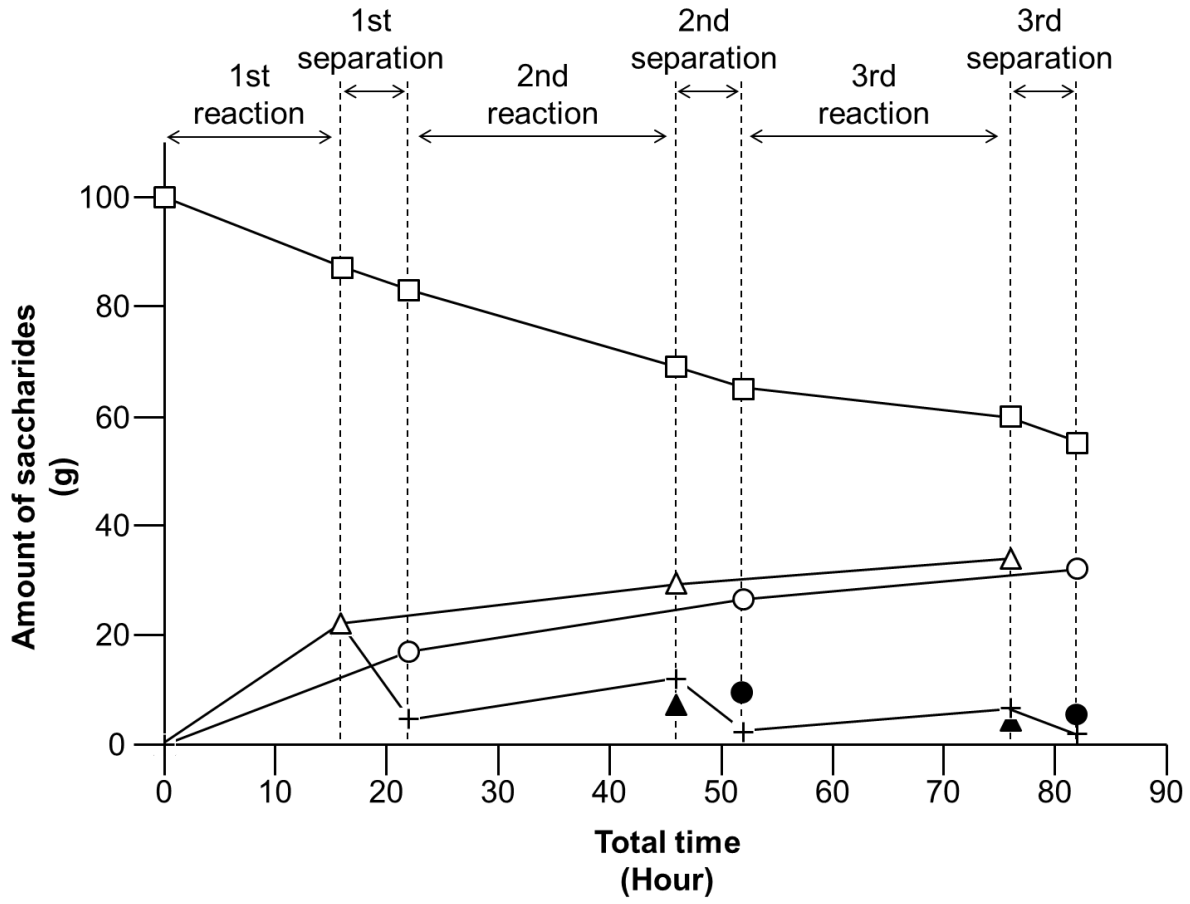

Figure 2-12 The amount of the produced CI4 and the recovered CI4.

□, Dextran T70 in the reaction mixture; +, CI4 in the reaction mixture; △, total produced CI4 in the reaction; ○, total recovered CI4; ▲, CI4 produced in each reaction; ●, CI4 recovered in each separation.

Table 2-5 Produced and recovered CI4 in each step.

Step		Time in each step (h)	Total run time (h)	Dextran (g), (%, w/v)	CI4 in each solution (g)	Produced CI4[1] (g)	Total produced CI4 (g)	Recovered CI4 (g)	Total recovered CI4 (g)
1st reaction	Start	16	16	100, 0.50	0.0	0	-	-	-
	End			87, 0.44	22	22	22	-	-
1st separation	Start	6	22	87, 0.44	22	-	-	-	-
	Permeate			2.3, 0.013	17	-	-	17	17
	Retentate			83, 3.3	4.7	-	-	-	-
2nd reaction	Start	24	46	83, 0.42	4.7	-	-	-	-
	End			69, 0.34	12	7.4	29	-	-
2nd separation	Start	6	52	69, 0.34	12	-	-	-	-
	Permeate			3.4, 0.019	9.5	-	-	9.5	27
	Retentate			65, 2.5	2.3	-	-	-	-
3rd reaction	Start	24	76	65, 0.33	2.3	-	-	-	-
	End			60, 0.30	6.7	4.4	34	-	-
3rd separation	Start	6	82	60, 0.30	6.7	-	-	-	-
	Permeate			3.3, 0.018	5.6	-	-	5.6	32
	Retentate			55, 3.5	1.5	-	-	-	-

Produced CI4[1]: calculated by subtracting the amount of CI4 at the start of the reaction from one at the end of the reaction.

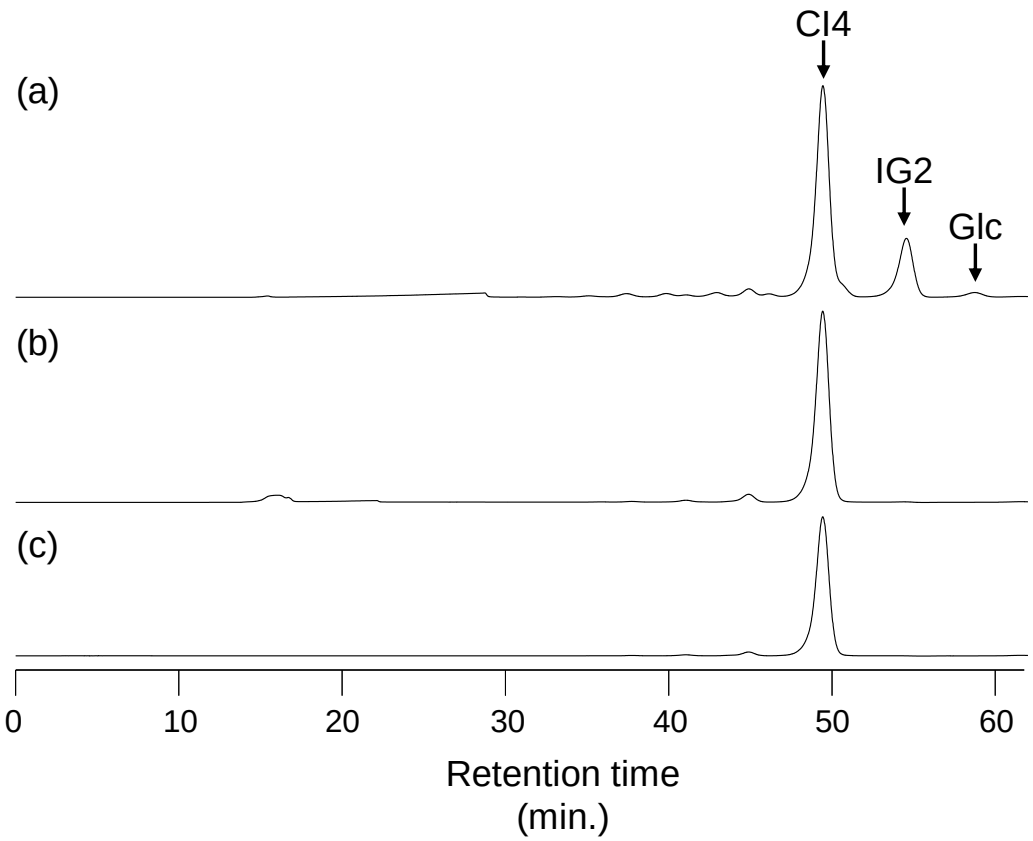

Figure 2-13 HPLC analysis of CI4 solution at each purification step.

(a) CI4 solution after dextranase reaction, (b) CI4 solution after alkaline treatment and decolorization, (c) purified CI4 after desalinization. Refractive indexes monitored in HPLC are shown.

Table 2-6 Sugar compositions in CI4 solution at each purification step.

Purification step	CI4	Glc	IG2	Others
Dextranase digestion	66.1	1.60	19.0	13.3
Alkaline treatment and decolorization	87.5	N.D.[1]	0.1	12.4
Desalinization	96.0	N.D.	N.D.	4.00

N.D.[1], Not detected.

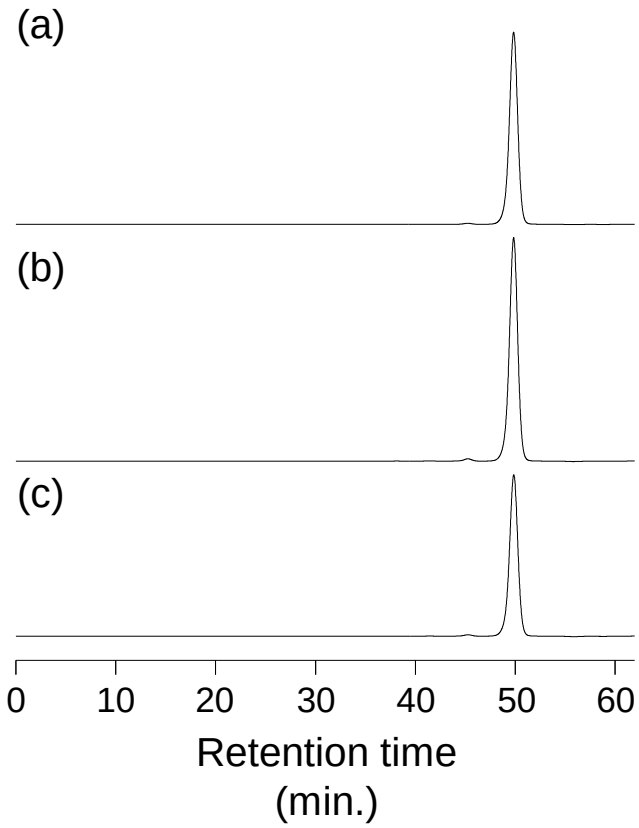

Figure 2-14 HPLC analysis of the purified CI4 crystals.

(a) CI4 crystal Lot 1, (b) CI4 crystal Lot 2, (c) CI4 crystal Lot 3. Refractive indexes monitored in HPLC are shown.

(b) Crystal structure analysis of CI4

Single crystals of CI4 were prepared and the X-ray crystal structure was determined. The CI4 crystal Lot 3 was dissolved in water and the solution (purity 98.1%) was condensed to Brix 48.0% at 60℃ and incubated at room temperature to obtain single crystals of CI4. The obtained single crystal was colorless and transparent (Figure 2-15). The X-ray data collection and refinement statistics of the CI4 crystal (CCDC deposition number 2003643) are summarized in Table 2-7. Figure 2-16 shows an asymmetric unit in the CI4 crystal where 2 CI4 molecules (molecule 1 composed of Ring1, Ring2, Ring3 and Ring4 and molecule 2 composed of Ring5, Ring6, Ring7 and Ring8), 6 water molecules, and 4 non-stoichiometric water molecules were present. The result suggested the CI4 crystal was pentahydrate, which was consistent with the measured water content (13.9%). The two independent CI4 molecules in the asymmetric unit showed similar conformation (Figure 2-17 (a)). Torsion angles of α-(1→6)-glucosidic linkages (φ, ψ, ω) were in good agreement (Table 2-8), and the two molecules were overlaid well with an RMS value of 0.150 Å for the fitting on 44 atoms (carbon and oxygen) (Figure 2-17 (b)). In molecule 1, four glucosyl residues possess conformation of $^4C_1$ (Figure 2-17 (a)). In Figure 2-17 (a), Ring1, 4, 3 and 2 show α-, β-, β- and α- face, respectively. An intramolecular hydrogen bond was observed between Ring2-O4 (O124) and Ring4-O4 (O144) (Figure 2-16). The intramolecular hydrogen bond was observed in molecule 2. An intermolecular hydrogen bond between Ring4-O2 (O142) in molecule 1 and Ring6-O3 (O332) in molecule 2 was observed (Figure 2-16). Between β-face of Ring1 and β-face of Ring3, a cavity was observed (Figure 2-17 (c)). The distance between Ring1-O5 (O115) and Ring3-O5 (O135) was 3.1 Å and the one between Ring1-O3 (O113) and Ring3-O3 (O133) was 7.8 Å.

Table 2-7 X-ray data collection and refinement statistics of a CI4 crystal.

Empirical Formula	$C_{48}H_{100}O_{50}$
Formula Weight (g mol^{-1})	1480.53
Crystal size (mm)	0.200 × 0.180 × 0.140
Crystal color and shape	Colorless, transparent
Temperature (K)	100
Radiation (λ, Å)	0.71075
Crystal system	Orthorhombic
Space Group	$P222_1$
a (Å)	9.0682 (6)[1]
b (Å)	20.3935 (12)
c (Å)	35.781 (3)
α = β = γ (°)	90
V ($Å^3$)	6617.1 (8)
Z	4
d_{calcd} (g/cm^3)	1.486
R (int)	0.0481
No. of observations (all reflections)	15107
Reflection/Parameter Ratio	16.40
Final R indices (I>2.00σ(I))	0.0488
Final R indices (all data)	0.0552
Goodness of Fit	1.059

Crystallographic data for CI4 crystals are available in Cambridge Crystallographic Data Center (CCDC number 2003643). Numbers in the round brackets[1], standard deviations.

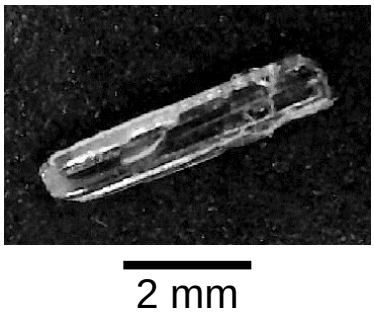

Figure 2-15 Picture of the CI4 single crystal.

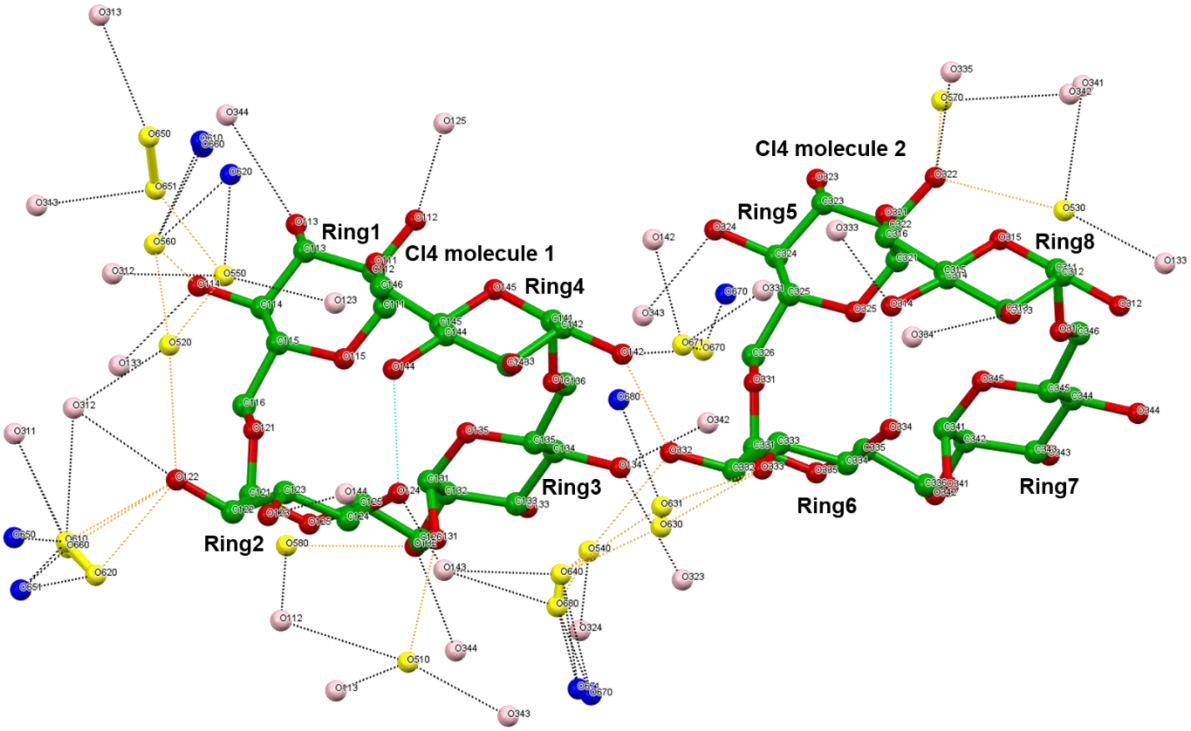

Figure 2-16 An asymmetric unit consisting of two CI4 molecules and water molecules in the CI4 crystal (CCDC deposition number 2003643).

Carbon atoms: green; oxygen atoms in CI4: red; oxygen atoms in CI4 in different asymmetric units: pink; oxygen atoms in water: yellow; oxygen atoms in water in different asymmetric units; blue. Intramolecular hydrogen bonds: cyan broken line; intermolecular hydrogen bonds within asymmetric unit: orange broken line; intermolecular hydrogen bonds with molecules in different asymmetric unit: black broken line.

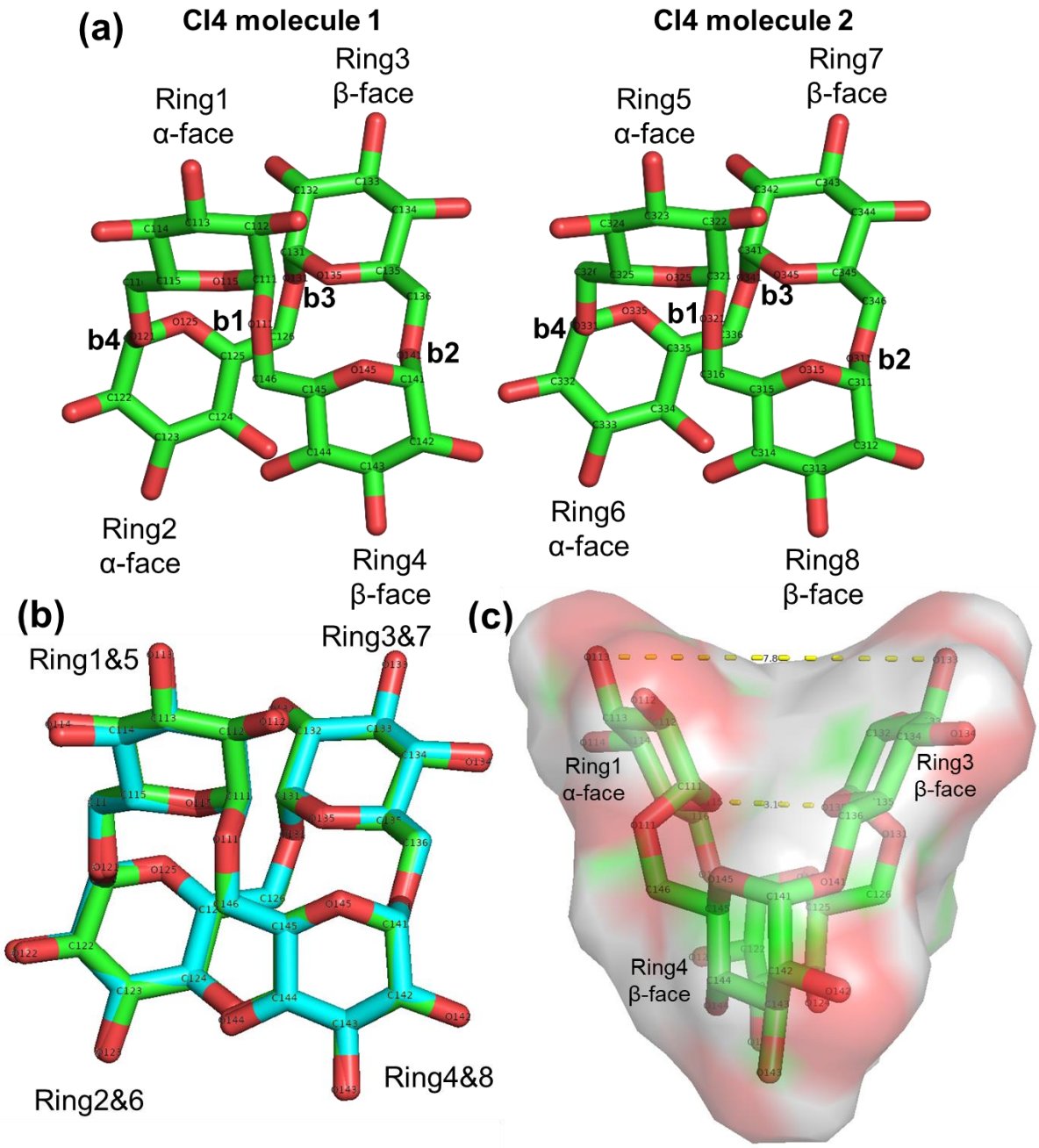

Figure 2-17 CI4 molecules in the asymmetric unit.

Carbon atoms: green and cyan; oxygen atoms: red. (a) CI4 molecule1 and molecule 2 in the asymmetric unit. (b) Comparison of two independent CI4 molecules. Two independent CI4 molecules in an asymmetric unit were fitted using Pymol ver 2.1.0. Fitting was performed on 44 atoms of carbon and oxygen atoms. (c) A cavity observed between β-face of Ring1 and β-face of Ring3.

Table 2-8 Torsion angles of glucosyl linkages in two CI4 molecules in an asymmetric unit.

		angles (°)			
	torsion angles	b1[1]	b2[2]	b3[3]	b4[4]
molecule 1	φ	56.0(3)[5]	78.2(3)	60.1(3)	82.5(3)
	ψ	51.8(3)	-152.3(2)	41.9(4)	-153.8(2)
	ω	47.7(3)	69.2(3)	51.6(4)	69.3(3)
molecule 2	φ	56.3(3)	80.5(3)	61.8(3)	77.5(3)
	ψ	52.7(3)	-150.8(2)	43.9(4)	-147.6(2)
	ω	45.4(3)	65.3(3)	52.6(4)	73.7(3)

Definitions of torsion angles are: O5-C1-O6'-C6' for φ, C1-O6'-C6'-C5' for ψ and O5'-C5'-C6'-O6' for ω. b1[1], a glycoside bond between Ring1 and Ring4 for molecule 1 and one between Ring5 and Ring8 for molecule 2 ; b2[2], a glycoside bond between Ring 4 and Ring 3 for molecule 1 and one between Ring8 and Ring7 for molecule 2; b3[3], glycoside bond between Ring 3 and Ring 2 and one between Ring7 and Ring6 for molecule 2; b4[4], glycoside bond between Ring 2 and Ring 1 and one between Ring6 and Ring5; numbers in the round brackets[5], standard deviations.

Digestibility test

The digestibility of CI4 was determined by AOAC2001.03 method. After the digestion using α-amylase, protease and amyloglucosidase, the amount of undigested CI4 was quantified by HPLC analysis. The analysis showed that 99.84% of CI4 was remained after the digestion. This result suggested that CI4 is an indigestible cyclic oligosaccharide for human.

Discussion

In this chapter, *Microbacteriaceae* strains, *Agreia* sp. D1110 and *M. trichothecenolyticum* D2006 were isolated using the gellan gum plate containing dextran as a sole carbon source, indicating these strains would assimilate dextran as carbon source. Different *Microbacteriaceae* strains, *Microbacterium hydrothermale* sp. nov., assimilates dextran and *Microbacterium dextranolyticum* IFO 14592 was reported to possess 1,6-α-isomaltotriosidase to produce IG3 from dextran (M. Kobayashi *et al*., 1983; Mitsuishi *et al*., 1979, 1980; Yokota *et al*., 1993; Zhang *et al*., 2014). These results suggest that some *Microbacteriaceae* bacteria have the ability to utilize dextran as a carbon source.

Agreia sp. D1110 and *M. trichothecenolyticum* D2006 were found to produce extracellular activity to produce CI4 from dextran. CI4, consisting of four glucosyl residues, is the smallest CI. Previously, CI7, which is synthesized with CI8 and CI9 by CITase, was the smallest CI. The CI4 was successfully crystalized and the CI4 single crystal was obtained. There have been no reports of CI crystals. The problems associated with crystallization of CIs whose DP is 7 or more seem to be due to the α-(1→6)-glucosidic linkages exhibiting higher flexibility than other glucosyl linkages (Pereira *et al*., 2006). Successful crystallization of CI4 is presumed to be due to its stable 3D structure, in which the intramolecular hydrogen bonds in CI4 molecules and the intermolecular hydrogen bonds between a CI4 and other molecules exist.

The digestibility of CI4 in the human gastrointestinal tract was also demonstrated in this chapter. CI4 would be used as a soluble dietary fiber and potentially contributes to the maintenance and promotion of intestinal health.

One of the issues to be resolved in developing CI4 as a commercial ingredient is the establishment of a mass production method. In the enzymatic reaction using the culture supernatant of *Agreia* sp. D1110, IG4 was increased as the enzymatic reaction progressed (Figure 2-11(a)). I assumed that production of IG4 is due to the hydrolysis of the CI4. The

culture supernatant of *M. trichothecenolyticum* D2006 showed lower production of IG4 than one of *Agreia* sp. D1110 (Table 2-4). Based on these results, the culture supernatant of *M. trichothecenolyticum* D2006 was used to prepare CI4 crystals. To increase the yield of CI4, ultrafiltration was exploited to separate CI4 from the reaction mixture. This separation method increased the yield compared to the single-batch reaction. Ultrafiltration membrane is widely used at production plants for a variety of purposes (Jönsson & Trägårdh, 1990), and is suitable for mass production of CI4.

The cost of starting materials is also an important consideration for industrial applications. Herein, dextran was used as a substrate to produce CI4. Dextran is industrially produced from purified sucrose (150 yen/kg) by the fermentation reaction using *Leuconostoc mesenteroides* (Naessens *et al*., 2005). In the fermentation reaction, dextran sucrase acts on sucrose and catalyze α-(1→6)-transglycosylation to produce dextran (Sidebotham, 1974). In this method, fructose residue is not used, and the conversion efficiency from sucrose does not exceed 50%. Theoretical cost of dextran exceeds 300 yen/kg. Alternatively, continuous α-(1→6)-glucosidic linkages can be formed from inexpensive starch using DDase or 6GT (Ichinose *et al*., 2017; Sadahiro *et al*., 2015; Tsusaki *et al*., 2009, 2012), and CIs can be produced from the α-(1→6)-linked substrates by CITase (Ichinose *et al*., 2017). The methods using these enzymes and starch have potential to produce α-(1→6)-glucan in yields of 50% or higher. Application of this method offers the possibility that CI4 may be able to be produced from inexpensive starch.

Chapter 3

Purification and characterization of cycloisomaltotetraose-forming enzymes from *Agreia* sp. D1110 and *Microbacterium trichothecenolyticum* D2006

Introduction

The culture supernatant of *Agreia* sp. D1110 and *M. trichothecenolyticum* D2006 possessed the CI4 production activity from dextran. In this chapter, the enzymes to produce CI4 from dextran (CI4-forming enzymes) were purified to homogeneity from the culture supernatant of *Agreia* sp. D1110 and *M. trichothecenolyticum* D2006 and their enzymatic properties were analyzed. For the practical production of CI4, isomaltooligosyl parts were formed at the non-reducing ends of starch using 6GT and then the CI4-forming enzyme from *M. trichothecenolyticum* D2006 acted on the isomaltooligosyl parts to produce CI4.

Materials and Methods

Saccharides

Partially hydrolyzed starch, Pinedex #4, was purchased from Matsutani Chemical Industry (Hyogo, Japan). Amylose EX-I (average DP = 17) was a product of Hayashibara (Okayama, Japan). IG2, IG3, IG4, isomaltopentaose (IG5), isomaltohexaose (IG6) and isomaltoheptaose (IG7) were purified from acid-hydrolysates of dextran T-40. Briefly, dextran T40 hydrolysates, prepared by the method described in chapter 2, were fractionized using three-tandemly connected Toyopearl HW-40S columns (Tosoh; Tokyo, Japan) (55 mm i.d. × 600 mm). Each fraction was further fractionized using a D-ODS-5 column (20 mm i.d. × 250 mm) purchased from YMC to prepare IG2, IG3, IG4, IG5, IG6 and IG7. CI4 crystal (Lot 1, 99.5%) prepared in chapter 2 was used for substrate specificity analysis and coupling reaction. Kojibiose, nigerose

and maltose were purchased from Fujifilm Wako Pure Chemical. CNN and CMM were synthesized in accordance with previously published methods (Mukai *et al*., 2005; Nishimoto *et al*., 2002)

Enzymes

α-Amylase from *Bacillus amyloliquefaciens* was purchased from Amano Enzyme. 6GT from *P. alginolyticus* and isoamylase (EC 3.2.1.68) from *Pseudomonas amyloderamosa* were prepared from the supernatant of the each culture broth (Harada *et al*., 1968; Tsusaki *et al*., 2012).

TLC analysis

AWPE, 2-propanol: 1-butanol: water = 12: 3: 4 (PBW) or 1-butanol: ethanol: water =4: 3: 3 (BEW) were used as developing solvents. For the separation, the developing solvent was ascended twice independently. Other conditions are same as described in chapter 2.

Culture of *Agreia* sp. D1110 and enzyme purification

Agreia sp. D1110 was cultured at 27°C on a rotary shaker for 66 h in a 500-mL Erlenmeyer flask containing 100 mL of medium (total 2.0 L) described in "Screening of enzymes derived from bacteria isolated from the soil" section in chapter 2. After removal of the cells by centrifugation at 23,800 ×*g* for 15 min, the supernatant of the culture broth was used for enzyme purification. The culture supernatant (1.8 L) was brought to 80% saturation by adding solid ammonium sulfate and incubated 4°C overnight. The resulting precipitate was collected by centrifugation at 23,800 ×*g* for 30 min and dissolved in 20 mM Tris-HCl buffer (pH 7.5). After dialysis overnight against 20 mM Tris-HCl buffer (pH 7.5), the enzyme solution was heated to 80°C for 30 min to deactivate and to remove contaminating enzymes. In the preliminary

experiments, it is confirmed that the CI4-forming enzyme from *Agreia* sp. D1110 showed activity to produce CI4. After removal of precipitants by centrifuge at 23,800 ×*g* for 10 min, the solution was put on a 24 mL (bed volume) DEAE-Toyopearl 650S (Tosoh) column equilibrated with 20 mM Tris-HCl buffer (pH 7.5) and attached on ÄKTA fast protein liquid chromatography (FPLC) system (Cytiva; Marlborough, MA, United States). Proteins adsorbed on the column were eluted with a linear gradient of 0 to 0.50 M NaCl in 20 mM Tris-HCl buffer (pH 7.5). The active fractions were pooled and brought to 1.0 M ammonium sulfate by adding solid ammonium sulfate. Using ÄKTA FPLC, the enzyme solution was then loaded onto an 11-mL (bed volume) Phenyl-Toyopearl 650M (Tosoh) column equilibrated with 20 mM Tris-HCl buffer (pH 7.5) containing 1.0 M ammonium sulfate. The adsorbed proteins were eluted with a linear gradient of 1.0 to 0 M ammonium sulfate in 20 mM Tris-HCl buffer (pH 7.5). The active fractions were pooled and dialyzed against 20 mM Tris-HCl (pH 7.5). The resulting enzyme solution was used as a purified preparation. The protein concentration of the purified preparation was 0.25 mg/mL (2.0 U/mL). The preparation was stored at 4℃.

Culture of *M. trichothecenolyticum* D2006 and enzyme purification

M. trichothecenolyticum D2006 was cultured at 27°C on a rotary shaker for 66 h in a 500 mL-Erlenmeyer flask containing 100 mL of the same medium (total 1.5 L) as that of the *Agreia* sp. D1110. After removal of the cells by centrifugation at 23,800 ×*g* for 15 min, the supernatant of the culture broth was used for enzyme purification. The culture supernatant (1.4 L) was brought to 80% saturation by adding solid ammonium sulfate and incubated at 4℃ overnight. The resulting precipitate was collected by centrifugation at 23,800 ×*g* for 30 min and dissolved in 20 mM Tris-HCl buffer (pH 7.5) containing 1.0 mM $CaCl_2$. After dialysis overnight against 20 mM Tris-HCl buffer (pH 7.5) containing 1.0 mM $CaCl_2$, the solution was put on a 20-mL (bed volume) DEAE-Toyopearl 650S column attached on ÄKTA FPLC and equilibrated with 20

mM Tris-HCl buffer (pH 7.5) containing 1.0 mM $CaCl_2$. Proteins adsorbed on the column were eluted with a linear gradient of 0 to 0.50 M NaCl in 20 mM Tris-HCl buffer (pH 7.5) containing 1.0 mM $CaCl_2$. The resultant solution was dialyzed using 20 mM Tris-HCl (pH 7.5) containing 1.0 mM $CaCl_2$, and the dialysate was put on a 1.0-mL MonoQ 5/50L column (GE Healthcare Japan, Tokyo, Japan) attached on ÄKTA FPLC and equilibrated with 20 mM Tris-HCl (pH 7.5) containing 1.0 mM $CaCl_2$. Proteins adsorbed on the column were eluted with a linear gradient of 0 to 0.50 M NaCl in 20 mM Tris-HCl (pH 7.5) containing 1.0 mM $CaCl_2$. The active fractions were dialyzed against 20 mM Tris-HCl (pH 7.5) and the resulting enzyme was used as a purified preparation. The protein concentration in the purified enzyme was 2.7 mg/mL (9.5 U/mL). The purified enzyme was stored at 4°C.

CI4-forming activity

The standard method to assay CI4-forming activity was as follows. The enzyme solution (0.10 mL) diluted with 20 mM sodium acetate buffer (pH 6.0) was added to substrate solution (0.90 mL) containing 11 mg/mL dextran T70 in 20 mM sodium acetate buffer (pH 6.0). The enzyme concentration in the reaction mixture ranged from 1.0 mU/mL to 32 mU/mL. Within this range, the initial velocity of the CI4-forming enzymes was measured in a 30-minute reaction. After incubation at 40°C for 0.5 and 30.5 min, the reaction mixture (0.30 mL) was dispensed and added to 10 mM $CuCl_2$ solution (0.030 mL) to stop the reaction. After mixing, the solution was immediately boiled at 100°C for 10 min. CI4 concentration was determined by HPLC whose columns were two-tandemly connected MCI GEL CK04SS columns under the same conditions as described in chapter 2. The concentration of produced CI4 was calculated by multiplying the peak area percentage (%) of produced CI4 to the initial concentration of dextran T70. One U of CI4-forming enzyme activity was defined as the amount of enzyme producing 1 μmol of CI4 per min under the stated conditions.

Dependency of CI4 production on protein concentration and reaction time

Dependency of CI4 production on protein concentration and reaction time in the assay system was analyzed to found the range of protein concentration and reaction times suitable for the determination of the initial velocity. For protein concentration dependency, reaction mixture (1.0 mL) containing 10 mg/mL dextran T70, 20 mM sodium acetate buffer (pH 6.0) and diluted purified enzyme derived from *M. trichothecenolyticum* D2006 (0.28, 0.56, 1.1, 2.2, 4.5, 9.0 μg/mL) was incubated at 40℃ for 0.5 and 30 min. For reaction time dependency, reaction mixture (3.0 mL) containing 10 mg/mL dextran T70, 20 mM sodium acetate buffer (pH 6.0) and 3.4 μg/mL purified enzyme derived from *M. trichothecenolyticum* D2006 were incubated at 40℃ for 0.5, 10.5, 20.5, 30.5 and 40.5 min. CI4 concentration was determined in the standard method.

Effects of pH on the activity of the CI4-forming enzymes

The purified preparations were diluted using 20 mM sodium acetate buffer (pH 6.0). Reaction mixture (1.2 mL) containing 10 mg/mL dextran T70, 50 mM Britton-Robinson buffer (pH 2.0-10.0), the CI4-forming enzyme (one from D1110; 0.83 μg/mL, 6.7 mU/mL or one from D2006; 3.1 μg/mL, 11 mU/mL) and 2 mM sodium acetate buffer (pH 6.0) were incubated at 40℃. After incubation for 0.5 and 30.5 min, CI4 concentration was determined as described in the standard method.

Effects of temperature on the activity of the CI4-forming enzymes

The purified preparations were diluted using 20 mM sodium acetate buffer (pH 6.0). Reaction mixture (1.0 mL) containing 10 mg/mL dextran T70, 20 mM sodium acetate buffer (pH 6.0) and the CI4-forming enzyme (one from D1110; 1.3 μg/mL, 10 mU/mL or one from D2006; 3.1 μg/mL, 11 mU/mL) were incubated at 30, 35, 40, 45, 50, 55, 60 or 65℃. After incubation for

0.5 and 30.5 min, CI4 concentration was determined as described in the standard method. All measurements were performed once.

Effects of pH on the stability of the CI4-forming enzymes

Mixtures containing the CI4-forming enzyme (one from D1110; 25 μg/mL, 200 mU/mL or one from D2006; 67 μg/mL, 240 mU/mL) and 20 mM Britton-Robinson buffer (pH 2.0-12.0) were incubated at 4℃ for 18 h. After the incubation, the same volume of 500 mM sodium acetate buffer (pH 6.0) was added to adjust pH 6.0. Remaining activities were assayed in the standard method, but using the reaction mixture containing the CI4-forming enzyme (one from D1110; 1.3 μg/mL, 10 mU/mL or one from D2006; 3.3 μg/mL, 12 mU/mL), 25 mM sodium acetate buffer (pH 6.0) and 1.0 mM Britton-Robinson buffer (pH 2.0-12.0). All measurements were performed once.

Effects of temperature on the stability of the CI4-forming enzymes

The purified preparations were diluted using 20 mM sodium acetate buffer (pH 6.0). The purified enzymes solution containing 20 mM sodium acetate buffer (pH 6.0) and the CI4-forming enzyme (one from D1110; 12.5 μg/mL, 100 mU/mL or one from D2006; 36 μg/mL, 130 mU/mL) were incubated at 30, 35, 40, 45, 50, 55, 60, 65 or 70℃ for 30 min in the absence of the substrate and then immediately cooled. After stored at 4℃ and overnight, remaining activity was measured in the standard method, but using the reaction mixture containing the CI4-forming enzyme (one from D1110; 1.3 μg/mL, 10 mU/mL or one from D2006; 3.6 μg/mL, 13 mU/mL). All measurements were performed once.

Effects of metal ions on the activity of the CI4-forming enzymes

Enzyme activity was measured in the standard assay method but using reaction mixture containing the CI4-forming enzyme (one from D1110; 0.83 μg/mL, 6.7 mU/mL or one from D2006; 3.3 μg/mL, 12 mU/mL) and 1.0 mM metal salts. As metal salts, 1.0 mM $AlCl_3$, $BaCl_2$, $CaCl_2$, $CoCl_2$, $CuCl_2$, $FeCl_2$, $FeCl_3$, $HgCl_2$, KCl, LiCl, $MgCl_2$, $MnCl_2$, NaCl, $NiCl_2$, $PbCl_2$, RbCl, $SnCl_2$, $SrCl_2$ or $ZnCl_2$ were tested. All measurements were performed once.

Determination of protein concentration

Protein concentration was determined by the Bradford method using bovine serum albumin in Bio-Rad Protein Assay Standard II (Bio-Rad Laboratories, Hercules, CA, United States) and Bio-Rad Protein Assay Dye Reagent Concentrates (Bio-Rad).

SDS-PAGE analysis

The molecular weight of the enzyme was estimated by SDS-PAGE performed on an 8 to 16% gradient gel purchased from Cosmo Bio (Tokyo, Japan). The protein was stained by CBB-R250. The molecular weight marker was purchased from Bio-Rad. For the purified enzymes derived from *Agreia* sp. D1110 and *M. trichothecenolyticum* D2006, 1.3 and 1.4 μg-protein were applied on the gel, respectively.

N-terminal amino acid sequence analysis

The purified enzymes were separated using SDS-PAGE under the same condition as described above. After the separation, the enzymes were blotted on Immobilon-FL PVDF membrane (Merck) using an electroblotting method. In the blotting, buffer containing 10 mM *N*-cyclohexyl-3-aminopropanesulfonic acid (CAPS, Fujifilm)-NaOH buffer (pH 11) and 10% (v/v) methanol was used, and electroblotting was performed at 50 V for 90 min in a semidry

blotting apparatus. The blotted membrane was stained using a solution containing 0.10% (w/v) amido black 10B (Fujifilm), 40% (v/v) methanol and 1.0% (v/v) acetic acid. After washed with 50% (v/v) methanol and distilled water, the membrane was dried. The band stained by amido black 10B was applied to the N-terminal amino acid sequence analysis with a PPSQ-31A protein sequencer (Shimadzu) using the Edman degradation method.

Analysis of products in the reaction using the CI4-forming enzymes and various substrates

A reaction mixture (30 μL) containing 10 mg/mL substrates, 50 mM sodium acetate buffer (pH 6.0) and 20 or 200 mU/mL of CI4-forming enzyme from *Agreia* sp. D1110 or *M. trichothecenolyticum* D2006 was incubated at 40°C for 24 h. The reaction products were analyzed by TLC.

Coupling reaction between CI4 and acceptor molecules

A reaction mixture (1.0 mL) containing 15.4 mM CI4, 20 mM sodium acetate buffer (pH 6.0) and 10 mU/mL of the CI4-forming enzymes derived from *Agreia* sp. D1110 or *M. trichothecenolyticum* D2006 was incubated at 40°C for 60 min in the presence or absence of acceptor molecules. As the acceptor molecules, 100 mM Glc and 100 mM IG2 were used. After boiling the sample for 15 min to stop the reaction, the saccharide composition of the sample was analyzed by HPLC using two-tandemly connected MCI GEL CK04SS columns under the same conditions as described in chapter 2.

Reaction time dependency of the amount of CI4 in 8, 24, 48 or 72 h-reactions

Reaction mixtures (1.7 mL) containing 10 mg/mL dextran T70, 22 mU/mL CI4-forming enzymes derived from *Agreia* sp. D1110 or *M. trichothecenolyticum* D2006, 50 mM sodium acetate buffer (pH 6.0) and 1.0 mM $CaCl_2$ were incubated at 40℃. At 8, 24, 48 and 72 h, 400 μL of each reaction mixture was dispensed and boiled for 10 min to stop the reaction. Each boiled sample was analyzed in HPLC using two-tandemly connected MCI GEL CK04SS columns as described in chapter 2.

Preparation of starch-derived substrates

A reaction mixture (1.0 L) containing 300 g/L liquified starch (DE 3.2), 20 mM sodium acetate buffer (pH 5.5), 1.0 mM $CaCl_2$, 0.0060% (w/v) hinokitiol, 3.0 U/mL of 6GT, 750 U/mL of isoamylase and 3.0 U/mL of α-amylase from *Bacillus amyloliquefaciens* was incubated at 50°C for 72 h. After boiling the sample for 10 min to stop the reaction, the enzymatic reaction products were purified and condensed as follows: The activated carbon 1.0 g was added to the reaction mixture (0.8 L) and incubated at 50℃ for 18 h. The mixture was filtered using the diatomite. The filtered solution was desalted using SK1B, WA30 and IRA-411 resins. Desalted solution passed through the activated carbon again and was filtered using 0.22 μm filter CCS-020-E1HR (Advantec, Tokyo, Japan). Filtered solution was condensed to Brix 72.9% using the rotary evaporator. Brix 72.9% was set at 729 mg/mL. The solution was used as starch-derived substrates for the CI4-forming enzyme.

Production of CI4 from starch-derived substrates

Reaction mixtures containing 10 mg/mL starch-derived substrates, 100 mM sodium acetate buffer (pH 6.0), 1.0 mM $CaCl_2$ and 22 mU/mL CI4-forming enzyme derived from *M. trichothecenolyticum* D2006 were incubated at 40℃ for 24 and 72 h, and boiled at 10 min. The

saccharide compositions of the samples with and without digestion by α-glucosidase and glucoamylase were analyzed using HPLC as described in chapter 2. The digestion using α-glucosidase and glucoamylase were performed under the condition as described in chapter 2.

Methylation analysis

Each sample (5.0 mg) was methylated according to the method reported by Ciucanu and Kerek (Ciucanu & Kerek, 1984), and the products were isolated by partitioning between $CHCl_3$ and water. The methylated samples were hydrolyzed in acid, reduced with $NaBH_4$, and acetylated (Hakomori, 1964). The resulting partially methylated alditol acetates were separated by gas liquid chromatography (GLC) (GC-14B; Shimadzu) on a silica gel capillary column (DB-5; 0.25 mm × 30 m; J&W Science, Folsom, CA, United States), with a temperature program of 130 °C for 2 min followed by a 5 °C/min gradient up to 250 °C. Standards used were 2,3,4,6-tetra-*O*-methyl-1-*O*-acetyl-D-glucopyranoside, 3,4,6-tri-*O*-methyl-1,2-di-*O*-acetyl-D-glucopyranoside, 2,4,6-tri-*O*-methyl-1,3-di-*O*-acetyl-D-glucopyranoside, 2,3,6-tri-*O*-methyl-1,4-di-*O*-acetyl-D-glucopyranoside, 2,3,4-tri-*O*-methyl-1,6-di-*O*-acetyl-D-glucopyranoside, 2,3-di-*O*-methyl-1,4,6-tri-*O*-acetyl-D-glucopyranoside and 2,4-di-*O*-methyl-1,3,6-tri-*O*-acetyl-D-glucopyranoside. The standards are prepared from kojibiose, nigerose, maltose, CMM and CNN using the same methods shown in this section.

Results

Purification of the CI4-forming enzymes from *Agreia* sp. D1110 and *M. trichothecenolyticum* D2006

The CI4-forming enzymes were purified from the culture supernatant of *Agreia* sp. D1110 and *M. trichothecenolyticum* D2006 through precipitation with 80%-saturation ammonium sulfate and DEAE Toyopearl 650S column chromatography, followed by Phenyl Toyopearl 650M for the enzyme from D1110 strain and anion-exchange chromatography on MonoQ column for the other enzyme from D2006 strain. The purifications are summarized in Table 3-1. SDS-PAGE analysis showed that the purified preparations contained a single protein of molecular weight 86,000 for both (Figure 3-1). Therefore, the 86-kDa proteins were considered to be the enzyme showing CI4-forming activity. The CI4-forming enzymes were named as cycloisomaltotetraose glucanotransferase whose abbreviation is CI4Tase. The CI4Tase derived from *M. trichothecenolyticum* D2006 and the CI4Tase derived from *Agreia* sp. D1110 are abbreviated as MtCI4Tase and AgCI4Tase, respectively.

The AgCI4Tase (2.5 mg, 20 U) was purified from the culture supernatant (1.8 L). The enzyme was purified with an 18-fold purification index, and yield of 10%. The specific activity of the AgCI4Tase was 8.1 U/mg. The N-terminal amino acid sequence of the AgCI4Tase was ATVGDAWTD.

The MtCI4Tase (3.0 mg, 11 U) was purified from the culture supernatant (1.4 L). The enzyme was purified with a 14-fold purification index, and yield of 11%. The specific activity of the MtCI4Tase was 3.6 U/mg. The N-terminal amino acid sequence of the MtCI4Tase was ADLGDAWTD.

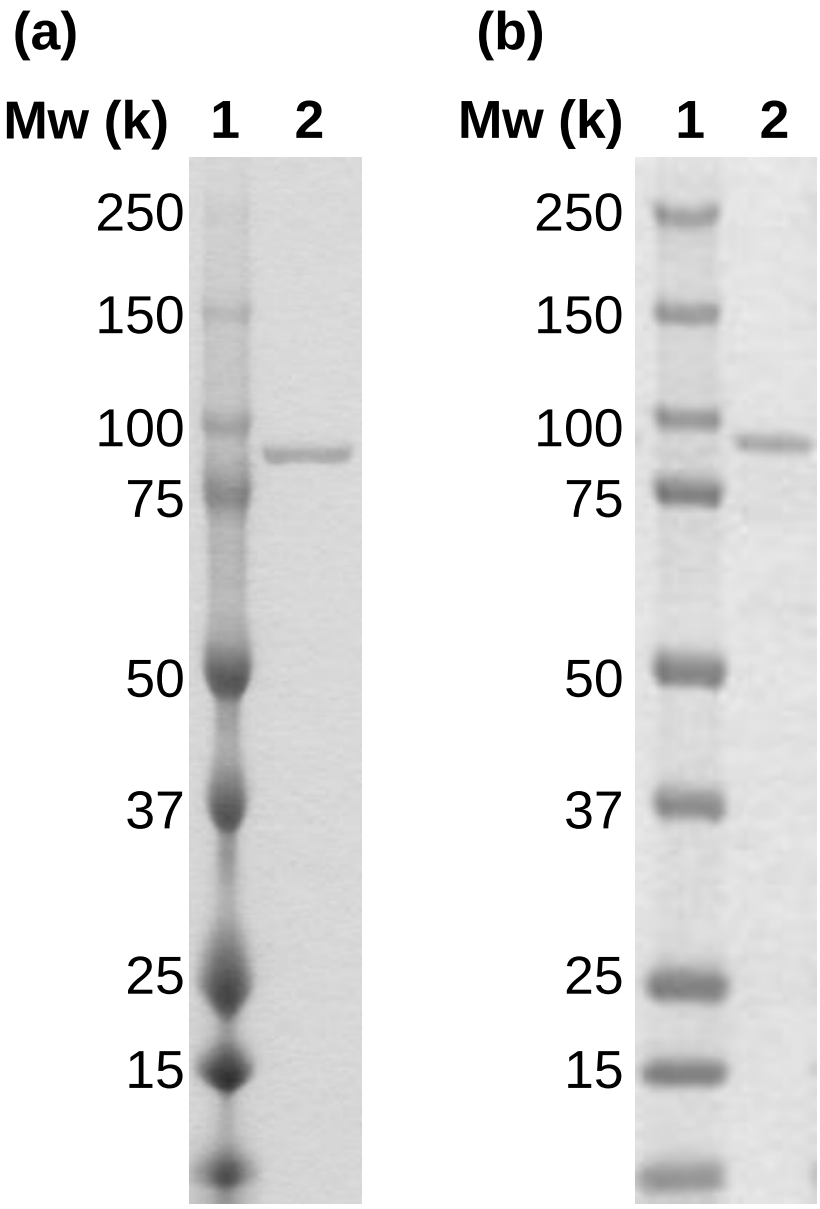

Figure 3-1 SDS-PAGE of the AgCI4Tase and MtCI4Tase.

Mw, Molecular weights of the standards; Lane 1, molecular weight markers; Lane 2, the purified CI4Tase. (a) the AgCI4Tase (1.3 μg-protein/lane). (b) the MtCI4Tase (1.4 μg-protein/lane).

Table 3-1 (a) Purification of the AgCI4Tase.

Step	Volume (mL)	Total protein (mg)	Total activity (U)	Specific activity (U/mg)	Purification index (fold)	Yield (%)
Culture supernatant	1800	440	200	0.46	1	100
80% saturation-ammonium sulfate precipitation and dialysis	153	260	33	0.13	0.28	17
DEAE-Toyopearl	37.5	25	22	0.88	1.9	11
Phenyl-Toyopearl	10	2.5	20	8.1	18	10

Table 3-1 (b) Purification of the MtCI4Tase.

Step	Volume (mL)	Total protein (mg)	Total activity (U)	Specific activity (U/mg)	Purification index (fold)	Yield (%)
Culture supernatant	1400	390	97	0.25	1.0	100
80% saturation-ammonium sulfate precipitation and dialysis	110	140	140	0.98	3.9	150
DEAE-Toyopearl	28	32	50	1.6	6.3	52
MonoQ	1.1	3.0	11	3.6	14	11

Dependency of CI4 production on protein concentration and reaction time

The CI4 production reaction was done for 30 min in the standard conditions for activity assay with 0.28–9.0 μg/mL MtCI4Tase, and CI4 produced was quantified (Figure 3-2(a), Table 3-2(a)). At lower protein concentrations such as 0.28, 0.56 μg/mL MtCI4Tase, the measured concentration of produced CI4 deviated significantly from the approximate curve. At higher protein concentration such as 2.2, 4.5 and 9.0 μg/mL MtCI4Tase, the difference between the approximate curve and the measured value was smaller. When the reaction was done for 40.5 min with 3.4 μg/mL MtCI4Tase, a proportional relationship was observed between the increase in CI4 concentration and reaction time (Figure 3-2(b), Table 3-2(b)).

On the basis of these results, the conditions of the assay system were determined as follows: Reaction time is 30 min, and the concentration of CI4 produced ranges from 39 to 540 μM. Since the velocity of the CI4 production (μmol/min/μg-protein) was almost constant at 10, 20, 30 and 40 min under the determined conditions, it was suggested that initial velocity of the CI4Tases can be measured under the determined conditions.

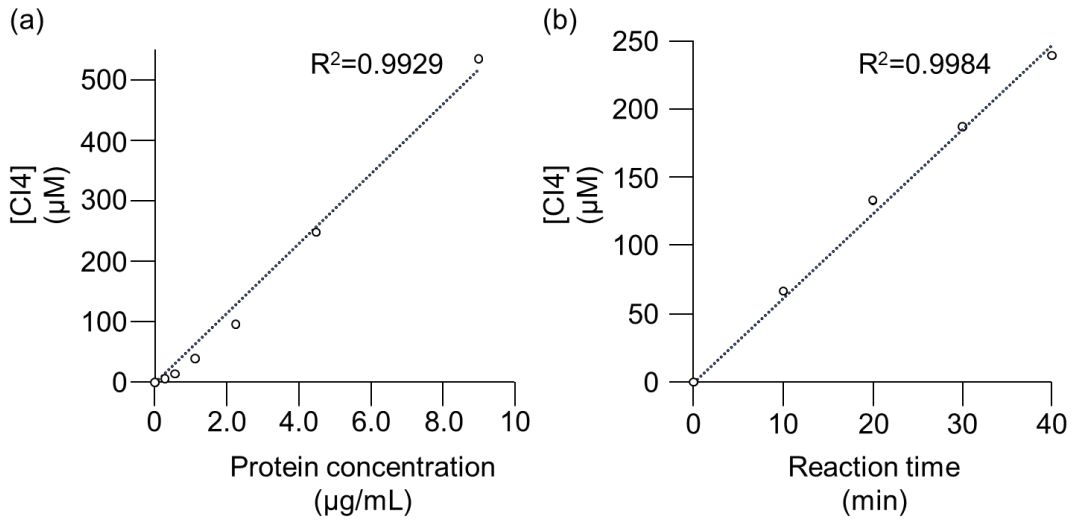

Figure 3-2 Effects of MtCI4Tase concentration and reaction time on CI4 production.

(a) CI4 production in 30-min reactions with 0.28–9.0 μg/mL MtCI4Tase, (b) time course of CI4 production with 3.4 μg/mL MtCI4Tase.

Table 3-2 (a) Effects of MtCI4Tase concentration on CI4 production.

Protein concentration (μg-protein/mL)	CI4-peak area percentage (%)	Produced CI4 (μmol)	Concentration of CI4 produced (μM)	Velocity (μmol/min/μg-protein)
0	0	0	0.0	0
0.28	0.036	0.0056	5.6	0.66
0.56	0.089	0.014	14	0.82
1.1	0.25	0.039	39	1.2
2.2	0.62	0.096	96	1.4
4.5	1.6	0.25	250	1.8
9.0	3.5	0.54	540	2.0

Table 3-2 (b) Effects of reaction time on CI4 production.

Reaction time[1] (min)	CI4-peak area percentage[2] (%)	Produced CI4 (μmol)	Concentration of CI4 produced (μM)	Velocity (μmol/min/μg-protein)
0	0	0	0	0
10	0.43	0.067	67	2.0
20	0.86	0.13	130	2.0
30	1.2	0.19	190	1.8
40	1.5	0.24	240	1.8

Reaction time[1], Reaction was stopped at 0.5, 10.5, 20.5, 30.5 and 40.5 min. CI4-peak area percentage[2], CI4-peak area percentage at each reaction time was subtracted from the CI4-peak area percentage at 0.5 min.

Enzymatic properties of the CI4Tases from two strains

The enzymatic properties of both purified CI4Tases were analyzed. The effects of pH on the activity are shown in Figure 3-3(a). The highest activity was obtained at pH 5.6-6.2 in AgCI4Tase and pH 5.7 in MtCI4Tase (Figure 3-3(a)).

The pH stability of the CI4Tases is shown in Figure 3-3(b). After kept at 4℃ for 18 h, 80% or higher residual activity was observed in the pH 4.6–9.9 in AgCI4Tase (Figure 3-3(b), circles) and in the pH 5.0–6.9 in MtCI4Tase (Figure 3-3(b), triangles). MtCI4Tase was less stable than the AgCI4Tase under basic pH conditions.

The effects of temperature on the activity of the CI4Tases in the standard assay conditions are shown in Figure 3-4(a). The CI4Tases derived from both bacterial strains showed the highest activity at 40°C.

The effects of temperature on the stability of the CI4Tases are shown in Figure 3-4(b). The enzymes were kept at various temperatures for 30 min, followed by 4℃, overnight, and remaining activities were measured. AgCI4Tase showed residual activity >80% under 40°C. As the incubation temperature increased, the residual activity decreased, but even after 30 min at 70°C, 40% activity still remained. MtCI4Tase showed residual activity >80% under 35°C. MtCI4Tase was found to be more susceptible to heat than AgCI4Tase.

Effects of 1.0 mM metal ions on the activity of the CI4Tases are shown in Table 3-3. The activity of AgCI4Tase and MtCI4Tase was significantly decreased by Al^{3+}, Cu^{2+}, Fe^{2+}, Fe^{3+}, Hg^{2+} and Pb^{2+} to less than 35% of their original activity. In addition, EDTA decreased MtCI4Tase activity to 26%, and Zn^{2+} inhibited AgCI4Tase to 29%. On the other hand, the activities were enhanced in the presence of Co^{2+}, Mg^{2+}, Mn^{2+}, and Ni^{2+} to 140–160%. Ca^{2+} ion increased MtCI4Tase activity to 130%.

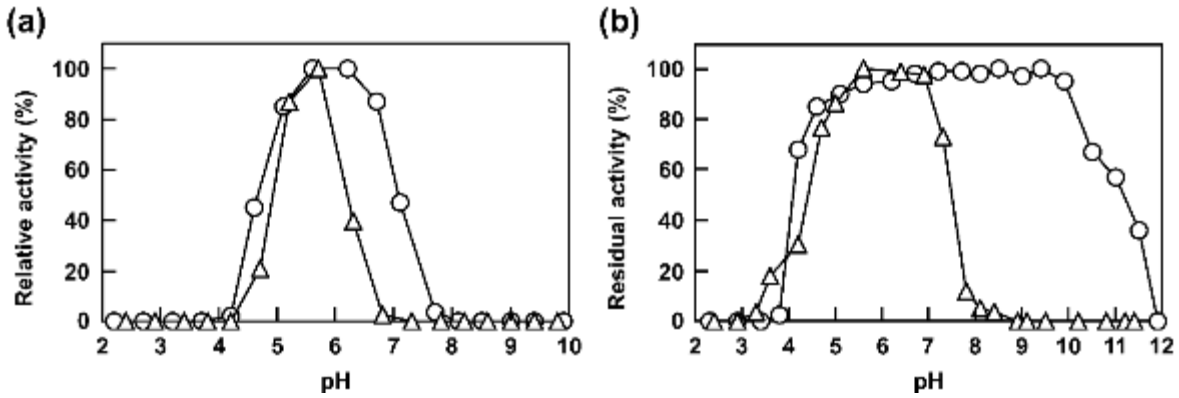

Figure 3-3 Effects of pH on the activity and the stability of the CI4Tases.

Circle, AgCI4Tase; triangle, MtCI4Tase. (a) Effects of pH on the activity of the CI4Tases. (b) Effects of pH on the stability of the CI4Tases. Remaining activities after kept at each pH at 4°C for 18 h are shown. All measurements were performed once.

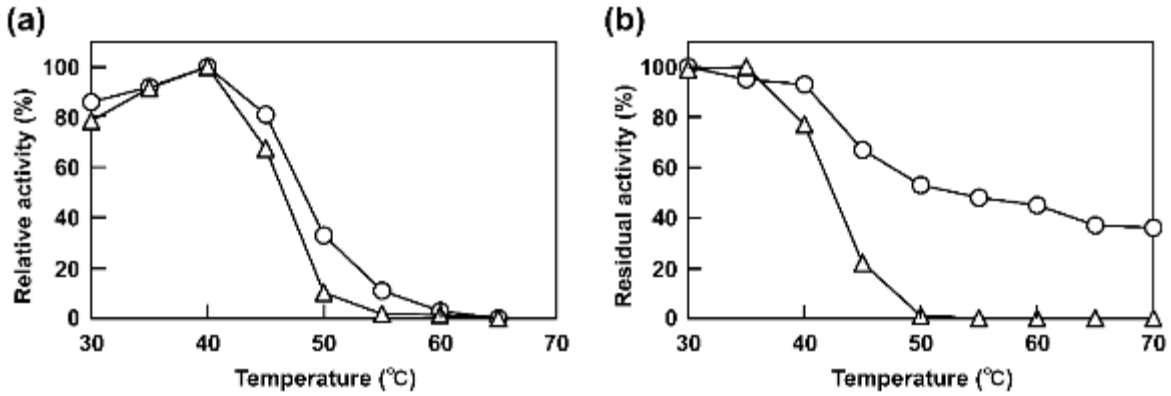

Figure 3-4 Effects of temperature on the activity and the stability of the CI4Tases.

Circle, AgCI4Tase; triangle, MtCI4Tase. (a) Effects of temperature on the activity of the CI4Tases. (b) Effects of temperature on the stability of the CI4Tases. Remaining activities after kept at each temperature at pH 6.0 for 30 min, followed by 4℃, overnight are shown. All measurements were performed once.

Table 3-3 Effects of metal ions on the activities of the CI4Tases.

	Relative activity (%)	
Metal salts	AgCI4Tase	MtCI4Tase
None	100	100
$AlCl_3$	2.5	N.D.[1]
$BaCl_2$	100	93
$CaCl_2$	110	130
$CoCl_2$	160	140
$CuCl_2$	N.D.	N.D.
$FeCl_2$	16	35
$FeCl_3$	0.20	N.D.
$HgCl_2$	N.D.	N.D.
KCl	100	96
LiCl	100	100
$MgCl_2$	140	140
$MnCl_2$	150	150
NaCl	110	100
$NiCl_2$	150	140
$PbCl_2$	4.5	N.D.
RbCl	100	100
$SnCl_2$	85	74
$SrCl_2$	94	99
$ZnCl_2$	29	85
EDTA	88	26

N.D.[1], Not detected. Concentration of all salts was 1.0 mM. All relative activities were calculated based on the enzymatic activity in the absence of metal salts. All measurements were performed once.

Analysis of products in the reaction using the CI4Tases and various substrates

The reaction products of AgCI4Tase and MtCI4Tase on various substrates were analyzed by TLC (Figure 3-5, 3-6 and 3-7). AgCI4Tase and MtCI4Tase produced predominantly CI4 and small amount of IG4 from dextran T10 (Figure 3-5). No reaction product was observed in the two CI4Tases reaction on Glc, IG2, IG3 (Figure 3-6). When 20 mU/mL AgCI4Tase or MtCI4Tase acted on IG4, no reaction product was observed, but with 200 mU/mL AgCI4Tase or MtCI4Tase, IG2, IG3, IG5 and IG8 were produced from IG4 (Figure 3-6). AgCI4Tase or MtCI4Tase (20 mU/mL) predominantly produced IG2, IG4, IG8 and IG9 from IG5. Also, IG2 to IG9 and Glc were produced from IG5 with 200 mU/mL of the enzymes (Figure 3-6). CI4 was also detected in the reactions. From IG6, 20 mU/mL of AgCI4Tase or MtCI4Tase predominantly produced CI4 and IG2. From IG7, 20 mU/mL of AgCI4Tase or MtCI4Tase predominantly produced CI4 and IG3.

These results indicate that AgCI4Tase and MtCI4Tase catalyzed intramolecular α-(1→6)-transglycosylation (cyclization) to produce CI4 from isomaltooligosaccharides with DP ≥5. Comparison of the residual amount of substrate in the reaction with 20 mU/mL of AgCI4Tase or MtCI4Tase suggested that IG7 and IG6 are more suitable substrates for CI4Tase than IG5. AgCI4Tase and MtCI4Tase mainly produced IG9 from IG5 and produced IG10 from IG6 (Figure 3-6). These results suggest that AgCI4Tase and MtCI4Tase mainly catalyzed intermolecular α-(1→6)-transglycosylation of IG4 units. AgCI4Tase and MtCI4Tase (20 mU/mL) produced IG2, IG3 and IG8 from IG5 and not produced Glc from IG5, suggesting that the CI4Tases weakly catalyze intermolecular α-(1→6)-transglycosylation of IG3 unit. AgCI4Tase and MtCI4Tase (200 mU/mL) produced IG4 from CI4 (Figure 3-6) and 20 mU/mL AgCI4Tase and MtCI4Tase produced IG8 from CI4. These results indicate that the enzymes catalyzed hydrolysis of CI4. The mechanism for IG8 production from CI4 is proposed as follows: 1) The CI4Tases hydrolyzed CI4 into IG4, and 2) The CI4Tases catalyzed

intermolecular α-(1→6)-transglycosylation (coupling reaction) between produced IG4 (acceptor) and CI4 (donor). AgCI4Tase and MtCI4Tase did not act on pinedex#1, pinedex#4, amylose, CNN or CMM (Figure 3-7).

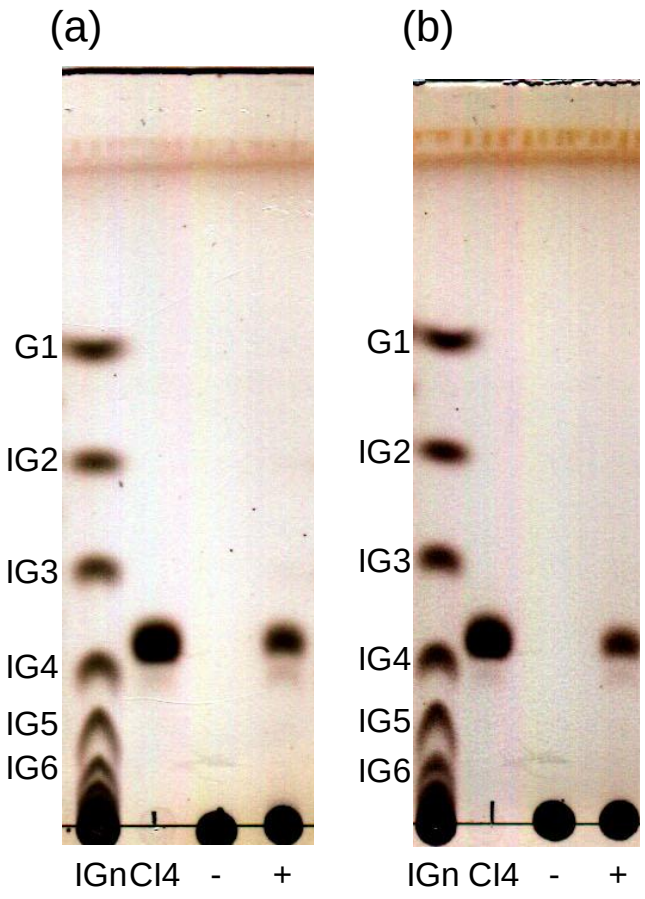

Figure 3-5 TLC analysis of reaction products from dextran T10 by the two CI4Tases.

(a) AgCI4Tase, (b) MtCI4Tase. IGn, standards containing glucose (G1) and isomaltooligosaccharides from isomaltose (IG2) to isomaltohexaose (IG6). - +, reaction for 24 h on 10 mg/mL dextran with CIT4Tase (0 and 20 mU/mL), respectively. The developing solvent, 2-propanol:1-butanol:water = 12:3:4 (v/v, PBW).

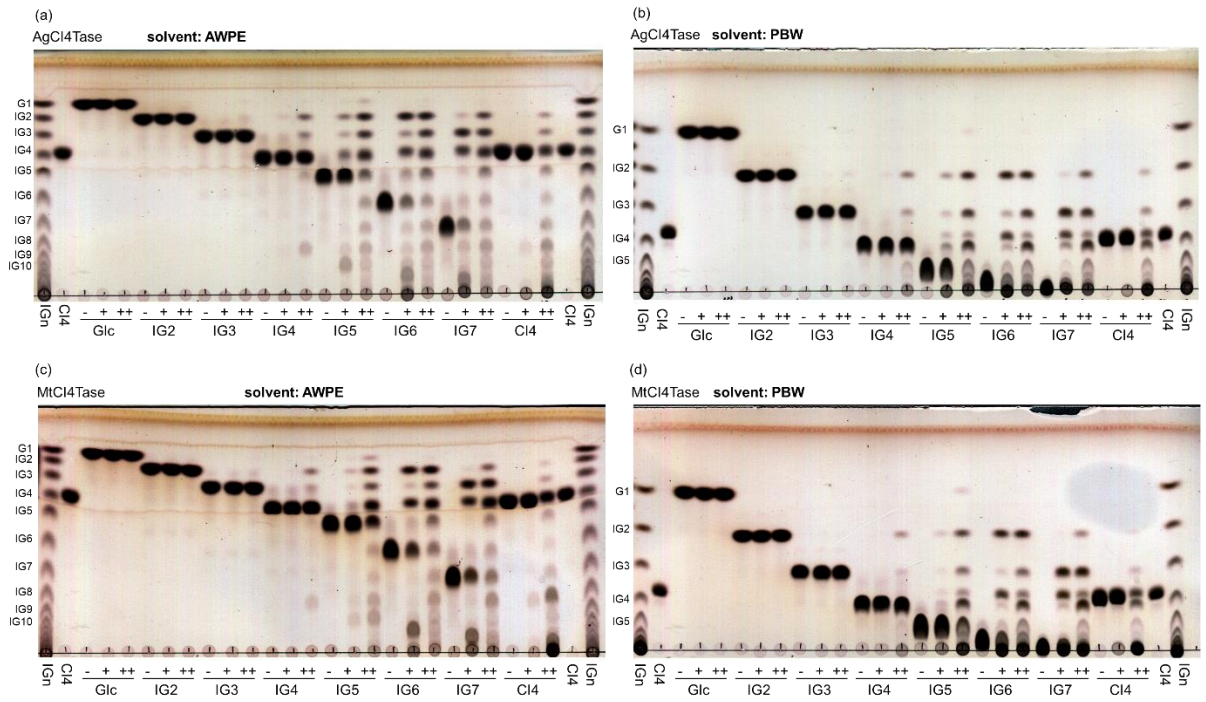

Figure 3-6 TLC analysis of reaction products from isomaltooligosaccharides by the two CI4Tases.

(a) and (b) AgCI4Tase; (c) and (d) MtCI4Tase. −, +, ++, reaction for 24 h on 10 mg/mL substrate (Glc–CI4) with CI4Tase (0, 20, and 200 mU/mL), respectively. IGn and CI4, the same as in Figure 3-5, but to isomaltodecaose (IG10). The developing solvents are acetonitrile:water:1-propanol:ethyl acetate = 85:70:50:20 (v/v, AWPE) or 2-propanol:1-butanol:water = 12:3:4 (v/v, PBW).

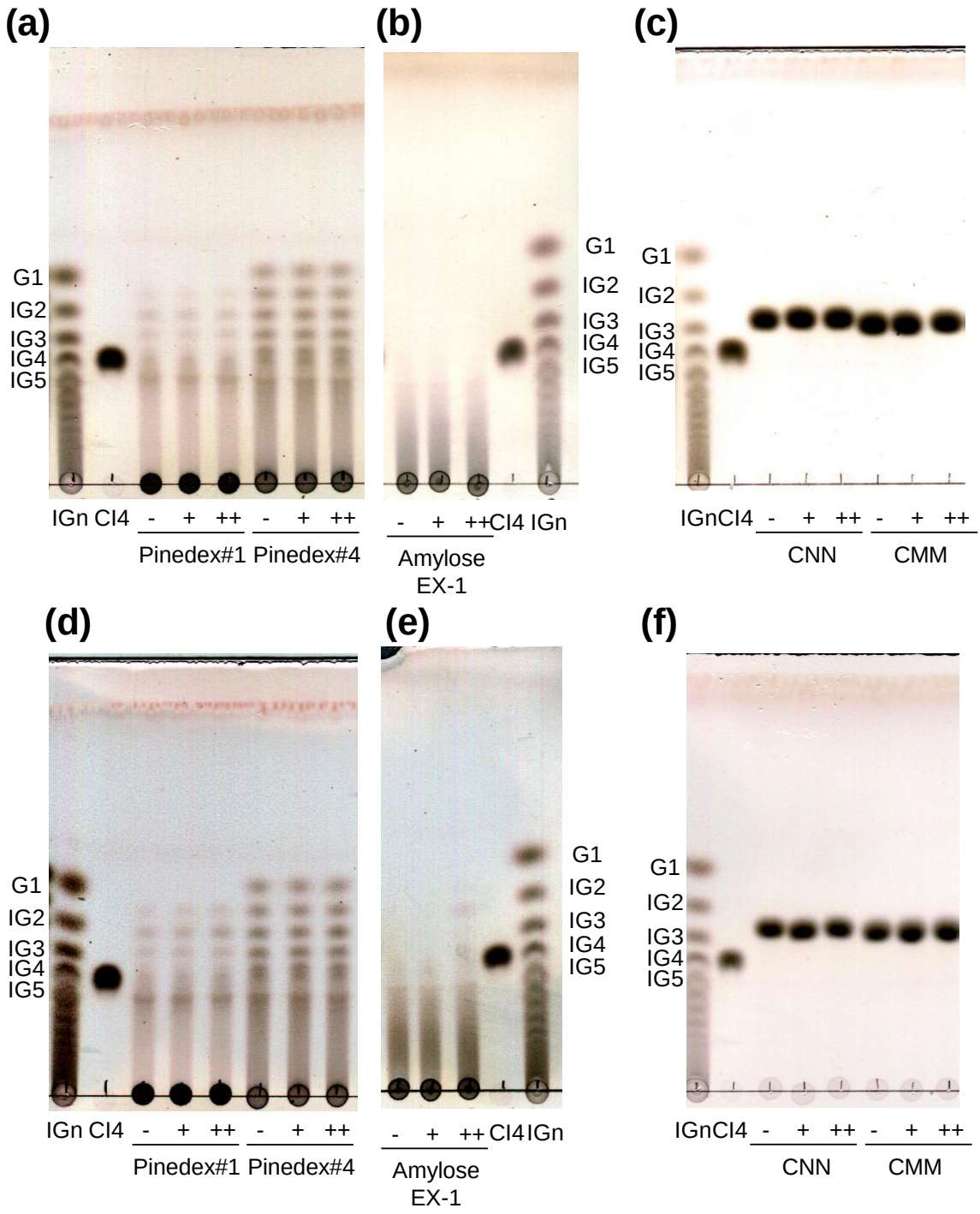

Figure 3-7 Substrates that the CI4Tases did not act on.

The abbreviations and symbols are same as Figure 3-6. Solvent is 1-butanol: ethanol: water =4: 3: 3. (a), (b) and (c) The AgCI4Tase. (d), (e) and (f) The MtCI4Tase.

Coupling reaction catalyzed by AgCI4Tase and MtCI4Tase

The CI4Tases (10 mU/mL) were reacted with 15.4 mM CI4 with 100 mM Glc and IG2. Products at 5 and 60 min of the reactions were analyzed by HPLC (Figure 3-8). In the reaction of CI4 alone and with Glc, no product was detected under the analytical conditions (Figure 3-8(a), (b), (d) and (e)). From CI4 and IG2, only IG6 was detected and increased for 60 min (Figure 3-8 (c) and (f)). These results suggest that AgCI4Tase and MtCI4Tase use IG2 as acceptor in their coupling reactions, but not D-Glc.

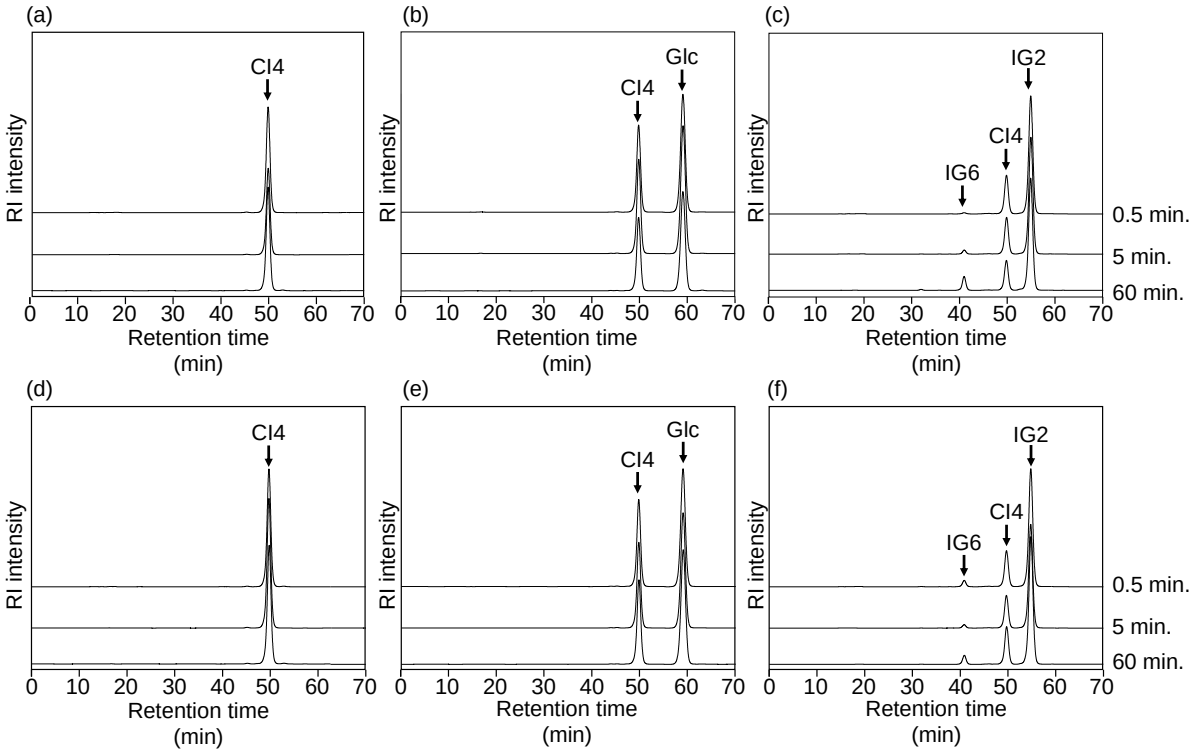

Figure 3-8 Coupling reaction between CI4 and acceptor molecules.

CI4Tase (10 mU/mL) were incubated with 15.4 mM CI4 only (a,d) and with 100 mM Glc (b,d). and 100 mM IG2 (c,f) for 0.5, 5, and 60 min. (a-c) AgCI4Tase, (d-f) MtCI4Tase. Products were analyzed by HPLC.

Reaction time dependency of the amount of CI4 in 8, 24, 48 or 72 h-reactions

AgCI4Tase and MtCI4Tase was reacted with dextran, and the time-dependent change in products was analyzed (Figures 3-9, 3-10, Table 3-4). With the progression of both the reaction, dextran decreased. CI4 was the most predominant product, but its composition was highest at 8 h for AgCI4Tase (19%) and 24 h for MtCI4Tase (14%) and gradually decreased to 12-13% as the reactions progressed (Figure 3-10, Table 3-4). Meanwhile, short oligosaccharides, particularly IG4, IG8 and IG12 were increased. The tendency of sugar composition of CI4, IG4, IG8 and IG12 in the reaction using MtCI4Tase was similar to one of AgCI4Tase (Table 3-4).

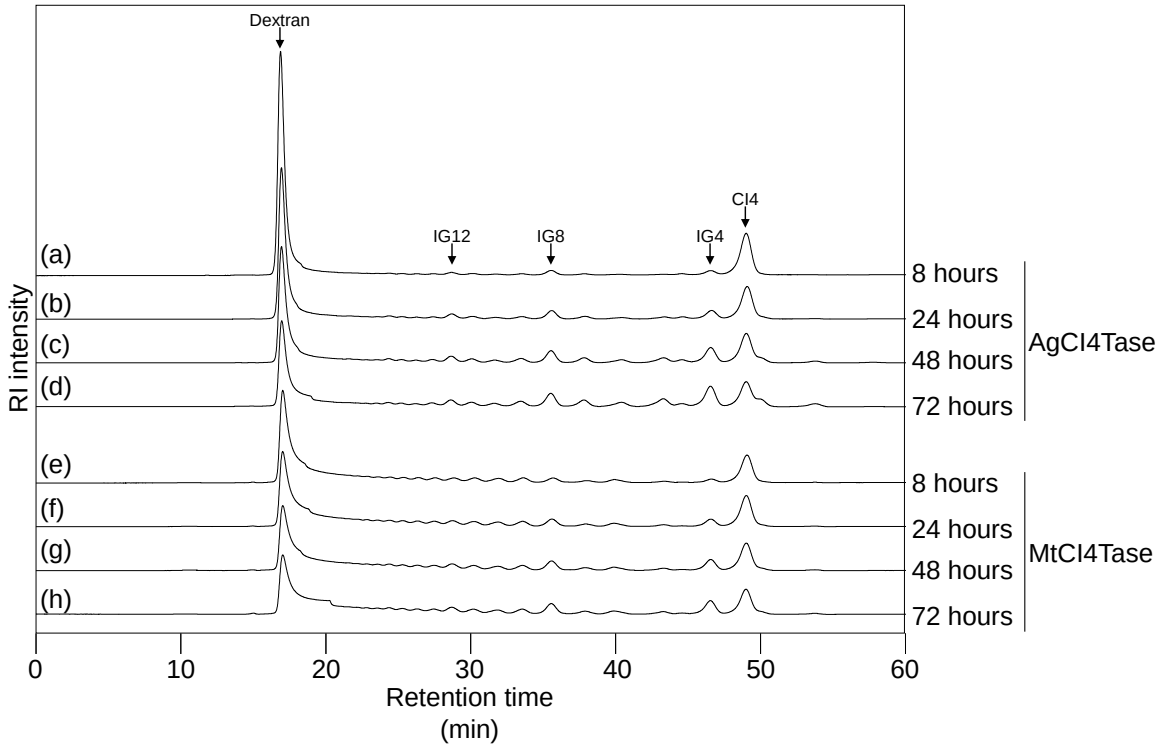

Figure 3-9 HPLC analyses of products from dextran by CI4Tases.

CI4Tases (22 mU/mL) was reacted with 10 mg/mL dextran for 8, 24, 48, and 72 h. (a)-(d), Products by AgCI4Tase. (e)-(h), Products by MtCI4Tase.

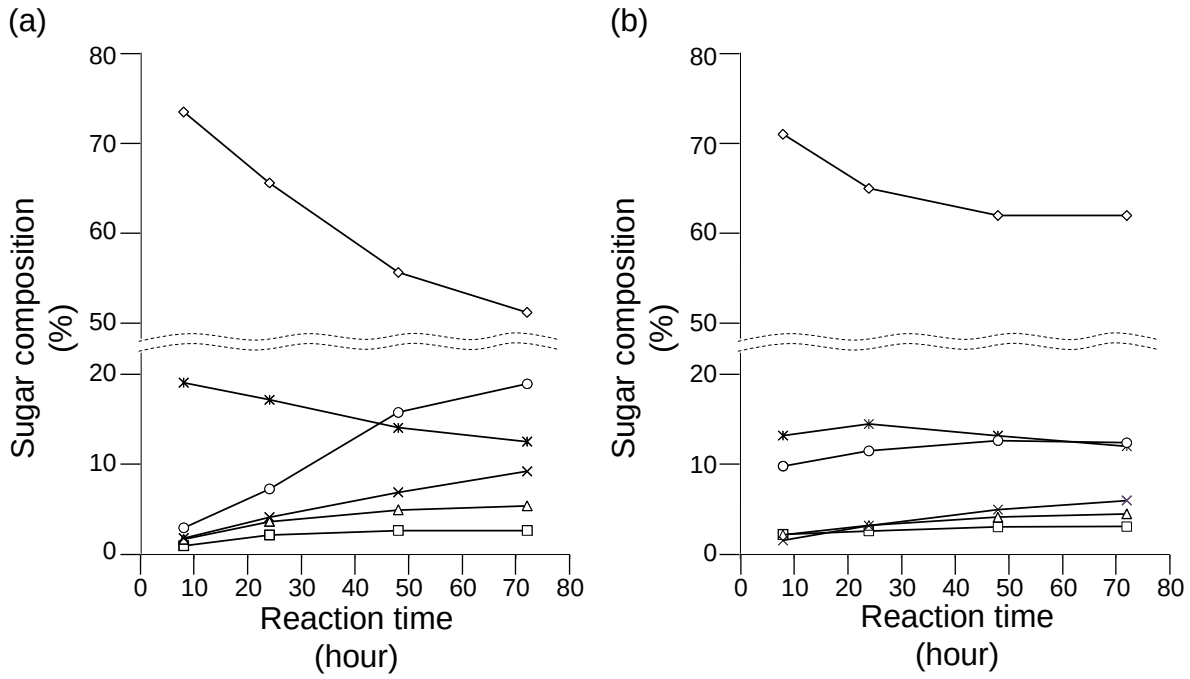

Figure 3-10 Time-dependent conversion of isomaltooligosaccharides from dextran.

◇, IG>12; *, CI4;×, IG4; △, IG8; □, IG12; ○, others.

Table 3-4 Time-dependent conversion of isomaltooligosaccharides from dextran.

	Reaction time (h)	Sugar composition (%)					
		DP>12	IG12	IG8	IG4	CI4	Others
AgCI4Tase	8	73	0.96	1.7	1.8	19	3.0
	24	66	2.2	3.7	4.1	17	7.3
	48	56	2.7	4.9	6.9	14	16
	72	51	2.7	5.4	9.2	13	19
MtCI4Tase	8	71	2.2	2.2	1.6	13	9.8
	24	65	2.6	3.2	3.2	14	11
	48	62	3.1	4.2	5.0	13	13
	72	62	3.1	4.5	6.0	12	12

Production of CI4 from starch-derived substrates

Using a liquefied starch as a starting material, the ability of 6GT and CI4Tase to produce CI4 was tested. First, α-(1→6)-linked glucan was prepared from 300 g/L of the liquified starch in a 72-h reaction with 6GT. Isoamylase and α-amylase were also added to digest a liquefied starch to provide substrate suitable for 6GT. HPLC analysis indicates that the products were isomaltooligosaccharides and Glc judging from their retention times, and almost (80%) were tetramer or saccharides with higher DP (Figure 3-11, Table 3-5 (0 h)). The methylation analysis of the prepared α-(1→6)-linked glucan showed that 45.4% of 6-linked Glc existed in its structure (Table 3-6). Taken together with the HPLC profiles consistent with isomaltooligosaccharide standards, the α-(1→6)-linked glucan was composed of isomaltooligosaccharides mostly. After thermal inactivation of the enzymes in the solution, the sample was briefly purified by active carbon and ion exchange resins, concentrated and used as a starch-derived substrate for MtCI4Tase. The reaction products of MtCI4Tase (22 mU/mL) with starch-derived substrates after 24 or 72 h, as well as samples after treatment of the products with α-glucosidase and glucoamylase, were analyzed by HPLC (Figure 3-11, Table 3-5). In the 24-h reaction, CI4 was 7.3% of all saccharides, and the substrates with DP ≥4 remained (Table 3-5). In the 72-h reaction, increase in CI4 and drastic decrease in the substrates were not observed, indicating that CI4 production have reached a plateau at 24-h reaction. Most of the linear saccharides were degraded into Glc by digestion with α-glucosidase and glucoamylase, while CI4 was not considerably degraded, and occupied 6.2 and 4.8% of all saccharides in the 24- and 72-h reactions. These studies clearly indicate that the combination of 6GT and CI4Tase can produce CI4 from starch as a starting material.

Table 3-5 Production of CI4 from the starch-derived substrate.

	Sugar composition (%)							
Reaction time	CI4	DP ≥4	IG4	G3[a]	IG3	G2[b]	IG2	Glc
0 h (α-(1→6)-glucan)	0	80	4.0	1.3	4.8	0.6	4.7	4.3
24 h	7.3	73	5.3	0	4.5	0.9	4.9	4.4
72 h	5.6	71	5.7	2.3	4.6	1.2	4.9	4.6
24 h + digestion[c]	6.2	3.8	0.2	0	0	5.1	0	85
72 h + digestion	4.8	4.6	0.6	0	0	0.1	0.7	89

G3[a], maltotriose; G2[b], maltose; digestion[c], boiled sample of the 24 h and 72 h reaction was treated with α-glucosidase and glucoamylase to degrade linear oligosaccharides and remaining starch-derived substrate.

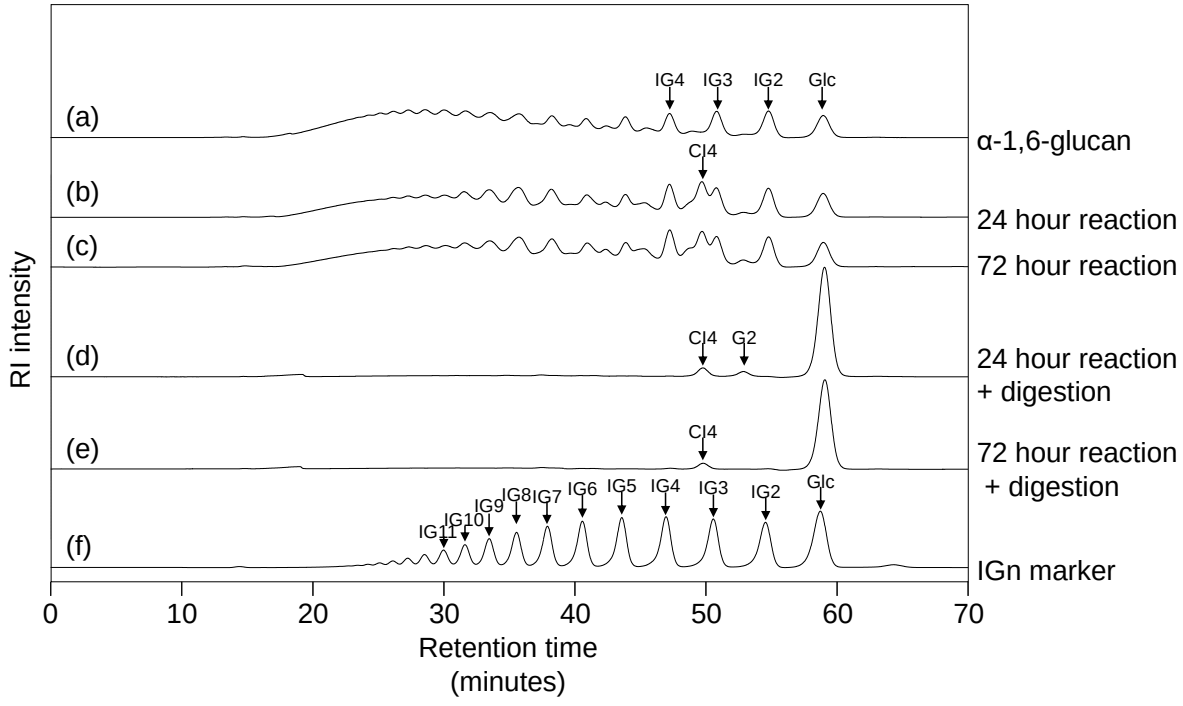

Figure 3-11 Production of CI4 from the starch-derived substrate.

(a) Prepared starch-derived α-(1→6)-glucan, (b) 24-h reaction using MtCI4Tase, (c) 72-h reaction using MtCI4Tase, (d) α-glucosidase and glucoamylase digestion of (b), (e) α-glucosidase and glucoamylase digestion of (c), (f) isomaltooligosaccharide marker.

Table 3-6 The proportion of each glucosyl linkage in the prepared α-(1→6)-glucan.

Non-reducing (%)	2-linked Glc (%)	3-linked Glc (%)	4-linked Glc (%)	6-linked Glc (%)	3,6-linked Glc (%)	4,6-linked Glc (%)
28.9	0	2.4	18.5	45.4	2.4	2.4

The proportion of each glucosyl linkage in the prepared α-(1→6)-glucan was analyzed using the methylation analysis.

Discussion

In this chapter, the CI4-forming enzymes from *Agreia* sp. D1110 and *M. trichothecenolyticum* D2006 were purified to homogeneity from the culture supernatants of both strains and their enzymatic properties were described. Based on the activity to produce CI4 from dextran, the purified enzymes were named cycloisomaltotetraose glucanotransferase whose abbreviation is CI4Tase. The purified CI4Tases, AgCI4Tase from *Agreia* sp. D1110 and MtCI4Tase from *M. trichothecenolyticum* D2006, produced CI4 from dextran. The results suggested that the CI4-forming activity observed in the culture supernatants of both strains was the activity of one type of enzyme. In SDS-PAGE analysis of the AgCI4Tase and MtCI4Tase, only one band was observed. This result suggested that AgCI4Tase and MtCI4Tase are composed of only one polypeptide, respectively. Molecular weight of both enzymes was 86,000 and was comparable between both enzymes. Compared with AgCI4Tase, MtCI4Tase showed lower specific activity, lower pH stability and lower temperature stability. AgCI4Tase was inhibited by $ZnCl_2$, while MtCI4Tase was less inhibited by $ZnCl_2$ than AgCI4Tase. EDTA inhibited MtCI4Tase and less inhibited AgCI4Tase than MtCI4Tase. Both enzymes showed higher activity in the presence of 1.0 mM Mg^{2+}, suggesting that addition of Mg^{2+} ion to the reaction mixture to produce CI4 in from dextran would increase the production rate of CI4.

The study revealed that the two CI4Tases mainly catalyze the following four reactions (Figure 3-12): a) intramolecular α-(1→6)-transglycosylation (cyclization) to produce CI4 from isomaltooligosaccharides with DP ≥5; b) intermolecular α-(1→6)-transglycosylation (disproportionation) between isomaltooligosaccharides; c) hydrolysis of CI4 to produce IG4; d) coupling reaction between CI4 (donor) and isomaltooligosaccharides (acceptor) with DP ≥2. Other CI-forming enzymes CITases also catalyze intramolecular α-(1→6)-transglycosylation, intermolecular α-(1→6)-transglycosylation, hydrolysis of CIs (DP≥7) and coupling reaction. Considering the similarity of substrates and catalyzed reactions, CITase and CI4Tases are

presumed to be the similar enzyme. The most striking difference between the CITases and CI4Tases are product specificities. CITase produces CIs of various DP (7 and more) (Funane *et al*., 2007; Oguma *et al*., 1994, 2014), while the CI4Tases produced CI4. The specific production of CI4 suggested that intramolecular transglycosylation strictly occurs at IG4 unit.

During the reaction using 20 mU/mL CI4Tases, IG9 and IG10 were mainly produced from IG5 and IG6, respectively (Figure 3-6). These results suggest that CI4Tase mainly catalyzes intermolecular α-(1→6)-transglycosylation of IG4 unit. When the intermolecular transglycosylation at IG4 unit is strictly carried out, only products of a certain DP would be produced even if the reaction sufficiently progresses. In the reaction using IG5 and 20 mU/mL CI4Tases, no Glc was produced, and instead, IG2 and IG3 accumulated. In the reaction using IG6 as the substrate, a small amount of IG3 was produced by 20 mU/mL CI4Tases, and a small amount of IG2 and a small amount of IG5 were produced in the reaction using IG7 as the substrate. These results suggest the possibility that the CI4Tases weakly catalyze hydrolysis at IG3 unit besides the intermolecular transglycosylation at IG4 unit. Furthermore, production of IG8 from IG4 was observed. In the reaction using IG4 as substrate, IG2 are also produced. Therefore, the CI4Tases would act on IG4 and weakly catalyze intermolecular transglycosylation of IG2 units to produce IG6 from IG4. The produced IG6 would be immediately used as substrate to produce CI4. IG8 would be produced in the coupling reaction between CI4 and IG4.

Dextran is a suitable starting material for CI4 production, but more expensive than starch which is widely used to produce various oligosaccharides. Partially hydrolyzed starch, pinedex#1 and pinedex#4, was not substrate for CI4Tases (Figure 3-7), suggesting that it is predicted that starch itself is not substrate for CI4Tase. However, α-(1→6)-glucan synthesized from starch using 6GT derived from *P. alginolyticus* can serve as substrate for CI4Tase. These

results suggest that CI4 can be produced using starch as a starting material without using dextran.

However, CI4 was produced only 6.2% of all saccharides after MtCI4Tase reaction and enzymatic digestion of remaining linear saccharides. Improvements is necessary to increase the yield. The 6GT used catalyzes α-(1→6)-transglycosylation only on the non-reducing ends (Tsusaki *et al*., 2009, 2012), suggesting that a large number of unreacted glucosyl residues remain within the starch. The proportion of α-(1→6)-linkages was 45.4% in the substrates for CI4 production, and 4-linked Glc (18.5%), 3-linked Glc (2.4%), 4,6-linked Glc (2.4%), and 3,6-linked Glc (2.4%) were present in the substrate. Figure 3-6 (b) and (d) showed that more CI4 was produced from IG6 than from IG5, suggesting that IG6 is substrate more suitable than IG5. If the ratio of α-(1→6)-glucan structure (DP≥6) in the substrate can be increased via combination with other enzymes, the glycosyl residues available for the reaction of the CI4Tases will increase and the CI4 yield would also increase. Also, CI4 produced using dextran and the CI4Tases was decreased with the progression of reaction as shown in Table 3-4. The decrease in CI4 can be attributed to the coupling and hydrolysis ability that CI4Tases intrinsically possess. The separation using ultrafiltration membrane shown in chapter 2 would be suitable for avoiding the decrease of CI4 due to the coupling reaction and hydrolysis, which would lead to increase the yield of CI4.

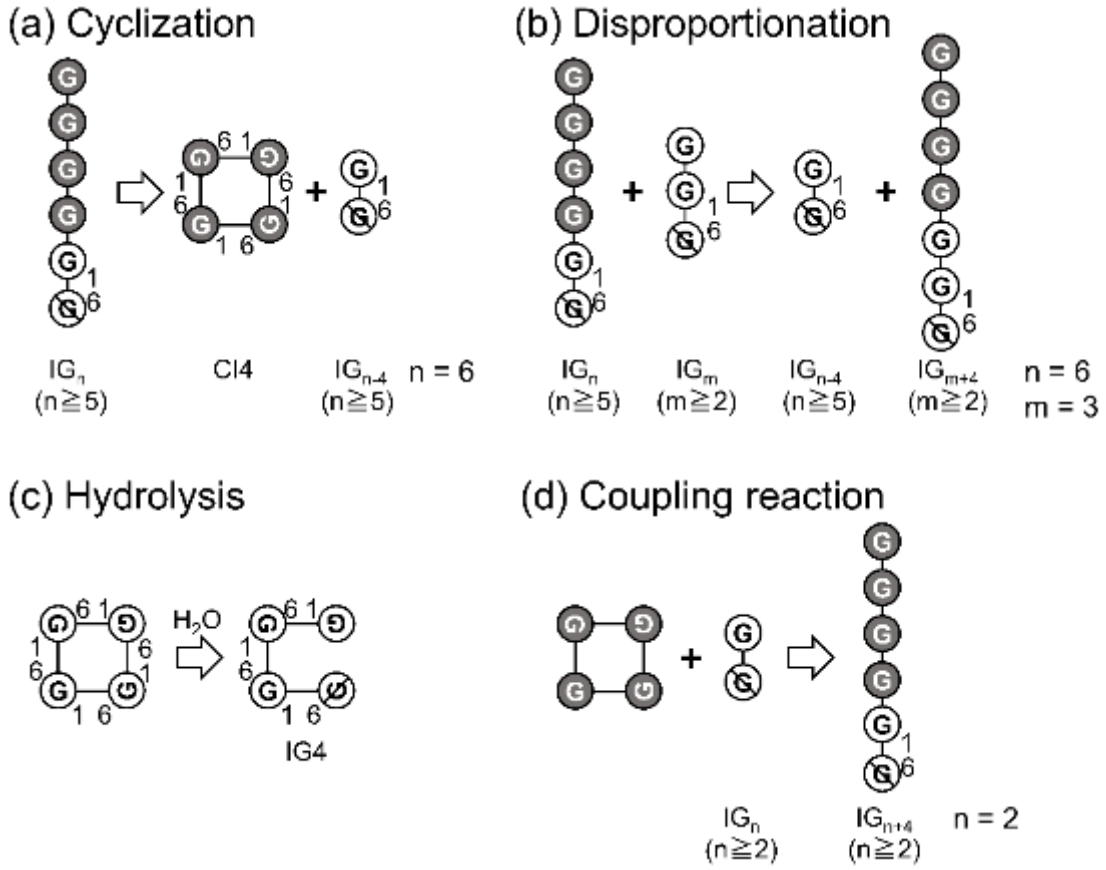

Figure 3-12 Four reactions catalyzed by CI4Tase.

IG_n, IG_{n-4}, IG_{n+4}, IG_m, IG_{m+4} isomaltooligosaccharides; IG4, isomaltotetraose. (a) CI4Tase catalyzes intramolecular transglycosylation (cyclization) and produces CI4 from isomaltooligosaccharide (IG_n) with n ≥5. In the figure, case of (n = 6) is shown; (b) CI4Tase catalyzes intermolecular transglycosylation (disproportionation) of IG4 units to produce products with DPs different from that of the substrates. In the figure, case of (n = 6, m = 3) is shown; (c) CI4Tase catalyzes hydrolysis and cleaves α-(1→6)-glucosidic linkages in CI4 to produce IG4; (d) Coupling reaction catalyzed by CI4Tase. In the figure, case of (n = 2) is shown.

Chapter 4

Sequence analysis of the CI4Tases using draft genome sequence analyses and model for CI4-production and metabolism

Introduction

In this chapter, draft genome sequence analyses of *Agreia* sp. D1110 and *M. trichothecenolyticum* D2006 were performed and protein coding sequences (CDSs) encoding the CI4Tases were discovered. Amino acid sequence comparison between CI4Tases and CITases was also described. Gene clusters containing a *ci4tase* gene were identified in the two CI4-producing bacteria, and two enzymes encoded in the gene cluster, intracellular GH66-like protein (ORF9042) and an annotated intracellular oligo-1,6-glucosidase (ORF9041), were recombinantly expressed as His-tag fusion proteins in *E. coli.* The enzymes were purified to homogeneity and analyzed its activity. A CI4 metabolic pathway was suggested based on the results.

Materials and Methods

Saccharides

CI4 (Lot 1, purity 99.5%) prepared in chapter 2 was used.

Draft genome sequence analysis, assembly and prediction

Agreia sp. D1110 and *M. trichothecenolyticum* D2006 were cultured at 27℃ on a rotary shaker for 66 h in a 500-mL Erlenmeyer flask containing 50 mL of medium described in chapter 2. DNeasy Blood and Tissue kit (QIAGEN N.V., Venlo, Netherlands) was used for the extraction and purification of total DNA from the cultured bacterial cells were performed using. A Nextera XT DNA Sample Prep Kit (FC-131-1024) (Illumina, Little Chesterford, UK) was

used for the preparation of the genomic DNA library from the total DNA. The next generation sequencer MiSeq (Illumina) and MiSeq Reagent Kit v3 (600) (MS-102-3003) were used to read the genomic DNA library in paired-ends read manner. Read length is from 200 to 1,000 bp and average read length is 600 bp. Adaptor sequences in each read were removed using Trimmomatic (Bolger *et al*., 2014). FASTX-Toolkits (http://hannonlab.cshl.edu/fastx_toolkit/) was used to control the quality of each read. Platanus (Kajitani *et al*., 2014) was used for *de novo* assembly. After building contigs, each open reading frame (ORF) in all contigs was predicted using Glimmer3 (Delcher *et al*., 2007). The predicted ORFs were annotated using BLASTP (NCBI Resource Coordinators, 2018) against Uniprot (The Uniprot Consortium, 2021). On proteins encoded by genes in the gene cluster including ORF9038 or ORF5328, homologous amino acid sequences were manually researched using BLASTP. Localization of the proteins encoded the genes in the gene cluster was predicted using SignalP ver 5.0 (Almagro Armenteros *et al*., 2019). A putative promoter region and a putative terminator region were predicted by searching pribnow BOX −10 and −35 for the promoter region and palindrome sequence for the terminator region using GENETYX ver. 15.

Cloning of ORF9038 and ORF5328

Genomic DNA prepared as described above was used as template in PCR to amplify ORF9038 from *Agreia* sp. D1110 and ORF5328 from *M. trichothecenolyticum* D2006. To prepare ORF9038 without region encoding signal peptide, PCR using 50% (v/v) PrimeSTAR Max premix solution, 8.0 mg/mL genomic DNA, 0.12 μM the forward primer (5´-GGAGATATACATATGGCAACCGTCGGCGACGCGTGG-3´) and 0.12 μM the reverse primer (5´-GCTAGCCATACCATGCTATTACTGGGGCAGCGTCCACTTCTG-3´) were performed. Obtained PCR fragment is named ORF9038(-pep). For ORF5328, PCR using the forward primer (5´-GGAGATATACATATGGCCGACCTCGGCGACGCGTGG-3´) and the

reverse primer (5´-GCTAGCCATACCATGCTATTAGCCCGGCAGCGTCCATTTCTG-3´) was performed to obtain ORF5328(-pep) without region encoding signal peptide. Concentrations of each reagent in PCR for ORF5328 was same as one for ORF9038. With homologous sequences in the primers (underlined sequences), the amplified fragments of ORF9038(-pep) and ORF5328(-pep) were introduced into linearized pRSETA (Thermo Fisher Scientific, Waltham, MA, United States) using the In-Fusion® HD Cloning Kit (Takara Bio). With the prepared plasmids, pRSETA-ORF9038(-pep) and pRSETA-ORF5328(-pep), *Escherichia coli* HST-08 (Takara Bio) was transformed and selected on LB agar medium (pH 6.8) containing 1.0% (w/v) hipolypepton, 0.50% (w/v) Bacto™ yeast extract (Thermo Fisher), 1.0% (w/v) NaCl, 1.5% (w/v) agar (Fujifilm Wako Pure Chemical) and 100 μg/mL ampicillin. The two plasmids, pRSETA-ORF9038(-pep) and pRSETA-ORF5328(-pep), were collected from the proliferating cells using QIAprep Spin Miniprep Kit (QIAGEN, Venlo, Netherlands). DNA sequencing was outsourced to Eurofins Genomics K.K. The sequence of oligonucleotides used for sequence analysis was shown below. For pRSETA-ORF9038(-pep), forward primer 1 (5´-GGAGACCACAACGGTTTCCCTC-3´), forward primer 2 (5´-TGTGGCGGCACGAAGCTCCCA-3´), forward primer 3 (5´-GGCATCCGACGGTGG GATGAA -3´), forward primer 4 (5´-GGCGACAGTGTCACGCTGAGC -3´), forward primer 5 (5´-AGATGAGCACCGAACTGCAGG -3´) and forward primer 6 (5´-CACGGT GCCGGAGCTGAAGAA -3´). For pRSETA-ORF5328(-pep), forward primer 1 (5'-GGAGACCACAACGGTTTCCCTC -3'), forward primer 7 (5'-TGTGGCGGCACGAGAAGCCTG-3'), forward primer 8 (5'-AGTGGACGGCGGCATGGACGA-3'), forward primer 9 (5'-GGGGATGCCGTCACCGTGACG-3'), forward primer 10 (5'-AGATGAACCACGAACTGCAAG -3') and forward primer 11 (5'-CTTCACCGTGCCCGAGCTGAA -3'). DNA sequencing was performed by Eurofins

Genomics K.K. Using the two plasmids, *E. coli* BL21(DE3) was transformed and selected on LB agar medium containing 100 μg/mL ampicillin.

Expression of ORF9038(-pep) and ORF5328(-pep)

E. coli BL21(DE3) transformants harbouring pRSETA-ORF9038(-pep) or pRSETA-ORF5328(-pep) were cultured in 5 mL of TB medium containing 47 g/L terrific broth (Thermo fisher scientific), 4 g/L glycerol (Fujifilm Wako Pure Chemical) and 100 μg/mL ampicillin at 37℃ with shaking at 240 rpm for 8 h. After adding isopropyl β-D-1-thiogalactopyranoside (IPTG) to bring the concentration in the culture medium to 100 μM, the culture was continued at 37℃ and 240 rpm for 16 h. Cells were collected by centrifugation at 5800 ×*g* at 4℃ for 10 min and were suspended in 3.0 mL of 20 mM sodium phosphate buffer (pH 7.0). The cells were lysed by incubating with 0.20 mg/mL lysozyme and 0.10% (v/v) Triton X-100 at 27℃ with shaking at 240 rpm for 1 h and then by freezing at −80℃ for 1 h and incubating at 37℃ for 1 h. Lysed cells were further disrupted using sonication and then centrifuged at 15,000 ×*g* and 4℃ for 10 min. The supernatant was filtered through 0.22-μm membrane (Millex®-LG). The filtered supernatant was used as a crude enzyme solution.

Enzyme reaction to analyze the abilities of the recombinant enzymes to produce CI4

A reaction mixture containing 10 mg/mL dextran T70, 50% (v/v) crude enzyme solution of wild-type CI4Tase or mutant enzyme and 50 mM sodium acetate buffer (pH 6.0) was incubated at 40℃ for 16 h. The reaction solutions were filtered, deionized and analyzed by HPLC using two-tandemly connected MCI GEL CK04SS columns. These methods and the calculation of CI4 yields followed the methods described in Chapter 2.

Preparation of CI4Tase mutants

Plasmids for expression of CI4Tase mutants were prepared by amplifying the entire plasmid in PCR using pRSETA-ORF9038(-pep) as template and following primers. Primer sets used are as follows: for CI4Tase(D289A), the forward primer 1 (5′-CACCTCGCTCAGCTCGGCAACTGG-3′) and the reverse primer 1 (5′-GAGCTGAGCGAGGTGGGTGCCGTCG-3′); for CI4Tase(E356A), the forward primer 2 (5′-CTACACGGCTCTGTGGGAGAACCACG-3′) and the reverse primer 2 (5′-CACAGAGCCGTGTAGAGGTAGTCAC-3′); for CI4Tase(L291M), the forward primer 3 (5′-GATCAGATGGGCAACTGGGGCAGCG-3′) and the reverse primer 3 (5′-GTTGCCCATCTGATCGAGGTGGGTGC-3′). Underlined sequence corresponds to the oligo-nucleotide sequences to introduce the mutation. For double mutant CI4Tase(D289A/E356A), E356A mutation was introduced with the forward primer 2 and the reverse primer 2 in the plasmid for CI4Tase(D289A) production as template. All the four plasmids were prepared as the wild-type but using *E. coli* JM109 (Takara Bio) and used for transformation of *E. coli* BL21(DE3). The transformants of both the strains were selected as done for the wild-type, but on plate containing 50 μg/mL ampicillin. The transformants harbouring plasmid for wild-type CI4Tase or mutants were cultured as done in the culture of transformants for wild-type CI4Tase, but volume of the medium was 20 mL and shaking was done at 200 rpm for 16 h for seed culture. As main culture, 2.0 mL of the seed culture was inoculated into 200 mL of TB medium containing 50 μg/mL ampicillin. After shaking at 37°C and 120 rpm for 3 h, final 100 μM IPTG was added followed by further culturing for 16 h. Collection, lysis and disruption of the cells and preparation of crude enzyme solution were performed under same conditions as recombinant CI4Tase wild-type, but without incubation with lysozyme and Triton X-100. Expression of the CI4Tase mutants were analyzed by SDS-PAGE

Constructing expression vectors for ORF9042-derived protein and ORF9041-derived protein

The intracellular GH66-like protein (ORF9042) and the annotated oligo-1,6-glucosidase (ORF9041) from *Agreia* sp. D1110 were expressed in *E. coli* as His-tag fusion proteins (ORF9042-derived protein and ORF9041-derived protein). Genes encoding the intracellular GH66-like protein and the annotated oligo-1,6-glucosidase were introduced into the pRSET A expression vector. The expression plasmid DNAs were designed to have a 6 × His-tag at the N-terminus of the recombinant proteins. Synthesis of the expression vectors pRSETA-ORF9042-derived protein and pRSETA-ORF9041-derived protein (Figure 4-1) were outsourced to Azenta Japan (Tokyo, Japan).

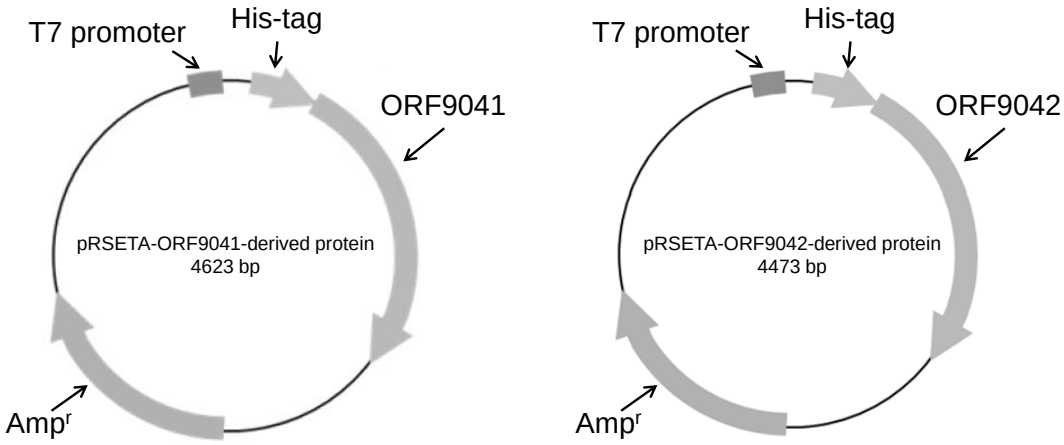

Figure 4-1 Constructed expression vectors.

Amp^r, genes for ampicillin resistance.

Expression of recombinant ORF9042-derived protein and ORF9041-derived protein

E. coli BL21 (DE3) transformants harboring pRSETA-ORF9042-derived protein or pRSETA-ORF9041-derived protein were cultured in 200 mL of TB medium containing 47 g/L terrific broth, 7.9 mL/L glycerol, 2.2 g/L KH_2PO_4 9.4 g/L K_2HPO_4 and 100 μg/mL ampicillin. After shaking at 37°C and 120 rpm for 3 h. IPTG was added to bring the concentration in the culture

medium to 10 μM, and the culture was shaken for another 16 h. Collection, lysis and disruption of the cells and preparation of crude enzyme solution were performed under same conditions as recombinant CI4Tase wild-type, but without incubation with lysozyme and Triton X-100. Expression of the proteins were analyzed by SDS-PAGE.

Purification of ORF9042-derived protein and ORF9041-derived protein

Crude enzyme solutions containing ORF9042-derived protein or ORF9041-derived protein were applied to 1.0 mL (bed volume) of HisTrap^{TM} HP columns (Cytiva) equilibrated with 50 mM sodium phosphate buffer (pH 8.0) containing 20 mM imidazole. After washing with 50 mM sodium phosphate buffer (pH 8.0) containing 40 mM imidazole, ORF9042-derived protein or ORF9041-derived protein were eluted using 50 mM sodium phosphate buffer (pH 8.0) containing 300 mM imidazole. Eluted enzymes were used as purified protein preparations without dialysis. The purified protein preparations were stored at 4℃.

Enzyme reaction to analyze the activities of ORF9042-derived protein

Reaction mixtures (1.0 mL) containing 95 μg/mL ORF9042-derived protein, 10 mg/mL CI4 and 50 mM sodium acetate buffer (pH 6.0) were incubated at 37℃ for 1 h. The solution was kept at 95 °C for 10 min to inactivate the enzyme. The samples were analyzed by HPLC using two-tandemly connected MCI GEL CK04SS columns under the the condition described in chapter 2.

Enzyme reaction to analyze the activities of ORF9041-derived protein

The 1-h ORF9042-derived protein reaction mixture, described in the preceding section, was used after boiling as substrate solution. A reaction mixture (1.0 mL) consisting of purified ORF9041-derived protein (66 μg/mL), the above-mentioned boiled reaction mixture as

substrate and 50 mM sodium acetate buffer (pH 6.0) was incubated at 37℃ for 1 h. The substrate solution was added at 50% volume of the reaction solution. The reaction solution was kept at 95°C for 10 min to terminate the reaction, and the products contained were analyzed by HPLC after pre-treatment using the method described in Chapter 2. The column used was two-tandemly connected MCI GEL CK04SS columns.

The reaction using purified ORF9042-derived protein and each substrate

Reaction mixtures containing 10 mg/mL each substrate, 0, 1.0 or 10 μg/mL purified ORF9042-derived protein and 50 mM sodium acetate buffer (pH 6.0) were incubated at 40℃ for 16 h. As substrate, Glc, IG2, IG3, IG4, IG5, IG6, IG7, dextran T40, CNN, CMM and CI4 (lot 1) were used. After the reaction, the reaction mixtures were boiled for 10 min to stop the reaction. The reaction products were analyzed using TLC under the same condition as described in chapter 2, but the PBW solvent and BEW solvent were developed once and twice, respectively.

Determination of protein concentration

Protein concentrations of the purified ORF9042-derived protein solution and ORF9041-derived protein solution were determined using the Bradford method under the same conditions as described in chapter 3.

SDS-PAGE

E. coli cell extracts were mixed with a equal volume of 50 mM Tris-HCl (pH 6.8), 2.0% (w/v) sodium dodecyl sulfate, 10% (w/v) glycerol, 100 mM dithiothreitol and 0.010% (w/v) bromo phenol blue, and incubated at 95℃ for 5 min. The gel, the dye and the molecular weight marker were one same as in chapter 3. For the CI4Tase (WT) and the CI4Tase mutants, 100 μg-crude protein was applied on the gel. For the crude extract, the flow-through fraction, the wash

fraction and the elution fraction of ORF9041-derived protein, 21, 13, 7.5 and 1.6 μg-protein were applied, respectively. For the ones of ORF9042-derived protein, 11, 7.0, 5.5 and 6.0 μg-protein were applied, respectively.

Multiple alignments

The sequences of CITase-T-3040 (Genbank accession BAA09604.1), CITase-598K (Genbank accession BAL21555.1) and CITase-U-155 (Genbank accession BAA13595.1) were obtained from Genbank (Sayers *et al*., 2020). The sequences of the known oligo-1,6-glucosidases from *Bacillus cereus* ATCC7064 (Uniprot accession P21332), *Bacillus* sp. F5 (P29093), *Bacillus subtilis* HB002 (Q9F4G4), *Bacillus subtilis* subsp. *subtilis* 168 (A0A6M4JPF4), *Parageobacillus thermoglucosidasius* KP1006 (P29094) and *Weizmannia coagulans* ATCC7050 (Q45101) were obtained from Uniprot (The Uniprot Consortium, 2021). All multiple alignments were performed using GENETYX ver. 15.

Analyses of identity of amino acid residues

Identity of amino acid residues between two sequences was calculated as follows except for the results in BLASTP search: 1) The two sequences were applied to pair-wise alignment using GENETYX ver. 15. 2) Identity of amino acid residues between two sequences was calculated with and without gaps, respectively.

BLASTP search

BLASTP (https://blast.ncbi.nlm.nih.gov/Blast.cgi?PAGE=Proteins) was used to search for proteins encoded by bacteria of the *Microbacteriaceae* family that displayed sequence similarity to the protein encoded by ORF9038, ORF5328, ORF9042 or ORF5324. Algorithm parameters were default setting. The protein sequences similar to the protein derived from each

ORF were outputted in the order of E value. *Microbacteriaceae* proteins were extracted from the list of proteins outputted in the search on the basis of the categorization of the bacteria in list of prokaryotic names with Standing in Nomenclature (LPSN) (Parte *et al*., 2020).

Results

Sequence analysis of the gene encoding the CI4Tases

Draft genome sequence analyses of the two strains were performed using the next-generation sequencer MiSeq and the gene sequences encoding the AgCI4Tase and MtCI4Tase were searched in the draft genome. Analysis of the *Agreia* sp. D1110 genome showed that the assembled data contained 145 contigs, yielding a 10.4 Mbp redundant draft genome. Gene prediction and functional annotation showed that there were 9139 ORFs in the draft genome. Analysis of *M. trichothecenolyticum* D2006 showed that the assembled data contained 422 contigs, yielding a 11.9 Mbp redundant draft genome. There were 11068 ORFs in the draft genome.

From the ORFs, the genes encoding the CI4Tases were searched using the determined N-terminal amino acid sequences (described in Chapter 3). Gene products of *Agreia* sp. D1110 ORF9038 and *M. trichothecenolyticum* D2006 ORF5328 possessed the sequence that fully matched with the 9-residue-long N-terminal amino acid sequences of the CI4Tases (Figure 4-2). No other assumed protein sequences were found to carry the 9-residue-long sequences. Therefore, ORF9038 and ORF5328 were annotated as the gene coding for the AgCI4Tase and MtCI4Tase, respectively. The lacked sequences from Met1 to Ala31 in the AgCI4Tase and the sequence from Met1 to Ala32 in the MtCI4Tase matched with the signal peptide sequences predicted using SignalP ver 5.0 (Almagro Armenteros *et al.*, 2019). Molecular weights, calculated from the amino acid sequences excluding the signal peptide sequences, were 86,364.1 and 86,675.1 for ORF9038 and ORF5328, respectively, which are consistent with molecular weight 86,000 determined by SDS-PAGE (Figure 3-1 in chapter 3).

(a)

MKSRFRRTLG ACGTAALIAA GVVLPAVPAS AATVGDAWTD KARYDPGQQV
TVTAEVDGSG PVEFSLVHLG ETVRTGTVQA TGSGTVTWTV TPPTTDFTGY
LVHADAGGST AQTAVDVSST WTRFPRMGYL DEYPADSTQA DRDAIVTDLA
NKYHLNALQF YDWMWRHEAP IERDGNGDLV GTWTAWNGDV IAPATVSGLV
DAGHAVNVAA LPYSMSYAAL EGFEAHGVDA DWRLKYRSDS SDWKFQMLPG
RPDTNLWIMN PSNPDWRDHI SAEYQDQIDT FGFDGTHLDQ LGNWGSGASD
GGMNDVAGNP VDIPVGFRDL VAETKAATGK PVGFNAVDGF AGSTLASSSS
DYLYTELWEN HETYSEVQSY LAGQRAESGG KAAVTAAYLN YRSNTGDRYE
AEDGTLIGVQ VNSNHPGYTG TGFVDQFGDV GDSVTLSVTV PESRRYGIVP
AWANDTATTA TRTVRVDGVP AGKLKMTPTG SWDSWNTEAG FGTYLSAGSH
TIEVSLDAGD TGFANLDSIT LGTFNTPSVQ LANAALAASG ASHIEMGQGD
QMLVAPYFLD DSKQMSTELQ AWMESYYDVI TGYENLLYGP TLRQLPNAVS
IAGHTTSTDG TGDTIWATPM RNDGMDVLHL INLEGNDGRW REPAAQAPTL
SNLPVKYYLA DRPVPADVRI ASPDNGGRSS TLAFTSGSDA GGNYISFTVP
ELKNWSFVYL GDSTRGNGNV VTQASTCLDV AGGNSADGTA VQVWNCASVP
AMQWTFQNNT LSALGKCLDL VAGGTADGTL AHLWTCSDVP SQTWERTGQG
QYLNPASGKC LDLVGGSTAN GTRAHLWSCH AGASQKWTLP Q

(b)

MRSSPFRRRL TAVTIAGLAV AGIIVPAAPA AAADLGDAWT DKARYAPGEQ
VTVTAEVSGT GSVQFSLVHL GDVVDTGTVT ATGSGQVNWT VTPPANDFTG
YMVHVDAGSS TTQTAVDVSS NWTRFPRTGF LDTYPIDLDS TEQAATVDEL
SRNYHLNSLQ FYDWMWRHEK PVQRESNGDL VDTWTAWNGD VIAPDTVAGL
IDATHDVNAA ALPYSMSYAA LEGFQAHGVD ADWRLKYRSS GDDWKFQMLP
NEPDTTLWIM NPENPDWVSH ITEQYADQID ALGFDGTHID QLGNWGEAVD
GGMDDVAGDP VDIPQGFANL VAATKDATGK TTGFNAVDGF GSDWLAGSES
DYLYTELWEN HETYAQVQDY LAQQRAASGG KGAVLAAYLN YRSNTGDQYE
AEAGVLAGGV QVDSDHTGYT GTGFIDSYGA SGDAVTVTVA VPESRRYGIV
PRWTNGTGAT ATRTVTVDGT NVGRIKLPST ADWDTWNIEG GTAAYLTAGT
HTITLAVGSG DTGYVNLDSV TLGTFDTPSV QLANAAFAAN GASHIEMGQG
DQMLVAPYFL DETKQMNHEL QGWLEKYYDV ITGYENLFYG PTLRQLSNAV
TISGQPTSTD GAANTVWTNV MRNDGIDVIH LINLKGNNGS WRDPAATPST
LTNLPVKYYL GDSPVPASVH VASPDRDGGR STALPFTTGS DANGTYLSFT
VPELKSWDFV YLGDSTAGNG NVVTKASKCL DVAGGSAANG TAVQIWDCAS
VPAQDWDYAG EKLSALGKCL DLYQGGTANG TLAHLWDCAN VPSQQWVRTA
QSQYYNPASG RCLDTVGGGA ANGTRIHLWD CHAGPSQKWT LPG

Figure 4-2 Amino acid sequences of the CI4Tases.

(a) The amino acid sequence encoded by ORF9038 derived from *Agreia* sp. D1110; (b) The amino acid sequence encoded by ORF5328 derived from *M. trichothecenolyticum* D2006. The boxed sequences are assumed to be signal peptides. Underlined amino acid residues correspond to the N-terminal amino acid sequences of the purified proteins, described in chapter 3.

Recombinant expression of ORF9038 and ORF5328 in *E. coli*

Recombinant AgCI4Tase and MtCI4Tase eliminating the predicted signal sequence (Lys2-Ala31 and Arg2-Ala32, respectively) were produced in *E. coli*, and CI4-producing activity in crude enzymes were assayed (Figure 4-3). The CI4 production from dextran T-70 was detected in both the crude enzymes. CI4 was produced from dextran with 7.4% and 6.6% yields, respectively. In the control reaction (with the extract of *E. coli* carrying none of the CI4Tase genes), CI4 was not detected. These results confirm that ORF9038 and ORF5328 encode for the AgCI4Tase and the MtCI4Tase and the predicted signal sequence is not essential for activity (Figure 4-2 (a), (b)).

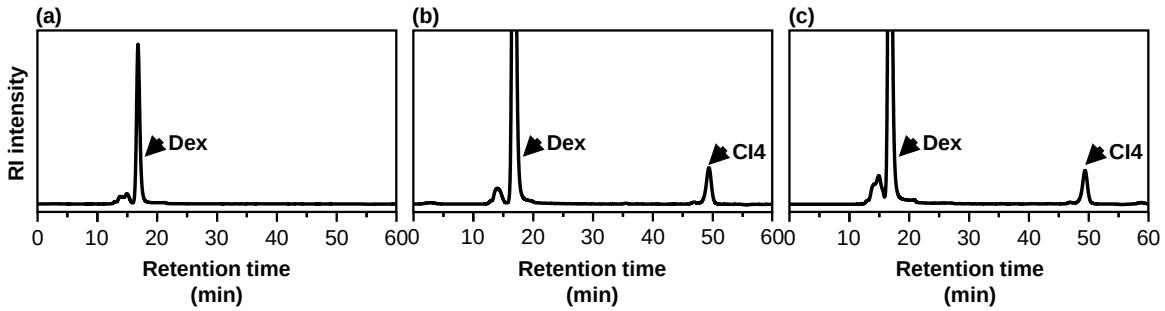

Figure 4-3 HPLC analysis of CI4 production from dextran T70 by the recombinant CI4Tases.

Enzyme reaction mixtures consisting of 10 mg/mL dextran T70, 50% (v/v) crude enzyme solution and 50 mM sodium acetate buffer (pH 6.0) were incubated at 40°C for 16 h. CI4 was detected by HPLC with two-tandemly connected MCI GEL CK04SS columns. Dex and CI4 indicate elution peaks of dextran and CI4 at retention time of 17.2 and 49.5 min. (a) *E. coli* extract without the two target gene products; (b) crude enzyme containing recombinant AgCI4Tase candidate (ORF9038) and (c) MtCI4Tase candidate (ORF5328).

Domain architecture of the CI4Tases

Pfam search (Mistry *et al*., 2021) was done using the full-length amino acid sequences of the CI4Tases as query sequence. Both CI4Tases derived from both strains possessed the Glyco_hydro_66 domain, the CBM35 domain and a Ricin_B_lectin domain, which is represented as CBM13 domain in CAZy (Figure 4-4 (a), (b)). The result indicated that these CI4Tases are classified into GH66 in CAZy. CITases, which are classified into GH66, have two CBM35 domains: one is inserted between β-strand 7 and α-helix 7 of the catalytic TIM barrel domain and the other located at the C-terminal side of the catalytic domain (Figure 4-4 (c)-(e)). The domain organization of CI4Tases is similar to that of CITases. C-terminal structure of the CI4Tases is different from that of CITases (Figure 4-4). The Glyco_hydro_66 domain of CITases is reported to be the catalytic domain. Based on the similarity of the domain structure between the CITases and the CI4Tases, the Glyco_hydro_66 domain in the CI4Tases is assumed to be the catalytic domain as well as the CITases.

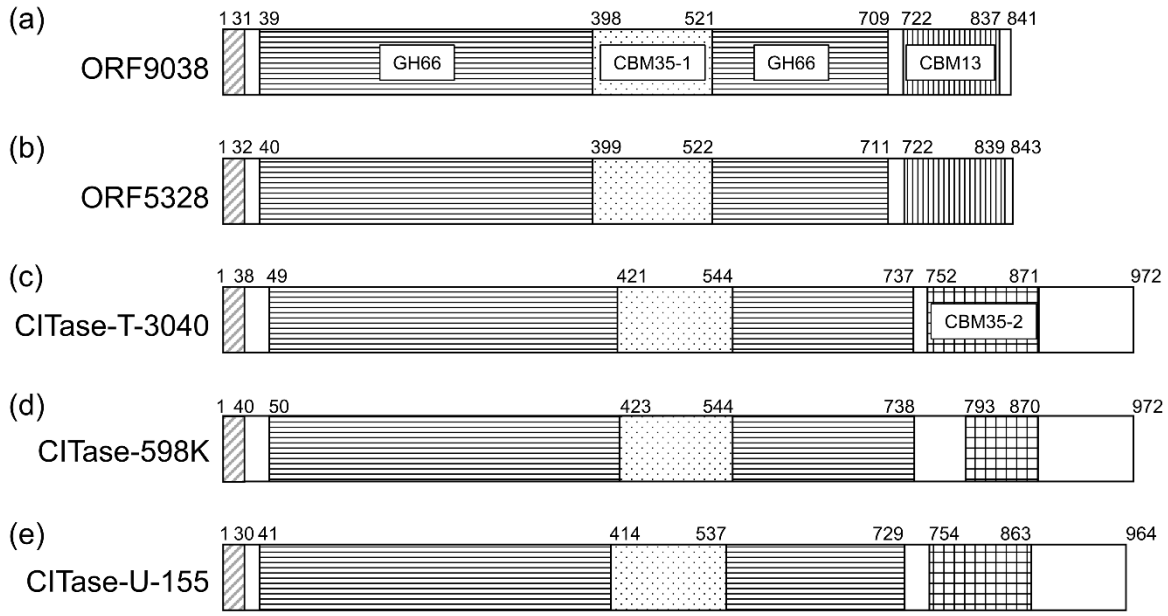

Figure 4-4 Domain architecture of the CI4Tases and CITases.

GH66, Glyco_hydro_66 domain (single domain carrying CBM35-1 in it); CBM35-1, Carbohydrate Binding Module family 35 domain inserted in the Glyco_hydro_66 domain; CBM13, Carbohydrate Binding Module family 13 domain (Ricin_B_lectin domain in Pfam); CBM35-2, Carbohydrate Binding Module family 35 domain in the C-terminal region. Diagonal stripe, signal peptide; Horizontal stripe, Glyco_hydro_66 domain; Dot, CBM35-1 domain; Vertical stripe, CBM13 domain; Plaid, CBM35-2 domain. (a) The CI4Tase precursor encoded by ORF9038 derived from *Agreia* sp. D1110; (b) The CI4Tase precursor encoded by ORF5328 derived from *M. trichothecenolyticum* D2006. (c) CITase derived from *B. circulans* T-3040 (Genbank ID BAA09604.1); (d) CITase derived from *Paenibacillus* sp. 598K (Genbank ID BAL21555.1); (e) CITase derived from *B. circulans* U-155 (Genbank ID BAA13595.1).

Comparison of amino acid sequences between the CI4Tases and the CITases

The amino acid sequences of the CI4Tases were compared with CITases (Figure 4-5). The amino acid sequences of the two CI4Tases showed 71% identities both with and without gaps to each other (Table 4-1). The highest identity between CI4Tase and CITase was 30% with gaps and 35% without gaps (Table 4-1). In the Glyco_hydro_66 domain of the CI4Tases, two acidic residues are conserved in the corresponding positions of catalytic residues of CITases, Asp308 (a nucleophile) and Glu380 (a general acid/base catalyst) in CITase-T-3040: Asp289 and Glu356 of AgCI4Tase and Asp290 and Glu356 of MtCI4Tase, respectively (Figure 4-5). Therefore, the residues are predicted to function as a nucleophile and a general acid/base catalyst, respectively. Compared with CITase sequences, CI4Tases sequences include some insertion (Insert 1 and 2) and deletion (Deletion 1 and 2), as shown in squares in Figure 4-5. Comparison with three dimensional structure of CITase-T-3040 (N. Suzuki *et al*., 2014) suggests that insert 1 in the CI4Tases was located in loop 4 between β-strand 4 and α-helix 4 in TIM barrel, that insert 2 was located near β-strand 1 in domain C and that deletion 1 and 2 were located at α-helix 4 and α-helix 5 in the TIM barrel, respectively. Met310 in CITase-T-3040, which is important residue for cyclization (N. Suzuki *et al*., 2014), is conserved in the CITases, but replaced by Leu in the CI4Tases. Also, the C-terminal region in the CITases is deleted in the CI4Tases (Figure 4-5, square).

Subsites in the CITase-T-3040 have been reported in the previous report (N. Suzuki *et al*., 2014). Following residues in the subsites of the CITase-T-3040 were conserved in the two CI4Tases (Figure 4-5, Table 4-2 (a)): Tyr182, Met235 and Asn354near subsite −1; Tyr233 near subsite −1 and −2; His188 and Leu275 near subsite −2; Asp183 near subsite −2 and −3; Tyr581 near subsite −3 and subsite −4. On the other hand, following residues in the CITase-T-3040 were not conserved in the two CI4Tases (Figure 4-5, Table 4-2(b)): Glu580 near subsite −1; His579 near subsite −3 and −4; Phe207 near subsite −3, −4, −5 and −7; Leu206 near subsite −3

and −5; Phe268 near subsite −5; Asn483 near subsite −6; Tyr499 near subsite −7; Phe501 near subsite −7; Gln496 near subsite −8; Leu498 near subsite −8; Trp514 near subsite −8; Tyr 515 near subsite −8. Leu206, Phe207, Phe268, Leu498, Trp514, His579 and Glu580 were conserved in 3 CITases (Figure 4-5).

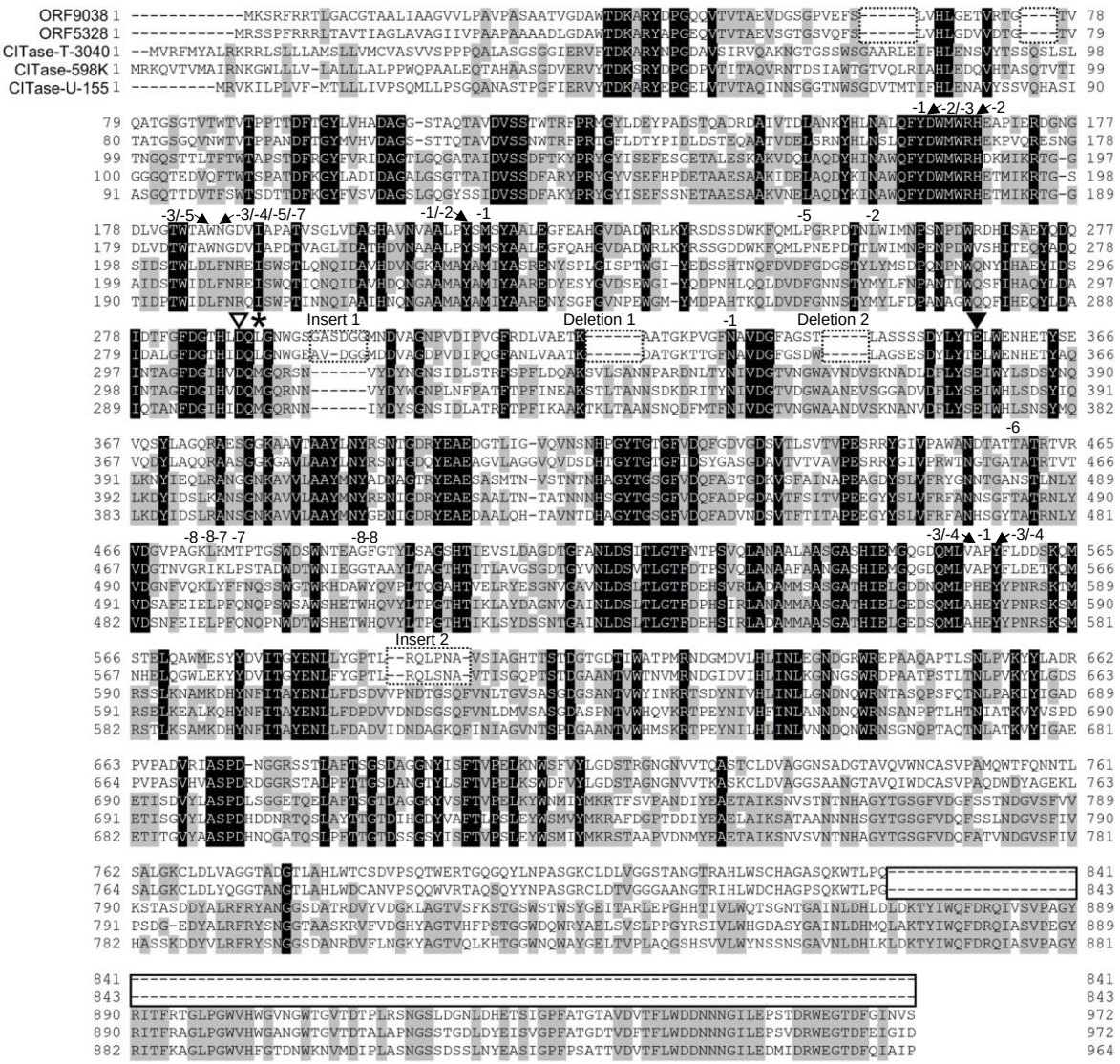

Figure 4-5 Comparison of amino acid sequences of the CI4Tases and the CITases.

White down-pointing triangle, nucleophile; black down-pointing triangle, general acid/base catalyst; asterisk, methionine residue important for determining DP of the products in CITase; dashed square, amino acid residues inserted or deleted in the CI4Tases; square, C-terminal region deleted in the CI4Tases; numbered residues, residues involved in each numbered subsite of CITase-T-3040.

Table 4-1 Identity of amino acid residues between the 2 CI4Tases and the 3 CITases.

Sequence 1	Sequence 2	Identity between sequence 1 and 2	
		With gaps	Without gaps
AgCI4Tase	MtCI4Tase	71% (599/844)	71% (599/841)
	CITase-T-3040	28% (277/974)	33% (277/841)
	CITase-598K	30% (293/980)	35% (293/841)
	CITase-U-155	30% (288/967)	34% (288/841)
MtCI4Tase	CITase-T-3040	29% (281/976)	33% (281/843)
	CITase-598K	30% (294/982)	35% (294/843)
	CITase-U-155	30% (288/974)	34% (288/843)

Table 4-2 (a) Conserved amino acid residues among CITase-T-3040, AgCI4Tase and MtCI4Tase

CITase-T3040		AgCI4Tase	MtCI4Tase
Subsites	Residues[1]	Residues	Residues
−1	Tyr182	Tyr161	Tyr162
−1	Met235	Met215	Met216
−1	Asn354	Asn335	Asn335
−1/−2	Tyr233	Tyr213	Tyr214
−2	His188	His167	His168
−2	Leu275	Leu256	Leu257
−2/−3	Asp183	Asp162	Asp163
−3/−4	Tyr581	Tyr557	Tyr558

[1]Residues involved in the formation of subsites in the CITase-T-3040 are shown.

Table 4-2 (b) Non-conserved amino acid residues among CITase-T-3040, AgCI4Tase and MtCI4Taes.

CITase-T3040		AgCI4Tase	MtCI4Tase
Subsites	Residues[1]	Residues	Residues
−1	Glu580	Pro556	Pro557
−3/−4	His579	Ala555	Ala556
−3/−4/−5/−7	Phe207	Asn187	Asn188
−3/−5	Leu206	Trp186	Trp187
−5	Phe268	Pro249	Pro250
−6	Asn483	Thr459	Thr460
−7	Tyr499	Lys475	Lys476
−7	Phe501	Thr477	Pro478
−8	Gln496	Gly472	Gly473
−8	Leu498	Leu474	Ile475
−8	Trp514	Gly490	Gly491
−8	Tyr515	Phe491	Thr492

[1]Residues involved in the formation of subsites in the CITase-T-3040 are shown.

Analysis of the ability of mutant enzymes to produce CI4

Four AgCI4Tase mutants, D289A, E356A, D289A/E356A and L291M, were prepared to confirm functions of the residues on catalytic activity. Asp289 and Glu356 are corresponding to catalytic residues, and Leu291 was corresponding to Met310 of CITase-T-3040, involved in the CI8 formation in the sequence alignment as described in the previous section. All the mutants along with the wild-type were produced in *E. coli*, and crude enzyme solutions were used for analysis. The SDS-PAGE analysis of the crude enzyme showed that the recombinant proteins were predominantly present in the extracts, and their content appeared to be comparable for all enzymes (Figure 4-6).

CI4-forming activities of the four mutants and wild-type of AgCI4Tase were assayed by incubation with dextran T-70, followed by HPLC analysis to detect CI4 (Figure 4-7). In the reaction with the wild-type enzyme, dextran was converted to CI4, but CI4 production by D289A, E356A, and D289A/E356A was not detected. Not only CI4 but no other products were detected in the reaction with these mutants. These results suggest that Asp289 and Glu356 of AgCI4Tase are essential for activity.

In the reaction with L291M, CI4 was clearly detected as a sole product (Figure 4-7(c)). These results suggested that Leu291 and Met in the position has no influence on reaction specificity of AgCI4Tase.

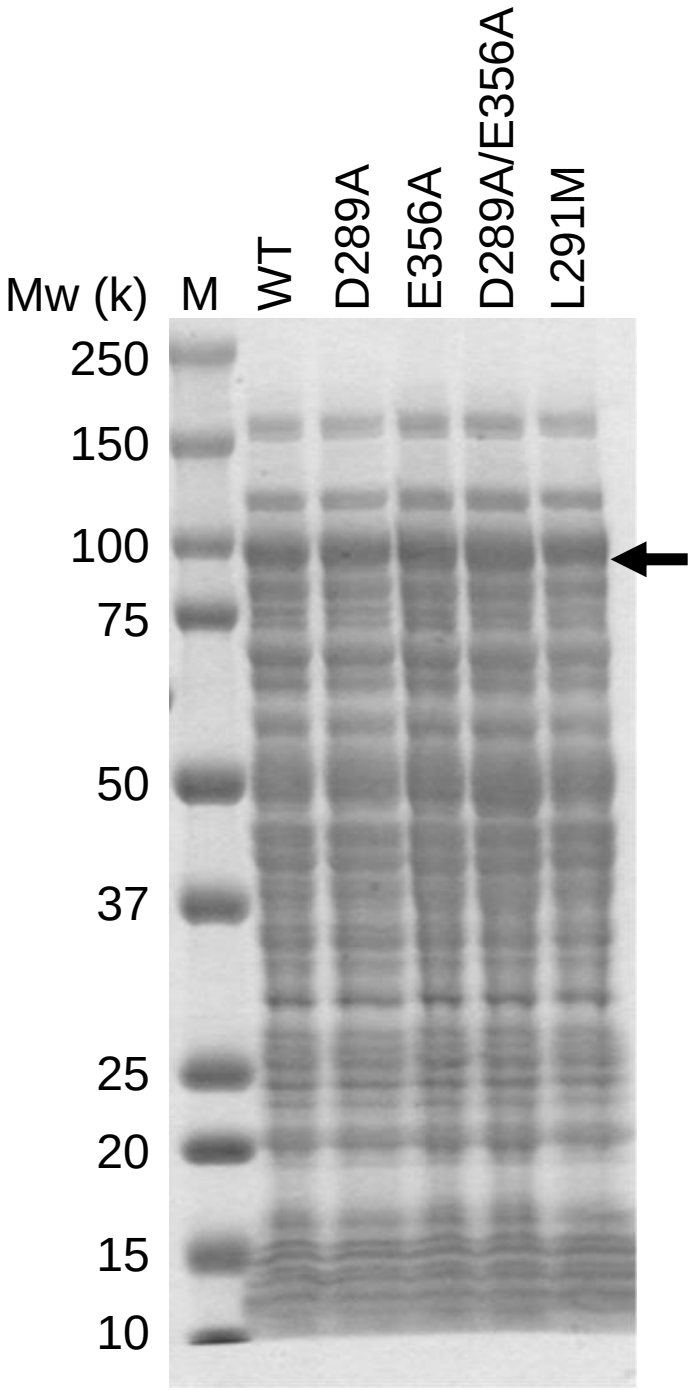

Figure 4-6 SDS-PAGE of the CI4Tase (WT) and the CI4Tase mutants.

Mw, molecular weight; M, molecular weight markers; WT, CI4Tase (WT); D289A, E356A, D289A/E356A, L291M, each CI4Tase mutants. An arrow indicates the bands of CI4Tases. In each lane, 100 μg-protein was applied.

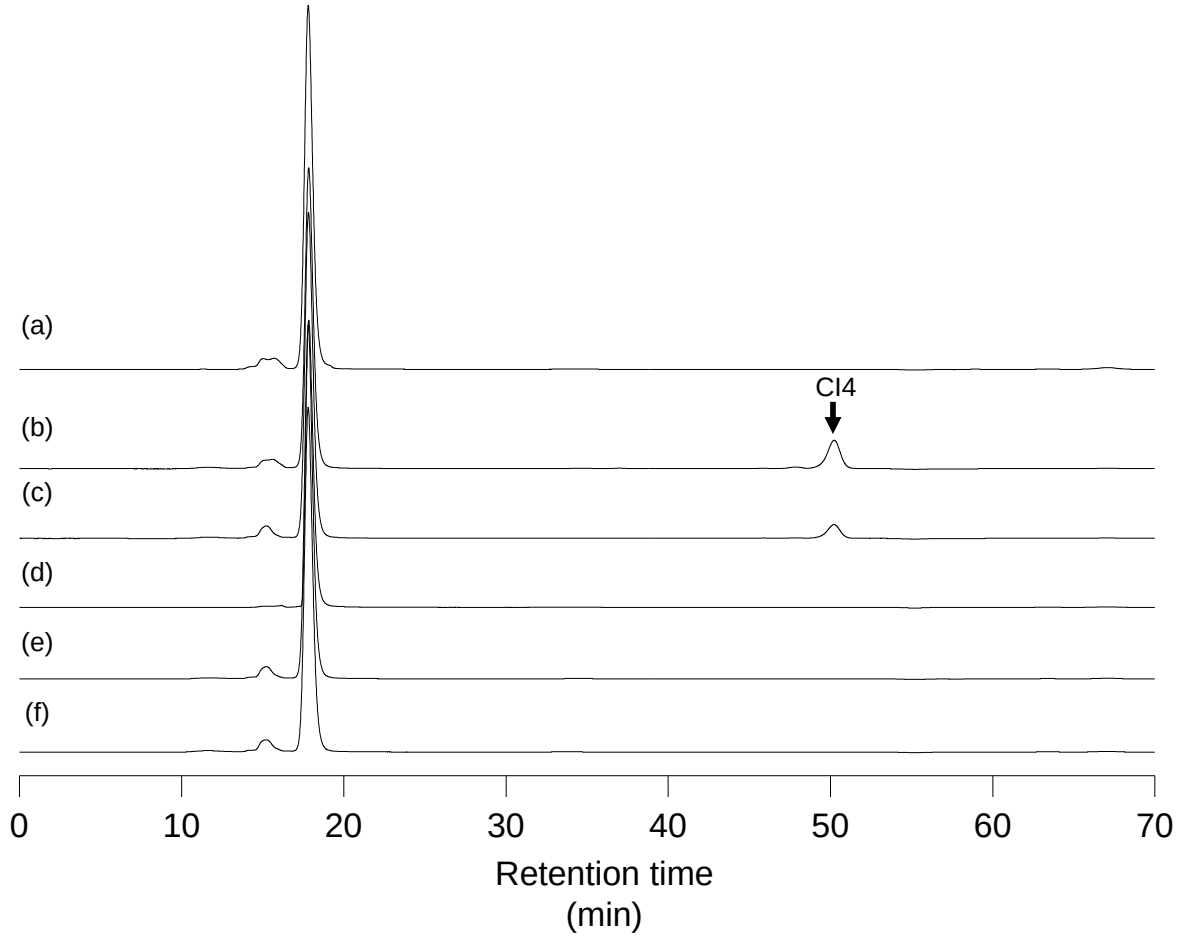

Figure 4-7 HPLC analysis of the enzymatic activities of AgCI4Tase mutants.

(a) no enzyme; (b) AgCI4Tase wild-type; (c) L291M; (d) D289A; (e) E356A; (f) D289A/E356A.

A gene cluster including the CI4Tase genes

The draft genome sequence of *Agreia* sp. D1110 and *M. trichothecenolyticum* D2006 indicated that several putative genes involving the dextran utilization were located near the gene for CI4Tase. Table 4-3 shows annotations of each gene and possible localizations of the proteins encoded by the genes. The gene cluster from *Agreia* sp. D1110 contains genes encoding the CI4Tase (ORF9038), putative oligo-1,6-glucosidase (ORF9041), GH66-like protein (ORF9042), putative transmembrane domains of ABC transporters (ORF9043 and ORF9044), and putative solute-binding protein (ORF9045) (Figure 4-8 (a)). A search using BLAST showed that an amino acid sequence encoded in ORF9042 displayed 61% identity to a protein annotate as CITase (GenBank accession number SIA27698.1) derived from *Mycobacteroides abscessus* subsp. *abscessus*. The search also showed that the solute-binding protein (ORF9045) has 62% amino acid sequence identity to an annotated maltose-binding protein (GenBank accession number ODU52991.1) derived from *Microbacterium* sp. SCN 70-10. A putative promoter region and a putative terminator region were located 45 bases upstream of the start codon of ORF9045 and 46 bases downstream of the stop codon of ORF9038, respectively. The similar gene cluster was observed in *M. trichothecenolyticum* D2006 (Table 4-3 (b), Figure 4-8 (b)) except for an annotated solute-binding protein (ORF12472). ORF12472 in *M. trichothecenolyticum* D2006 was not in the contig same with one of ORF5322, ORF5323, ORF5324, ORF5325 and ORF5328. Identities of amino acid sequences between ORF9045-derived protein (Figure 4-9(a)) and ORF12472-derived-protein (Figure 4-9 (b)) were 81% both with and without gaps, suggesting that these proteins possess similar function.

Table 4-3 (a) A gene cluster containing ORF9038 in *Agreia* sp. D1110

ORF	start	end	Annotation[1]	Localization[2]
ORF9045	8,172,241	8,170,961	Solute-binding protein	Extracellular
ORF9044	8,170,948	8,169,995	ABC transporter	Transmembrane
ORF9043	8,169,998	8,169,156	ABC transporter	Transmembrane
ORF9042	8,169,159	8,167,555	GH66-like protein	Intracellular
ORF9041	8,167,568	8,165,814	Oligo-1,6-glucosidase	Intracellular
ORF9038	8,165,753	8,163,228	CI4Tase	Extracellular

Table 4-3 (b) A gene cluster containing ORF5328 in *M. trichothecenolyticum* D2006.

ORF	start	end	Annotation	Localization
ORF5322	4,223,574	4,224,407	ABC transporter	Transmembrane
ORF5323	4,224,404	4,225,243	ABC transporter	Transmembrane
ORF5324	4,225,240	4,226,838	GH66-like protein	Intracellular
ORF5325	4,226,825	4,228,561	Oligo-1,6-glucosidase	Intracellular
ORF5328	4,228,618	4,231,149	CI4Tase	Extracellular
ORF12472[3]	9,774,201	9,772,927	Solute-binding protein	Extracellular

[1]All annotations except for CI4Tase and GH66-like protein were identified using BLASTP against Uniprot (NCBI Resource Coordinators, 2018). [2]Localization of all proteins except for CI4Tase were predicted using SignalP ver 5.0 (Almagro Armenteros *et al*., 2019). ORF12472[3], this gene was not in the contig same with one of ORF5322, ORF5323, ORF5324, ORF5325 and ORF5328.

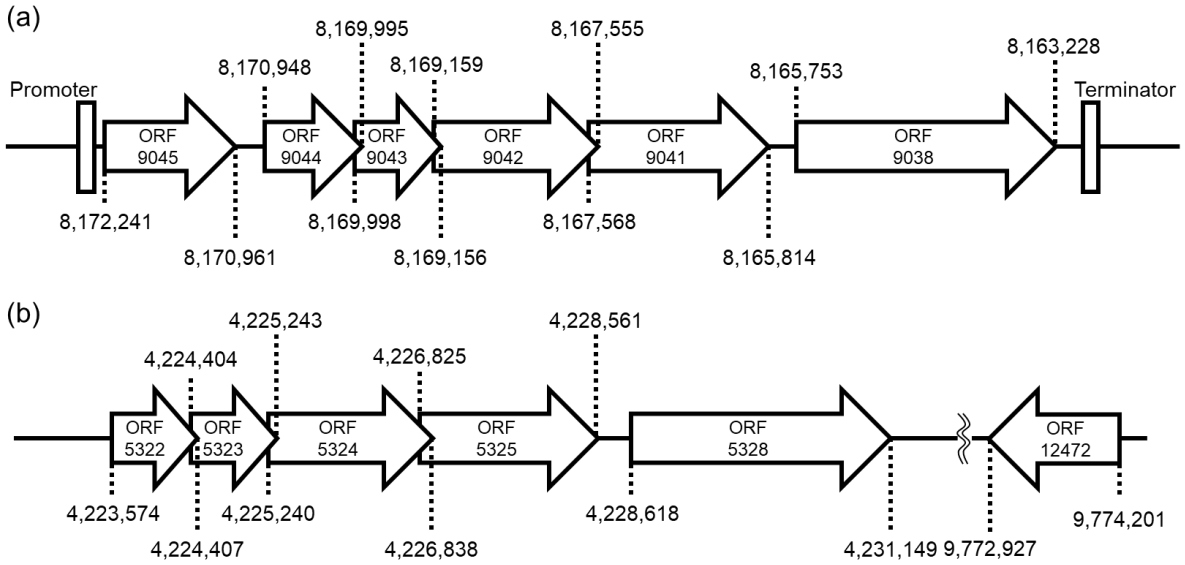

Figure 4-8 Gene clusters in *Agreia* sp. D1110 and *M. trichothecenolyticum* D2006.

(a) A gene cluster in *Agreia* sp. D1110. (b) A gene cluster in *M. trichothecenolyticum* D2006. ORF12472 existed in the genome region different from the gene cluster comprising ORF5322 to ORF5328.

(a)

MRHSRFAIVG ALTVAGALIL SGCSSSSEGS ADDPITLTFW GTYGNGGNSA
QTDVLENELI PAFEKSNPGI TVDYVDMPYD GLKQKLTTSA AGGELPDLVR
SDIGWVAQFA ELGVFKQLDG TMPGFDDLAG AVYPGTLETT SWNGHYYGLP
LNTNTRVLIS NQKALDAAGL SKPPATFDEL RALATKLNGT GVAAFADSGL
NAWNVMPWIW SAGGDIADAD LTTATGYLDS AESVAGVQLL VDLYREGAIP
NLITGNTGAT STSDGLPSGV YATVLDGPWM KEIWQGQYPE FAPVYSPVPA
GDGGSISVVG GESIVVSEGT KYADAAYKFL EFTQSEDYQV GMAGVGQMTV
KPEFAEQQAA IDPYYEAFST QLETARARLP IPQASEVDSI LNAELVPAFE
GTVTVKEALS KAATKITDLL AENKGK

(b)

MRQSRRFAAA GAFALVGVLV LGGCAASGSS ADEPVTLTFW GTYGNGGNSA
QTDVLENELI PAFEKANPGI EVDYVDMPYD GLKQKLTTSA AGGELPDLIR
SDIGWVAQFA ELGVFKQLDG QMPGFDDLAE AVYPGTLQTT SWNGHYYGLP
LNTNTRVLVA NQSALDAAGV AAPPATFDEM RALAAGLAGK GIAAFADSGL
SAWNVMPWIW SAGGDIADED LTTSTGYLDS DASVAGVQLL VDLYQEGAIP
NLITGNTGAT STSDGLPSGE YATILDGPWM QDIWAGQYPD FTPIYASVPA
GDGGSISVVG GESIVVTDAT EHADAAYKFV EFTQSEDYQL GMAKAGQMTV
KPEFAAAQAE IAPYYEAFSN QLETARARLP IPQAGEVDTI LNTELVPAFE
GEVSVKEALT AAAKQIDALL AENQ

Figure 4-9 Amino acid sequences encoded by ORF9045 and ORF12472.

(a) ORF9045-derived protein from *Agreia* sp. D1110, (b) ORF12472-derived protein from *M. trichothecenolyticum* D2006. The boxed sequences are assumed to be signal peptides using SignalP ver 5.0 (Almagro Armenteros *et al*., 2019).

Sequence characteristics of proteins encoded in the gene clusters

Both *Agreia* sp. D1110 and *M. trichothecenolyticum* D2006 possessed genes of GH66-like protein (ORF9042, 534 amino-acid-residue-long and ORF5324, 532 amino-acid-residue-long respectively) and putative oligo-1,6-glucosidase (ORF9041, 584 amino-acid-residue-long and ORF5325, 578 amino-acid-residue-long, respectively). Full amino acid sequences encoded by these ORFs are shown in Figure 4-10 and 4-11. The enzymes encoded by these genes possessed no signal peptide sequence, implying the enzymes are localized in the cytosol. Amino acid sequences derived from ORF9042 and ORF5324 displayed 67% identities both with and without gaps, while those derived from ORF9041 and ORF5325 displayed 66% identities both with and without gaps. Domains of each protein were searched using Pfam, and the results were shown in Table 4-4. ORF9042- and ORF5324-derived proteins possess Glyco_hydro_66 domain, indicating that the enzymes are categorized in GH66 in CAZy. These enzymes did not have a CBM35 domain, being similar to the GH66 dextranase (Table 1-1). Table 4-4(b) shows that ORF9041-derived protein and ORF5325-derived protein possessed Alpha-amylase domain and DUF3459 domain.

The amino acid sequences of the ORF9041- and the ORF5325-derived protein were compared with 6 known oligo-1,6-glucosidase (P21332, P29093, Q9F4G4, A0A6M4JPF4, P29094 and Q45101) (Figure 4-12, Table 4-5). Table 4-5 revealed that the ORF9041- and the ORF5325-derived protein showed identity higher than 42% to 6 known oligo-1,6-glucosidase. The ORF9041- and ORF5325-derived protein possessed 7 conserved regions (CSR from I to VII in Figure 4-12) which have been reported to be present in 6 known oligo-1,6-glucosidase (Berlina *et al*., 2021; Oslancová & Janeček, 2002). A nucleophile and a general/acid base catalyst were conserved in ORF9041- and the ORF5325-derived protein (Figure 4-12, white down-pointing triangle for nucleophile and black down-pointing triangle). Three residues ,Val, Lys and Glu, important for α-(1→6)-linkage selectivity in GH13 *exo*-glucosidase (Saburi *et al*., 2015) were

conserved in ORF9041- and ORF5325-derived protein.

(a)

```
MSSFELVAPF ATGTDAQWWK SAVVYQVYPR SFQDSDSDGI GDIRGVLNRL
DHLQRLGVDV IWLSPVYRSP QADNGYDISD YEEIDPVFGT MADFDELLAS
AHERGIKIVM DLVVNHTSDE HPWFVESRSS PDNPRRDWYW WRDARPGTIP
GEAGSEPNNW ESFFSGSTWE FDKSSGQYYL HLFDRKQPDL NWENPEVRHA
VYAMMRRWLD RGVDGFRMDV INLISKHPGL PDGQRSEPSR FGDGFPYFAH
GPRLHEYLRE MHREVFDGRD GLLTVGEMPG VTPGEAVLFT DQSRRELDMV
FQFEHVGLDH GDGSKFTHRE LAPGALAESL TRWQDALAET GWNSLYLSNH
DQPRAVSRFG DDANWWRESA TALATILHLQ RGTPYIYQGE ELGMTNRTFS
SIDEVRDVES INHYRDRVAS GDSDSDVLAA IGRIGRDNAR TPVQWDASQH
GGFTTGTPWL AVNPNTATIN AEDQYDVAGS VFEHYRALIR LRHERAVIAD
GSFRRITVTP ASDAVFAYER RLGNDTVLVV ANLSSQERVV RLDGYPAPWT
TGTLLLGNVT SIGYDGAQTE TELFAPWEAR VYAL
```

(b)

```
MTVHQISLLP TRSSFGTGDP VEIEIETGSA ELTGLLTVWR LGERVAERAV
SAPGVHRLPD LDDGSYGIEL DVDGLTVART AIEITADPRA RLRYGFVASY
APGKDVAAAA RLARRLHLNG IQFYDWAYRH ADLVGGGDVY TDALDQPIAL
DTVRQLVAAY RAVGTDSIGY AAVYAVGPNE WDDWKQHALL RPSGEPYALG
DFLFIVDPAA REWTAHFRAD LSKSTAAVGF DGYHLDQYGY PKFASTPDGT
PVDVAESFAR LIEEVRAELP DARLIFNNVN DFPTWRTAAL PQDAVYIEPW
VPNDTLESLA QIVNRARASS AGQPVVLAAY QHIYDSVPAR DADRATALTM
ATLFSHGATQ LLIGEDGRLL VDPYYVRNQQ ADSETLDVLA RWYDFVVEHD
ELLMDPGISE VTSSYVGEYN GDLDVLFSDV AVASTPLADS VWRRVTSSDR
GLVVHLINLC GQTDTLWDAA RADVVSPGSG ELRFRYTRGR IPRVRVADPD
GQSRLIDVDV RIDGDYAVAV LPPLNIWQVV HVIL
```

Figure 4-10 Amino acid sequences encoded by ORF9041 and ORF9042 from *Agreia* sp. D1110.

(a) An amino acid sequence encoded by ORF9041. (b) An amino acid sequence encoded by ORF9042.

(a)

```
MSLSEILVAE AAAEASSEWW KRAVVYQVYP RSFQDSDGDG IGDLRGILQR
LDHLERLGID VIWLSPIYRS PHADNGYDIS DYQDIDPAFG TFDDFTELLD
AVHTRGMKLV MDLVVNHTSD EHPWFLESRS SLDNPKRDWY WWRPARAGHH
PGELGAEPTN WESFFSGPTW TLDEHTGEYY LHLFAKKQPD LNWENPEVRE
AVYAMMRWWL DRGVDGFRMD VVNLISKHPG LPDGTVTEGK TYGDGFPHYS
AGPRLHEYLQ EMRREVFDGR GALLTVGETP GVTTDEAALF SDPARRELDM
VFQFEHVSLD HEDGKFRPRE LEPGELAASF TTWQDALAQI GWNSLYLANH
DQPRPVSRFG NATAWWRESA TALATVLHLQ RGTPYVYQGE ELGMTNAPFD
QIGDYRDVES LNHFTDAVGR GEQPDAVIAG LLRMSRDHAR TPVQWDDSLN
AGFTAGTPWI RVNPNHTRIN ALTQYDDPDS VFEHYRTLIA LRHRLPVVAD
GDFVRLDAGT PAVFAFQRTL DDERLLVVAN LSSSVVTPLL PDAICEEWHD
ARPVLTNRAG EHAVDAALHP WEAKVYTH
```

(b)

```
MNMPLTLLPT RASYRPADPI TIEIRDAEAP LDGTLTLWRL GELVHTQPLQ
PGPLQTLPDL SAGGYGIELD GPMGTARTAV EVTADPQSRL RYGFVASYNP
GKDVRAVADF ARRLHLNGIQ FYDWAYRHAD LLGGGEQYDD ALGQPITLST
VRELVDALRD AGSASYGYAA VYAVGPNEWP DWQHYALLRP TGEPYALGDF
LFILDPAARE WLAHFTADLS ASVDTVGFDG FHLDQYGYPK HAATPDGTAV
DVAASFTRLI EEVRQTLPDS RLIFNNVNDF PTWDTASSPQ DAVYIEPWKP
VVTLQALANV ATRARAVAGG LPVVLAAYQH TYDLAPAEAS DRAAAFTMAT
LLSHGATQLL AGEHGKLLVD PYYVRNHEAE PNTVEFLSRW YDFAVEHDAL
LLDPSIVDVT AAYVGDYNDD LDVMYDAIEV TETAVAGSVW RRVTRTSEGI
VVHLINLVGQ DDTLWDAPRN TPGATGEGEL RFKFVRGQIP RVRVADPDRN
PRLVDVPVRL DGDRAVATLP ALNIWQVVHV AL
```

Figure 4-11 Amino acid sequences encoded by ORF5325 and ORF5324 from *M. trichothecenolyticum* D2006.

(a) An amino acid sequence encoded by ORF5325. (b) An amino acid sequence encoded by ORF5324.

Table 4-4 (a) Domain of the ORF9042-derived protein and the ORF5324-derived protein.

Protein	Family[1]	Start	End
ORF9042-derived protein	Glyco_hydro_66	56	530
ORF5324-derived protein	Glyco_hydro_66	12	528

Domains were searched using Pfam. Family[1], notation of domain conforms to the one in Pfam.

Table 4-4 (b) Domain of the ORF9041-derived protein and the ORF5325-derived protein.

Protein	Family[1]	Start	End
ORF9041-derived protein	Alpha-amylase	41	397
	DUF3459	485	579
ORF5325-derived protein	Alpha-amylase	42	397
	DUF3459	485	575

Domains were searched using Pfam. Family[1], notation of domain conforms to the one in Pfam.

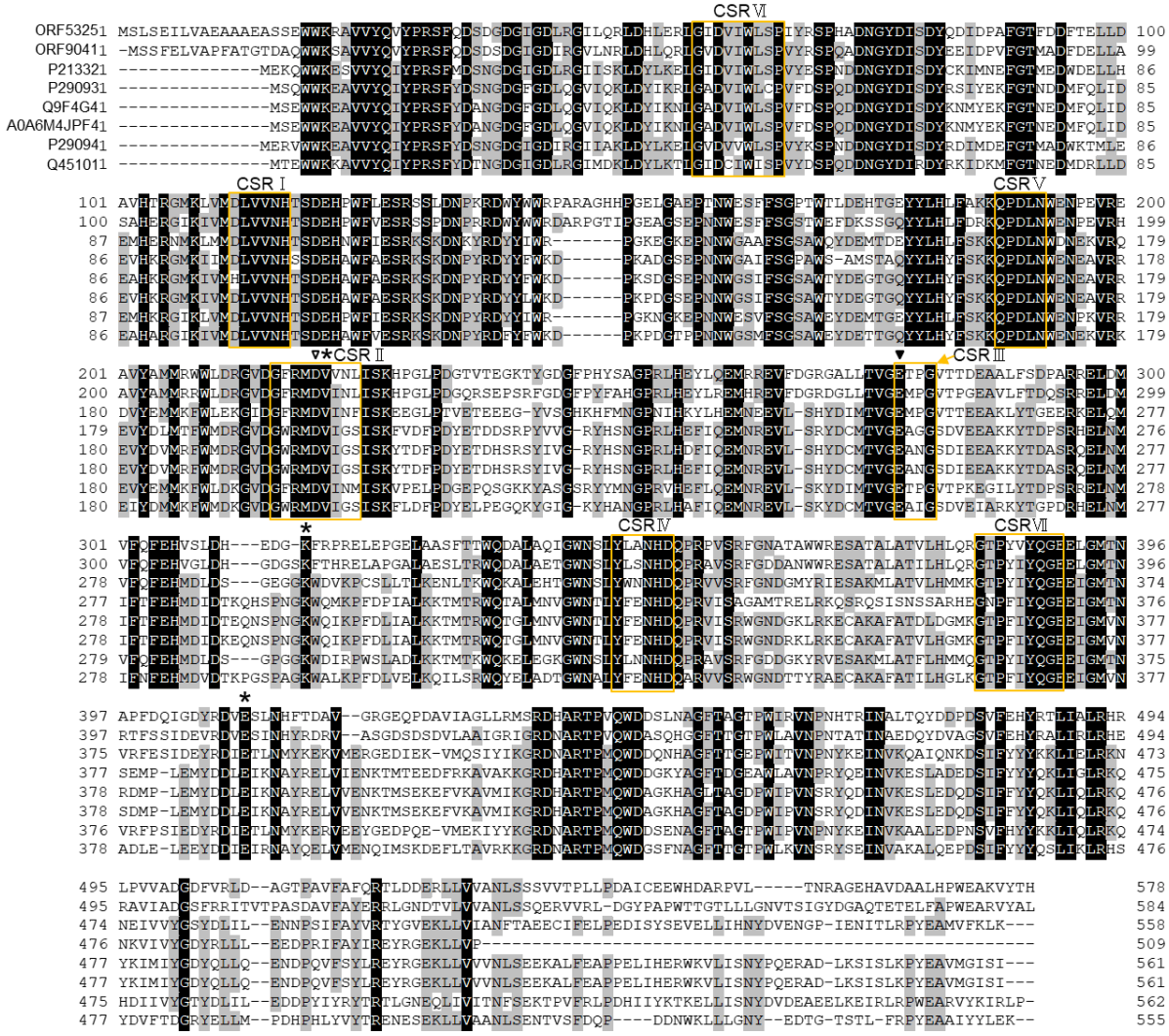

Figure 4-12 Comparison of amino acid sequences of the ORF9041-derived protein, the ORF5325-derived protein and the known oligo-1,6-glucosidases.

White down-pointing triangle, nucleophile; black down-pointing triangle, general acid/base catalyst; asterisk, residues important for α-(1→6)-linkage selectivity in GH13 *exo*-glucosidase (Saburi *et al*., 2015). CSR from I to VII, conserved region observed in α-amylase family proteins (Oslancová & Janeček, 2002). Multiple alignment of following proteins was shown: ORF5325-derived protein, ORF9041-derived protein and the known oligo-1,6-glucosidases from *Bacillus cereus* ATCC7064 (Uniprot accession P21332), *Bacillus* sp. F5 (P29093), *Bacillus subtilis* HB002 (Q9F4G4), *Bacillus subtilis* subsp. *subtilis* 168 (A0A6M4JPF4), *Parageobacillus thermoglucosidasius* KP1006 (P29094) and *Weizmannia coagulans* ATCC7050 (Q45101).

Table 4-5 Identity of amino acid residues among the ORF9041-derived protein, the ORF5325-derived protein and the known oligo-1,6-glucosidases.

Sequence 1	Sequence 2	Identity between sequence 1 and 2	
		with gaps	without gaps
ORF5325-derived protein	ORF9041-derived protein	66% (385/586)	67% (385/578)
	P21332	50% (292/581)	52% (292/558)
	P29093	42% (247/584)	49% (247/509)
	Q9F4G4	45% (261/585)	47% (261/561)
	A0A6M4JPF4	46% (267/585)	48% (267/561)
	P29094	53% (312/584)	56% (312/562)
	Q45101	46% (271/586)	49% (271/555)
ORF9041-derived protein	P21332	50% (295/586)	53% (295/558)
	P29093	42% (247/589)	49% (247/509)
	Q9F4G4	44% (258/589)	46% (258/561)
	A0A6M4JPF4	44% (261/589)	47% (261/561)
	P29094	54% (316/588)	56% (316/562)
	Q45101	49% (291/591)	52% (291/555)

Recombinant expression of ORF9041 and ORF9042 and their purification

To investigate the catalytic activity of proteins derived from ORF9041 and ORF9042 of *Agreia* sp. D1110, their recombinant proteins with a His tag fused at the N-terminus (Figure 4-13) were produced in *E. coli*. The recombinant enzymes were purified by immobilized metal affinity chromatography as confirmed by SDS-PAGE analysis (Figure 4-14). The molecular weights of the proteins derived from ORF9041 and ORF9042 were estimated to be 70,000 and 65,000 from the migration distance in SDS-PAGE, respectively. These molecular weights were matched well with the molecular weight calculated from the amino acid sequence, 70457.60 and 62975.47, respectively.

(a)

MRGSHHHHHH GMASMTGGQQ MGRDLYDDDD KDRWGSELES SFELVAPFAT
GTDAQWWKSA VVYQVYPRSF QDSDSDGIGD IRGVLNRLDH LQRLGVDVIW
LSPVYRSPQA DNGYDISDYE EIDPVFGTMA DFDELLASAH ERGIKIVMDL
VVNHTSDEHP WFVESRSSPD NPRRDWYWWR DARPGTIPGE AGSEPNNWES
FFSGSTWEFD KSSGQYYLHL FDRKQPDLNW ENPEVRHAVY AMMRRWLDRG
VDGFRMDVIN LISKHPGLPD GQRSEPSRFG DGFPYFAHGP RLHEYLREMH
REVFDGRDGL LTVGEMPGVT PGEAVLFTDQ SRRELDMVFQ FEHVGLDHGD
GSKFTHRELA PGALAESLTR WQDALAETGW NSLYLSNHDQ PRAVSRFGDD
ANWWRESATA LATILHLQRG TPYIYQGEEL GMTNRTFSSI DEVRDVESIN
HYRDRVASGD SDSDVLAAIG RIGRDNARTP VQWDASQHGG FTTGTPWLAV
NPNTATINAE DQYDVAGSVF EHYRALIRLR HERAVIADGS FRRITVTPAS
DAVFAYERRL GNDTVLVVAN LSSQERVVRL DGYPAPWTTG TLLLGNVTSI
GYDGAQTETE LFAPWEARVY AL

(b)

MRGSHHHHHH GMASMTGGQQ MGRDLYDDDD KDRWGSELET VHQISLLPTR
SSFGTGDPVE IEIETGSAEL TGLLTVWRLG ERVAERAVSA PGVHRLPDLD
DGSYGIELDV DGLTVARTAI EITADPRARL RYGFVASYAP GKDVAAAARL
ARRLHLNGIQ FYDWAYRHAD LVGGGDVYTD ALDQPIALDT VRQLVAAYRA
VGTDSIGYAA VYAVGPNEWD DWKQHALLRP SGEPYALGDF LFIVDPAARE
WTAHFRADLS KSTAAVGFDG YHLDQYGYPK FASTPDGTPV DVAESFARLI
EEVRAELPDA RLIFNNVNDF PTWRTAALPQ DAVYIEPWVP NDTLESLAQI
VNRARASSAG QPVVLAAYQH IYDSVPARDA DRATALTMAT LFSHGATQLL
IGEDGRLLVD PYYVRNQQAD SETLDVLARW YDFVVEHDEL LMDPGISEVT
SSYVGEYNGD LDVLFSDVAV ASTPLADSVW RRVTSSDRGL VVHLINLCGQ
TDTLWDAARA DVVSPGSGEL RFRYTRGRIP RVRVADPDGQ SRLIDVDVRI
DGDYAVAVLP PLNIWQVVHV IL

Figure 4-13 Expressed sequences derived from ORF9041 and ORF9042.

(a) The expressed sequence derived from ORF9041, (b) The expressed sequence derived from ORF9042. Underline, sequences added on the N-terminus.

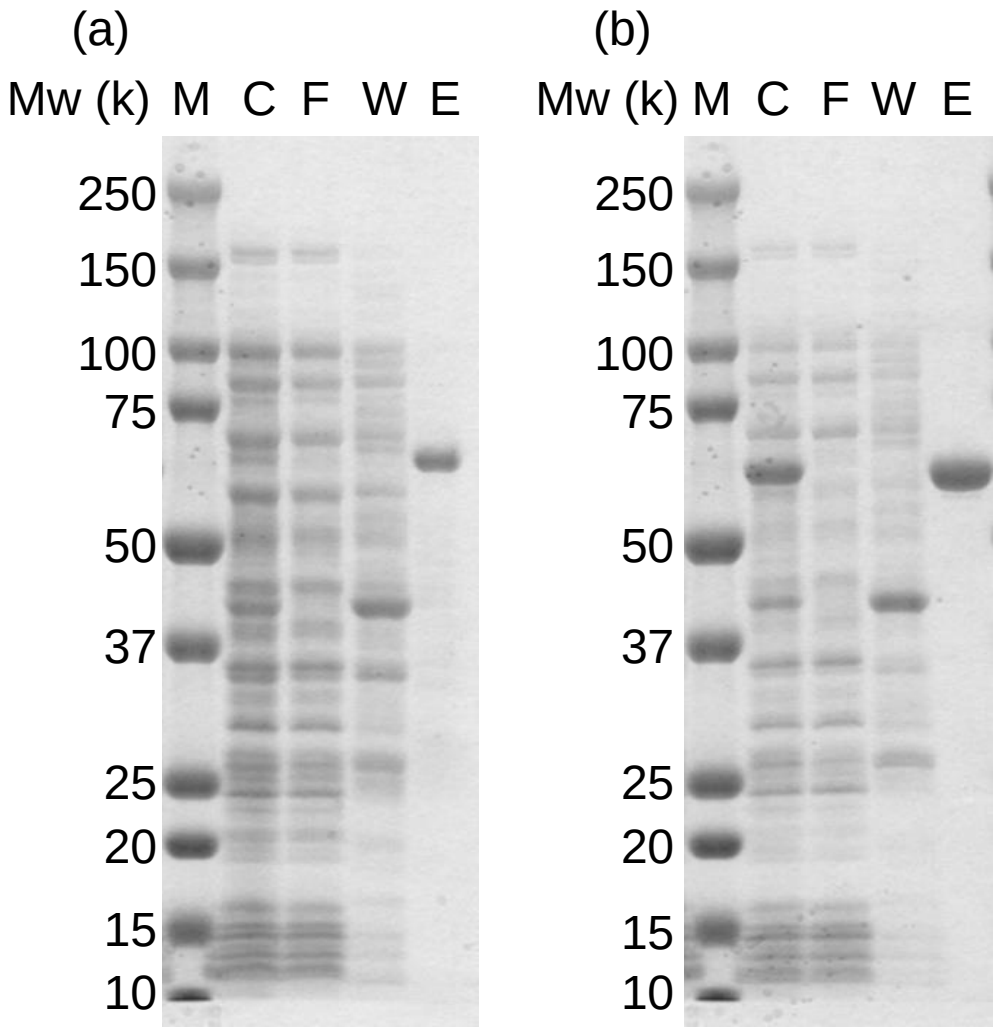

Figure 4-14 SDS-PAGE of purified proteins derived from ORF9041 and ORF9042.

Mw, molecular weight; M, molecular weight marker; C, crude extract of each transformant; F, flow-through fraction in HisTrap^{TM} HP column purification; W, wash fraction; E, elution fraction of the purification. (a) ORF9041-derived protein. In the lane of C, F, W and E, 21, 13, 7.5 and 1.6 μg-protein were applied, respectively. (b) ORF9042-derived protein. In the lane of C, F, W and E, 11, 7.0, 5.5 and 6.0 μg-protein were applied, respectively.

Analysis of enzymatic activity of ORF9042-derived protein and ORF9041-derived protein

The enzymatic activity of the ORF9042-derived protein was assessed using CI4 as substrate. Products from 10 mg/mL CI4 in 1-h reaction were analyzed by HPLC (Figure 4-15). In the 1-h reaction mixture, most CI4 was converted to IG4 and a small amount of IG3 and Glc (Figure 4-15 (b). This result indicates that ORF9042-derived protein has an activity to hydrolyze CI4 to IG4 and also hydrolyze IG4 to IG3 and Glc.

The enzyme activity of ORF9041-derived protein was assessed using the 1-h reaction mixture by ORF9042-derived protein. The predominant IG4 was degraded into IG3, IG2 and Glc (Figure 4-15 (c)). This result indicated that ORF9042-derived protein hydrolyzes IG4 to produce Glc. The result suggest that the enzyme hydrolyze an α-(1→6)-glucosidic linkage. Comparison of amino acid sequence among the ORF9041-derived protein, ORF5325-derived protein and 6 known oligo-1,6-glucosidases revealed that the ORF9041- and ORF5325-derived protein are homologous to the oligo-1,6-glucosidase, and that important residues for α-(1→6)-linkage selectivity are conserved in the ORF9041- and ORF5325-derived protein. Taken together with the results obtained in Figure 4-15 and sequence homology between the ORF9041-derived protein and 6 known oligo-1,6-glucosidases, the ORF9041-derived protein is assumed to be oligo-1,6-glucosidase. The oligo-1,6-glucosidase derived from *Agreia* sp. D1110 was named as Ag-oligo-1,6-glucosidase.

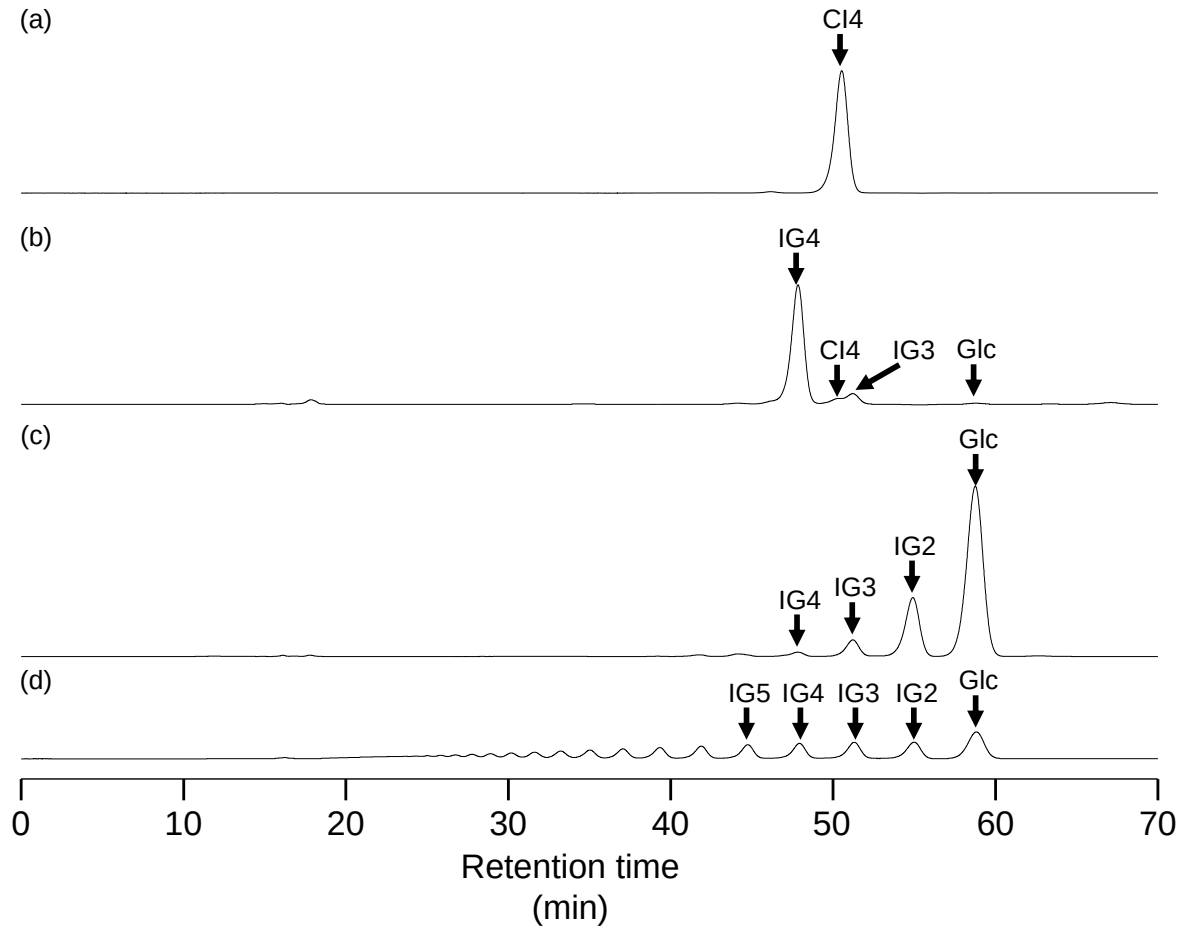

Figure 4-15 HPLC charts of reaction products in the reaction using ORF9042-derived protein and ORF9041-derived protein.

HPLC chromatograms of products in the reaction using ORF9042- and ORF9041-derived protein. (a) CI4. (b) Reaction product of ORF9042-derived protein. Purified ORF9042-derived protein and 10 mg/mL CI4 were incubated in 50 mM sodium acetate buffer (pH 6.0) at 37℃ for 1 h. The reaction mixture was heated at 95℃ for 10 min, deionized and applied to HPLC analysis. (c) Reaction products of ORF9041-derived protein. The reaction products obtained by reacting CI4 with purified ORF9042-derived protein (b) was heat treated and used as substrate. The reaction was done in 50 mM sodium acetate buffer (pH 6.0) at 37°C for 1 h. The reaction mixture heated and desalted was analyzed by HPLC. (d) Isomaltooligosaccharide marker.

The reaction using purified ORF9042-derived protein and each substrate

Action of ORF9042-derived protein on various saccharides (10 mg/mL) was analyzed (Figure 4-16). ORF9042-derived protein (1.0 μg/mL) weakly produced IG4 from CI4. In the reaction using 10 μg/mL ORF9042-derived protein, CI4 was completely degraded, and IG4, IG3 and Glc was produced (Figure 4-16 (a), (b)). ORF9042-derived protein (1.0 μg/mL) produced no reaction product from any other substrate candidates except CI4, while it produced reaction products from isomaltooligosaccharides (DP is from 4 to 7) at higher concentration (10 μg/mL). From IG5, 10 μg/mL ORF9042-derived protein produced Glc, IG3, and IG4 (Figure 4-16 (b)). From IG6, 10 μg/mL ORF9042-derived protein produced Glc, IG3, IG4 and IG5 (Figure 4-16 (b)). From IG7, 10 μg/mL ORF9042-derived protein produced Glc, IG6, IG5, IG4 and a small amount of IG3. IG2 was not produced from IG4-IG7. ORF9042-derived protein produced no reaction products from Glc, IG2, IG3, dextran T40, CNN and CMM. In the reaction with CI4 and 10 μg/mL ORF9042-derived protein, CI4 was completely degraded, whereas not all IG4 was degraded in the reaction with IG4 and 10 μg/mL ORF9042-derived protein. This result suggests that ORF9042-derived protein acted on CI4 more than IG4. ORF9042-derived protein produced no CI4 from dextran T40 (Figure 4-16 (a)) and no α-1,6 glucan longer than the substrates such as IG4, IG5, IG6 and IG7 (Figure 4-16 (b)). Based on the activity to hydrolyze CI4, ORF9042-derived protein was named as cycloisomaltotetraose hydrolase (CI4Hase). The CI4Hase encoded in ORF9042 from *Agreia* sp. D1110 was abbreviated as AgCI4Hase.

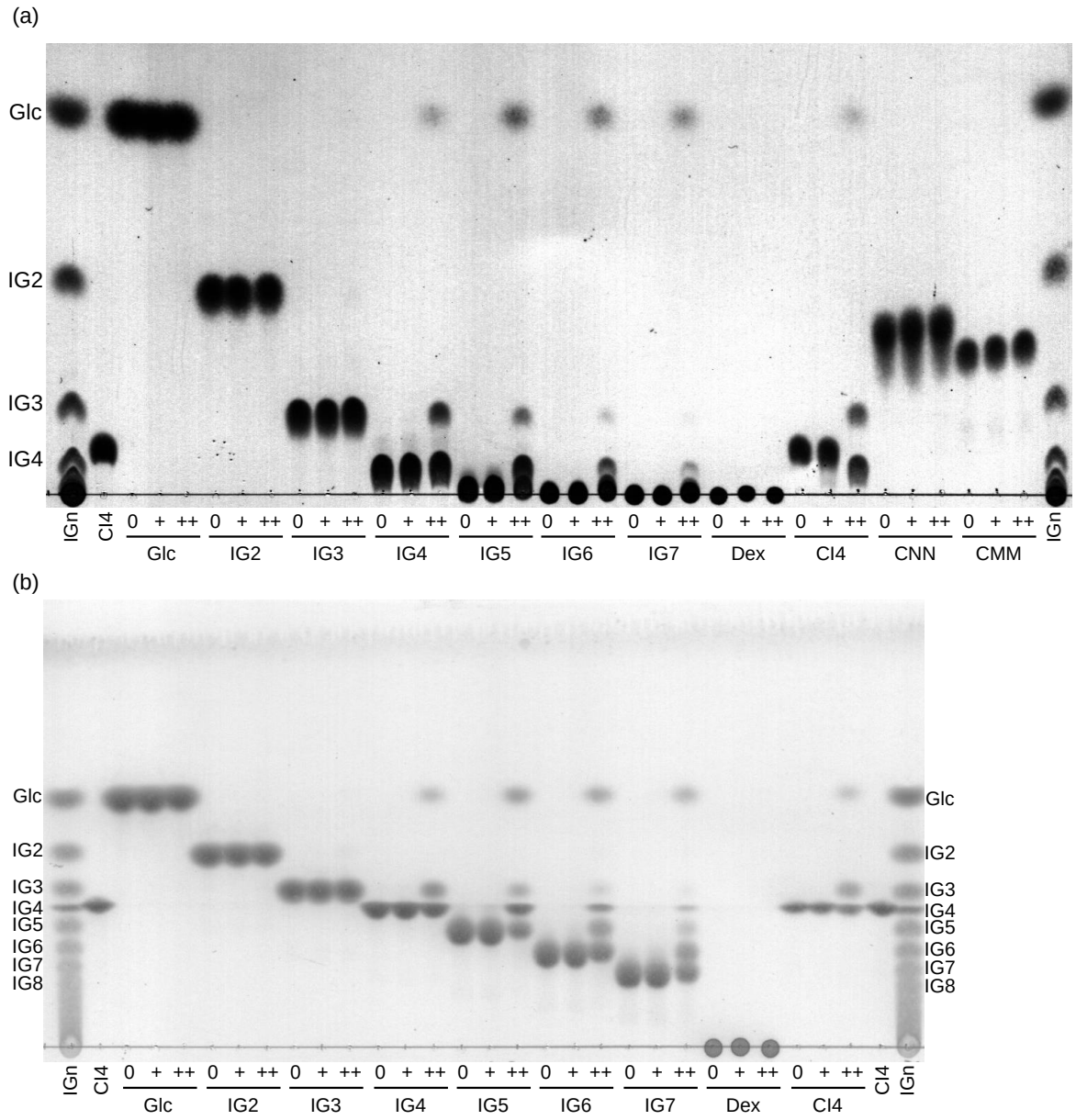

Figure 4-16 The reaction using purified ORF9042-derived protein and each substrate.

(a) Reaction products developed using the PBW solvent. (b) Reaction products developed using BEW solvent. +, 1.0 μg/mL ORF9042-derived protein, ++, 10 μg/mL ORF9042-derived protein. Dex, dextran T40. The plate was developed once using the PBW developing solvent.

BLASTP search

Agreia sp. D1110 and *M. trichothecenolyticum* D2006 belongs to *Microbacteriaceae* family and the two bacteria possessed gene clusters composed of genes encoding similar proteins (Table 4-3). To determine if bacteria of *Microbacteriaceae* family has AgCI4Tase, MtCI4Tase, AgCI4Hase and ORF5324-derived proteins, a BLAST search was performed using their sequences as query sequence. *Microbacteriaceae* protein sequences homologous to each query sequence were shown in Table 4-6. Table 4-6 (a) shows that *Microbacterium* sp. YMB-B2, *Microbacterium* sp. Leaf351, *Microbacterium* sp. Leaf347, *Leifsonia* bacteria., *Leifsonia* sp. ZF2019, *Leifsonia* sp. LS1 and *Leifsonia shinshuensis* possess the sequences homologous to the AgCI4Tase and MtCI4Tase. *Microbacterium* sp. YMB-B2, *Microbacterium* sp. Leaf351, *Leifsonia* sp. ZF2019, *Leifsonia* sp. LS1 also possessed the sequences homologous to the AgCI4Hase and the ORF5324-derived protein (Table 4-6(b)). These results suggested that *Microbacteriaceae* bacteria other than *Agreia* sp. D1110 and *M. trichothecenolyticum* D2006 possessed proteins homologous to the CI4Tases and proteins homologous to the AgCI4Hase and ORF5324-derived protein. *Microbacterium* sp. YMB-B2 and *Leifsonia* sp. ZF2019 possessed gene clusters similar to ones observed in *Agreia* sp. D1110 and *M. trichothecenolyticum* D2006 (Table 4-7, Figure 4-17). The proteins in *Microbacterium* sp. YMB-B2, WP_227529647.1, WP_227529648.1 and WP_227529649.1, showed 72%, 68% and 68% identity on AgCI4Tase, Ag-oligo-1,6-glucosidase and AgCI4Hase respectively (Table 4-7 (a)). The proteins in *Leifsonia* sp. ZF2019, WP_223359054.1, WP_223359059.1 and WP_223359060.1 showed 49%, 57% and 60% identity on AgCI4Tase, AgCI4Hase and Ag-oligo-1,6-glucosidase.

Table 4-6 (a) *Microbacteriaceae* protein sequences homologous to AgCI4Tase and MtCI4Tase encoded by ORF9038 or ORF5328, respectively.

Strain	Length	Accession	AgCI4Tase		MtCI4Tase	
			E value	Identity (%)	E value	Identity (%)
Microbacterium sp. YMB-B2	843	WP_227529647.1	0	72	0	94
Leifsonia	869	WP_208041632.1	0	49	0	52
Leifsonia sp. ZF2019	869	WP_223359054.1	0	49	0	52
Leifsonia sp. LS1	869	WP_226656701.1	0	49	0	52
Microbacterium sp. Leaf347	867	WP_056519258.1	0	50	0	53
Leifsonia shinshuensis	732	NYJ25833.1	0	49	0	52
Microbacterium sp. Leaf351	578	WP_156456236.1	4.0×10^{-159}	51	1.0×10^{-152}	54

Sequences homologous to AgCI4Tase and MtCI4Tase are shown in the table.

Table 4-6 (b) *Microbacteriaceae* protein sequences homologous to AgCI4Hase and ORF5324-derived protein encoded by ORF9042 and ORF5324, respectively.

Strain	Length	Accession	AgCI4Hase		ORF5324-derived protein	
			E value	Identity (%)	E value	Identity (%)
Microbacterium oryzae	533	WP_156241192.1	0	69	0	62
Microbacterium sp. YMB-B2	530	WP_227529649.1	0	68	0	94
Microbacterium saccharophilum	530	WP_147049665.1	0	67	0	77
Microbacterium flavum	527	WP_246539854.1	0	67	0	77
Microbacterium flavum	530	MBT8797499.1	0	67	0	77
Microbacterium aurum	532	WP_239541904.1	0	66	0	77
Microbacterium aurum	530	WP_076689203.1	0	66	0	77
Salinibacterium sp.	531	MBC7591431.1	0	61	0	62
Microbacteriaceae bacterium	539	RQP11821.1	0	60	0	62
Marisediminicola antarctica	538	QHO70311.1	0	57	0	59
Pseudolysinimonas yzui	542	WP_191282304.1	0	61	0	62
Leifsonia sp.	530	MBN9239222.1	0	61	0	64
Microbacterium sp. Leaf351	532	KQR93944.1	0	57	0	58
unclassified *Microbacterium*	529	WP_162237854.1	0	57	0	58
Leifsonia	539	WP_208041633.1	0	57	0	61
Leifsonia sp. LS1	539	WP_226656693.1	0	57	0	62
Marisediminicola antarctica	501	WP_236966531.1	0	59	0	62
Galbitalea soli	541	WP_163474539.1	0	57	0	60
Leifsonia sp. ZF2019	534	UAJ81377.1	0	57	0	61
Leifsonia sp. AG29	533	WP_158865878.1	0	57	0	59
Leifsonia sp. ZF2019	539	WP_223359059.1	0	57	0	62
Microbacteriaceae bacterium	535	TAM70476.1	0	57	0	60
Microbacteriaceae bacterium	466	HAM27874.1	0	62	0	63
Microbacterium immunditiarum	559	WP_179486708.1	8.0×10^{-177}	58	2.0×10^{-167}	59

Sequences homologous to AgCI4Hase and the ORF5324-derived protein are shown in the table.

Table 4-7 (a) A gene cluster in *Microbacterium* sp. YMB-B2.

Start	Stop	Genbank accession	Annotation
454,694	457,225	WP_227529647.1	ricin-type beta-trefoil lectin domain protein[1]
457,282	459,018	WP_227529648.1	alpha-glucosidase[2]
459,005	460,597	WP_227529649.1	hypothetical protein[3]
460,600	461,439	WP_227529650.1	carbohydrate ABC transporter permease
461,436	462,392	WP_227529651.1	sugar ABC transporter permease
462,392	463,663	WP_227529652.1	extracellular solute-binding protein

Ricin-type beta-trefoil lectin domain protein[1], amino acid sequence identity of this protein on AgCI4Tase is 72%; alpha-glucosidase[2], the identity of this protein on Ag-oligo-1,6-glucosidase is 68%; hypothetical protein[3], the identity of this protein on AgCI4Hase is 68%.

Table 4-7 (b) A gene cluster in *Leifsonia* sp. ZF2019.

Start	Stop	Genbank accession	Annotation
346,878	349,487	WP_223359054.1	carbohydrate-binding protein[1]
349,539	350,564	WP_223359055.1	ROK family protein
350,888	352,177	WP_223359056.1	extracellular solute-binding protein
352,308	353,204	WP_223359057.1	sugar ABC transporter permease
353,201	354,091	WP_223359058.1	carbohydrate ABC transporter permease
354,088	355,707	WP_223359059.1	hypothetical protein[2]
355,704	357,464	WP_223359060.1	alpha-glucosidase[3]

Carbohydrate-binding protein[1], amino acid sequence identity of this protein on AgCI4Tase is 49%; hypothetical protein[2], the identity of this protein on AgCI4Hase protein is 57%; alpha-glucosidase[3], the identity of this protein on Ag-oligo-1,6-glucosidase is 60%.

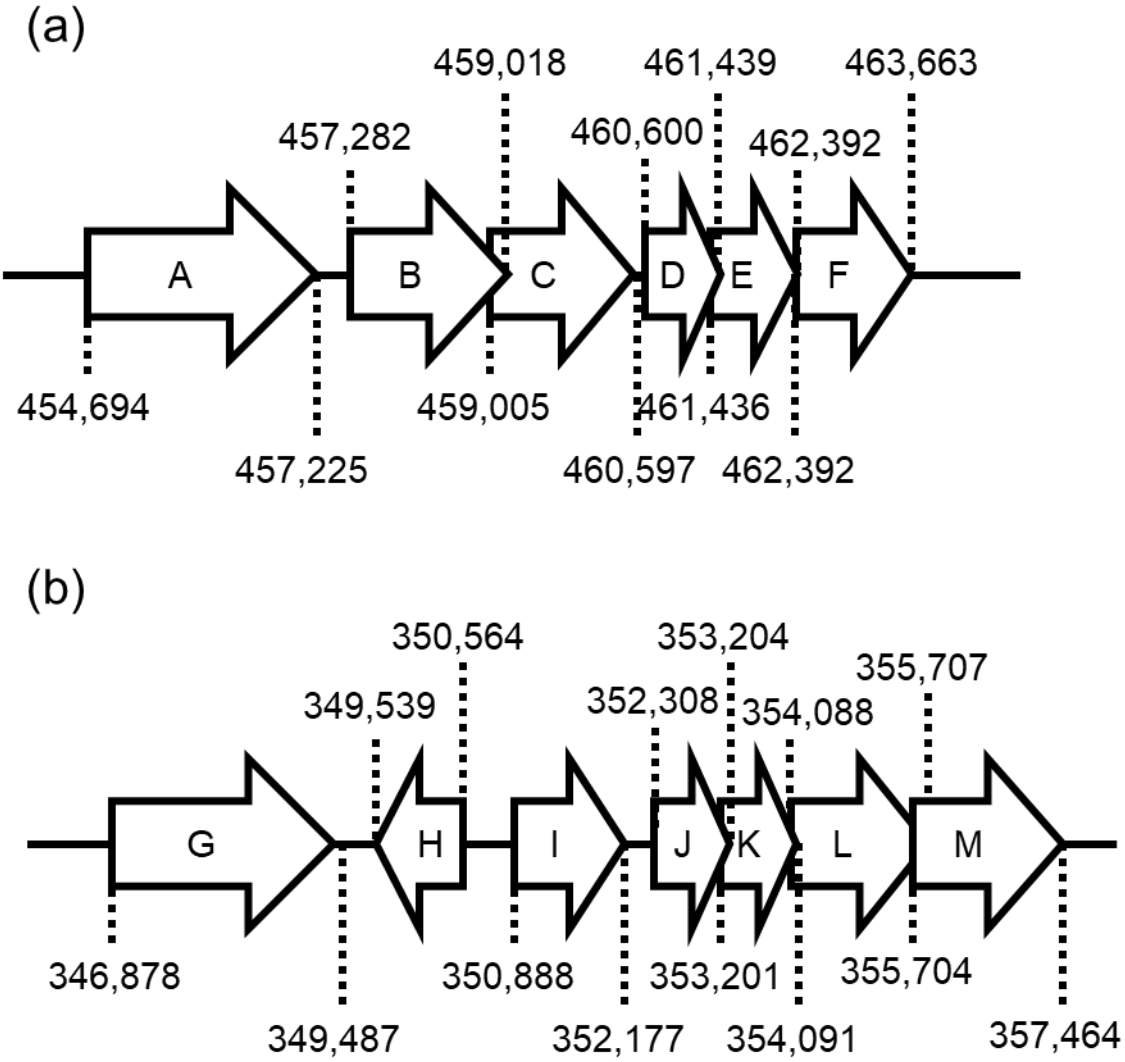

Figure 4-17 Gene clusters in *Microbacteriaceae* bacteria.

(a) A gene cluster in *Microbacterium* sp. YMB-B2. A, WP_227529647.1; B, WP_227529648.1; C, WP_227529649.1; D, WP_227529650.1; E, WP_227529651.1; F, WP_227529652.1. (b) A gene cluster in *Leifsonia* sp. ZF2019. G, WP_223359054.1; H, WP_223359055.1; I, WP_223359056.1; J, WP_223359057.1; K, WP_223359058.1; L, WP_223359059.1; M, WP_223359060.1

Discussion

In this chapter, based on the draft genome sequences of *Agreia* sp. D1110 and *M. trichothecenolyticum* D2006, the genes encoding AgCI4Tase and MtCI4Tase were identified with activity confirmation using recombinant enzymes. The sequences suggest that CI4Tases possess Glyco_hydro_66 domain, CBM35-1 domain and CBM13 domain and that the enzymes are thus categorized into GH66 together with CITases and dextranases (Figure 4-4). Identity of amino acid sequences between the CI4Tases was 71% both with and without gaps. Their highest identities to CITases were 30% with gaps and 35% without gaps (Table 4-1).

Not only the overall sequence similarity, but essential residues conserved in other GH66 CITases were conserved in both the CI4Tases (Figure 4-5). The CI4Tases possess Asp and Glu corresponding to invariant nucleophile and general acid/base catalysts of CITases, and the Ala substitution of the two residues of AgCI4Tase, D289A, E356A and D289A/E356A, resulted in significant loss of activity to produce CI4 from dextran (Figure 4-7). The results indicate that Asp289 and Glu356 in AgCI4Tase are essential for its enzymatic activity probably through functioning as catalytic residues. Several residues involved in the formation of subsites −1, −2, −3 and −4 in 3D-structure-available CITase-T-3040 were conserved in two CI4Tases (Table 4-2(a)). This suggests that active site and substrate binding site of CI4Tases are likely shared with CITases.

On the other hand, residues involved in the formation of subsite −5, −6, −7 and −8 were not conserved in two CI4Tases (Table 4-2(b)). Residues near subsite −5 of CITase-T-3040, Leu206, Phe207 and Phe268, were replaced by Trp, Asn and Pro, respectively, in two CI4Tases. Considering the CI4-formation of CI4Tase, CI4Tases require isomaltooligosaccharides binding to subsite −4, whereas CITases require their binding to subsite −8 for CI8 formation by cyclization. The difference in subsite −5 and farther subsites must be critical for CI4Tase activity. In addition, Met310 in CITase-T-3040 is conserved in the CITases and is reported to

be involved in the predominant production of CI8 (N. Suzuki *et al*., 2014), but replaced by Leu in two CI4Tases. The Met substitution for Leu291 of AgCI4Tase (L291M) gave no effect on the CI4-specific production of CI4Tase (Figure 4-7). The results suggested that the Leu residue in the AgCI4Tase is not involved in determination of DP of the products.

The draft genome sequence analyses of *Agreia* sp. D1110 and *M. trichothecenolyticum* D2006 revealed that the *ci4tase* gene constitutes a gene cluster, associated with dextran assimilation via CI4 in both the bacteria (Table 4-3). Putative promoter and terminator regions are in upstream and downstream regions of the gene clusters. These genes are predicted to be polycistronically expressed and the enzymes encoded in the gene clusters work in concert with CI4Tase. Bacteria producing other cyclic tetrasaccharides possess gene clusters similar to those found in *Agreia* sp. D1110 and *M. trichothecenolyticum* D2006 (Kohno *et al*., 2018; Light *et al*., 2016; Tagami *et al*., 2016), which are predicted to be involved in the production and degradation of the tetrasaccharides. CNN producing bacterium, *K. flavida* NBRC 14399, possesses two gene clusters involved in CNN production and metabolism (Tagami *et al*., 2016) and gene clusters involved in CNN production and metabolism are also reported in *L. monocytogenes* (Light *et al*., 2016). CMM producing bacterium, *A. globiformis* M6, possesses a gene cluster involved in CMM production and degradation (Kohno *et al*., 2018).

Two proteins encoded in the gene cluster of *Agreia* sp. D1110 were named as AgCI4Hase and Ag-oligo-1,6-glucosidase using recombinant enzymes. AgCI4Hase catalyzed the formation of IG4 from CI4 through hydrolysis of the α-(1→6)-glucosidic linkage in CI4 specifically, but not in CNN and CMM (Figure 4-16). The enzyme showed no other activities on dextran such as hydrolytic activity and intramolecular transglycosylation activity to produce CI4. AgCI4Hase acted on IG4 to IG7 with considerably less activity than on CI4. The substrates were degraded down to IG3, along with the formation of Glc. This suggests that the AgCI4Hase hydrolyzes linear isomaltooligosaccharides (DP≥4) in a glucosyl unit from the ends of the linear substrates,

although it is not clear from which ends of the linear substrates glucosyl residues are released. In summary, CI4Hase is a novel enzyme possessing following two activities: 1) Specific hydrolysis of an α-(1→6)-glucosidic linkage in CI4 to produce IG4, 2) Hydrolysis of linear isomaltooligosaccharides (DP≥4) to release Glc from the ends of the linear substrates with lower velocity than on CI4. The CI4Hase possess no intramolecular transglycosylation activity.

The Ag-oligo-1,6-glucosidase acted on the substrate containing a large portion of IG4 and a small portion of CI4, IG3 and Glc (Figure 4-15 (b)). The reaction product contained IG4, IG3, IG2 and Glc (Figure 4-15(c)). The production of Glc in Figure 4-15(c) would be the results of oligo-1,6-glucosidase's hydrolyzing IG4 to Glc. By the two enzymes, AgCI4Hase and Ag-oligo-1,6-glucosidase, CI4 was degraded mostly to Glc (Figure 4-15).

Agreia is a Gram-positive bacterium and it has been reported that solute-binding proteins in Gram-positive bacteria are membrane-anchored type (Singh & Röhm, 2008). Therefore, the putative solute-binding protein in *Agreia* sp. D1110 is assumed to be membrane-anchored type.

On the basis of the predicted localization of proteins encoded in the gene cluster and confirmed activities of AgCI4Tases, AgCI4Hase and Ag-oligo-1,6-glucosidase, a CI4 production and metabolism model in *Agreia* sp. D1110 is proposed (Figure 4-18): Here, *Agreia* sp. D1110 secretes CI4Tase (ORF9038) outside the bacterium to produce CI4 from dextran. This CI4 is captured by the putative solute-binding protein (ORF9045), and putative ABC transporter consisting of transmembrane domains (ORF9043 and ORF9044) takes up CI4 into the cell. Internalized CI4 is hydrolyzed to IG4 by AgCI4Hase (ORF9042) and degraded to Glc by Ag-oligo-1,6-glucosidase (ORF9041). As *M. trichothecenolyticum* D2006 possessed the gene cluster similar to one in *Agreia* sp. D1110, *M. trichothecenolyticum* D2006 is assumed to possess the CI4 production and metabolism pathway. Taken together with the results that two CI4-producing bacteria grow in the media containing dextran as a sole carbon source and CI4 and CI4Tases were isolated from the culture supernatant, it is concluded that these bacteria

assimilate dextran using the proposed CI4-production and metabolism pathway. *Microbacteriaceae* bacteria such as *Microbacterium* sp. YMB-B2, *Microbacterium* sp. Leaf351, *Leifsonia* sp. ZF2019 and *Leifsonia* sp. LS1 possessed a set of homologous to CI4Tase and CI4Hase (Table 4-6). Figure 4-17 showed that gene clusters similar to ones in *Agreia* sp. D1110 and *M. trichothecenolyticum* D2006 were observed in *Microbacterium* sp. YMB-B2 and *Leifsonia* sp. ZF2019, indicating these 4 bacteria also would assimilate dextran via the CI4-production and metabolism pathway (Figure 4-18). The pathway would be conserved in some of *Microbacteriaceae* bacteria.

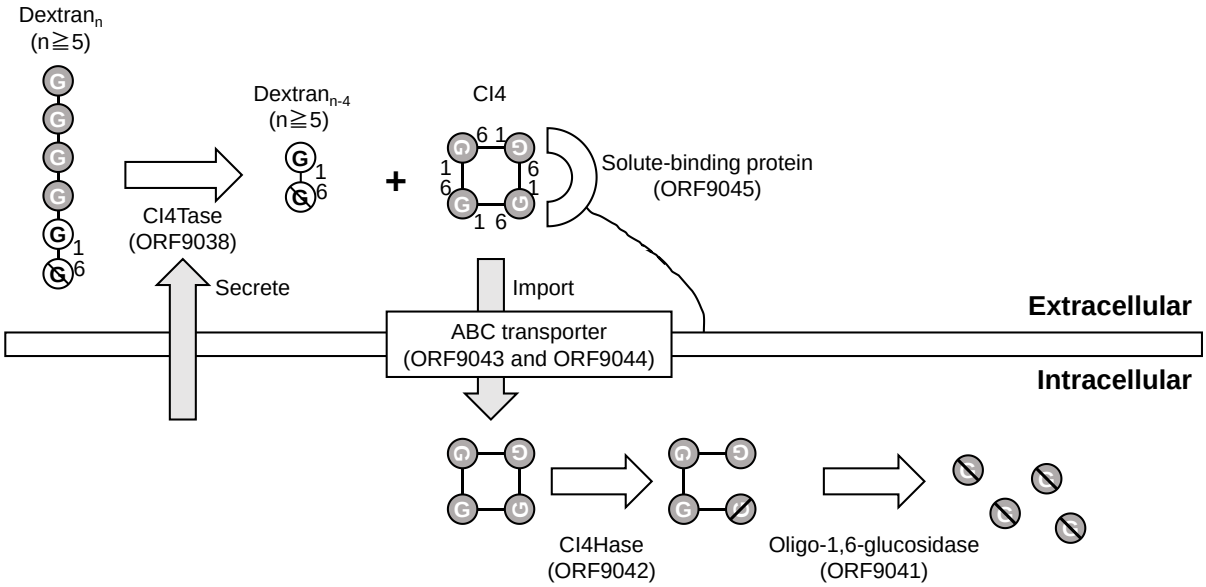

Figure 4-18 Model of CI4-production and CI4-metabolism in *Agreia* sp. D1110.

Similar model is proposed in *M. trichothecenolyticum* D2006.

Chapter 5 General conclusions

In this study, enzymes producing novel oligosaccharides from dextran were searched from soil-derived bacteria to expand oligosaccharide production technologies. The findings in this study are summarized as follows.

In chapter 2, it was described that the culture supernatants of *Agreia* sp. D1110 and *M. trichothecenolyticum* D2006, microorganisms in the *Microbacteriaceae* family, produced a novel cyclic tetrasaccharide, CI4, from dextran. CI4 is the smallest CIs, and the crystal of CI4 was firstly obtained in CIs. *In vitro* digestion experiments showed that CI4 is an indigestible carbohydrate.

In chapter 3, AgCI4Tase and MtCI4Tase were purified from the culture supernatants of *Agreia* sp. D1110 and *M. trichothecenolyticum* D2006, respectively, as CI4-producing enzymes. AgCI4Tase and MtCI4Tase had similar optimal temperature and optimal pH, while AgCI4Tase had a wider stability range in terms of pH stability and temperature stability. AgCI4Tase and MtCI4Tase catalyzed 1) cyclization reaction of isomaltooligosaccharides to produce CI4, 2) disproportionation reaction between isomaltooligosaccharides mainly at IG4 unit, 3) hydrolysis reaction of CI4, and 4) coupling reaction between CI4 and isomaltooligosaccharides. The known CITases produce CIs of various DPs, while the two CI4Tases specifically produced CI4 as cyclic oligosaccharides, which is the most striking difference between them. It was shown that the CI4-producing activity observed in the culture supernatants of *Agreia* sp. D1110 and *M. trichothecenolyticum* D2006 were the activity of the CI4Tases.

In chapter 4, the draft genome sequences of *Agreia* sp. D1110 and *M. trichothecenolyticum* D2006 were obtained. Full amino acid sequences of AgCI4Tase and MtCI4Tase were determined on the basis of the obtained draft genome sequences and activity of recombinant enzymes. The sequence identity between the two CI4Tases was 71% both with and without gaps, and their highest sequence identities with the three known CITases were 30% with gaps

and 35% without gaps. The two CI4Tase were composed of the Glyco_hydro_66 domain, the CBM35-1 domain inserted in the Glyco_hydro_66 domain, and the CBM13 domain at the C-terminus. The general acid/base catalytic and nucleophilic catalytic residues of the three CITases were conserved in the two CI4Tases. AgCI4Tase(D289A), AgCI4Tase(E356A), and AgCI4Tase(D289A/E356A), in which two putative catalytic residues were replaced by Ala, lost CI4-producing activity, indicating that both residues are essential for the activity. Met310 important for cyclization in the CITase-T-3040 was replaced by a Leu residue in the two CI4Tases. AgCI4Tase(L291M) produced CI4 and no other cyclic oligosaccharides, indicating that the Leu residue does not independently affect DP of the product. Compared with the CITases, the CI4Tases possessed characteristic insertions (Insert 1, 2) and deletions (Deletion 1, 2). The subsites from −1 to −4 in the CITase-T-3040 were conserved in the two CI4Tases, while the subsite −5 in the CITase-T-3040 was mutated to other amino acids in the CI4Tases. Insertions, deletions and amino acid mutations in the subsite −5 could affect the IG4 specificity of the CI4Tases.

The two CI4-producing bacteria possessed the gene clusters presumably involved in CI4 production and metabolism. The AgCI4Hase encoded in the gene cluster of *Agreia* sp. D1110 hydrolyzed CI4 to produce IG4. IG4 was degraded to Glc by Ag-oligo-1,6-glucosidase encoded in the gene cluster. Based on these results, the model for dextran metabolism pathway in the two CI4-producing bacteria was proposed. Other *Microbacteriaceae* microorganisms such as *Microbacterium* sp. YMB-B2, *Microbacterium* sp. Leaf351, *Leifsonia* sp. ZF2019 and *Leifsonia* sp. LS1 also had enzymes homologous to CI4Tase and CI4Hase.

These findings obtained in this study lead to the following general discussions.

CI4-producing bacteria, *Agreia* sp. D1110 and *M. trichothecenolyticum* D2006, extracellularly produce CI4 from dextran by the action of the CI4Tases, and the CI4 produced is incorporated into the bacteria. AgCI4Hase and AG-oligo-1,6-glucosidase intracellularly degrade the

incorporated CI4 into Glc, which the bacteria can assimilate (Figure 4-18). When α-glucosidase, glucoamylase or dextranase were acted on CI4 under the condition that other linear isomaltooligosaccharides were completely degraded to Glc, CI4 remained (Figures 2-2, 2-13). This result suggests that CI4 is less degradable by these enzymes. Other examples of production and metabolism of cyclic oligosaccharides which are less susceptible to enzymatic degradation have been reported in CNN and CMM-producing bacteria. This cyclic oligosaccharide production-degradation system is understood to have a physiological significance as follows: The cyclic oligosaccharide producing-bacteria monopolizes the carbon sources by converting carbon sources degradable for a wide range of enzymes into cyclic oligosaccharides undegradable without enzyme to degrade the cyclic oligosaccharides (Kohno *et al*., 2018; Tagami *et al*., 2016). Based on the results obtained in this study, CI4 is assumed to be less degradable by a wide range of microbial enzymes such as α-glucosidase, glucoamylase and dextranase, and CI4 production-metabolism is also assumed to have physiological significance to monopolize carbon sources.

Generally, dextran is not widely found in nature. Therefore, it is likely that CI4-producing bacteria produce dextran or alternative substrate from other widely available carbohydrates for the CI4 production. A CITase-producing bacterium *Paenibacillus* sp. 598K produces CIs from starch even in the absence of dextran using CITase and 6GT (Ichinose *et al*., 2017). The bacterium produces 6GT to yield α-1,6 glucan at the non-reducing ends of starch, and CITase acts on the α-1,6 glucan to produce CIs. In the draft genome sequences of *Agreia* sp. D1110 and *M. trichothecenolyticum* D2006, however, no genes involved in the production of α-(1→6)-glucan, such as homologous genes coding for dextran dextrinase from *G. oxydans* ATCC11894 (Sadahiro *et al*., 2015), dextran sucrase from *L. mesenteroides* NRRL B512F (Naessens *et al*., 2005) and 6GT from *Paenibacillus* sp. 598K (Tsusaki *et al*., 2009, 2012) were found. This suggests that the CI4-producing bacteria use dextran and related α-1,6 glucan, which are

produced by other bacteria.

Other than *Agreia* sp. D1110 and *M. trichothecenolyticum* D2006, microorganisms in the *Microbacteriaceae* family such as *Microbacterium* sp. YMB-B2, *Microbacterium* sp. Leaf351, *Leifsonia* sp. ZF2019 and *Leifsonia* sp. LS1 also have enzymes homologous to CI4Tase and CI4Hase, suggesting that these microorganisms would also have the CI4 production-metabolism system. *Microbacteriaceae* are known to live in soil and associated with plants (Evtushenko & Takeuchi, 2006). In particular, the bacteria in *Microbacterium* species are associated with plant roots, and volatile molecules produced by the bacteria have been reported to increase biomass in the roots and shoots of lettuce and tomatoes, thereby promoting their growth (Cordovez *et al*., 2022). Some strains of *Leifsonia* species are also known to promote plant growth, and the bacteria have been reported to improve stress tolerance and quality of water-stressed greenhouse ornamentals (Nordstedt *et al*., 2021). Looking ahead, investigating whether CI4 selectively proliferates these useful microorganisms of the *Microbacteriaceae* family will lead to the possibility of developing CI4 as biostimulants.

The establishment of an industrial manufacturing process is important for the commercial development of CI4. When purified AgCI4Tase and MtCI4Tase were acted on dextran, the maximum production rates were 19% for AgCI4Tase and 14% for MtCI4Tase (Table 3-4). When the reaction time was extended, CI4 was decreased and IG4, IG8, and IG12 were increased (Table 3-4). Since the CI4Tases catalyze hydrolysis of CI4 and coupling reactions between CI4 and isomaltooligosaccharides (Figures 3-6 and 3-8), the decrease in CI4 observed in Table 3-4 could be the result of hydrolysis and coupling reactions. In chapter 2, 34 g of CI4 was produced from 100 g of dextran in the system using ultrafiltration membrane (production rate: 34%. Table 2-5). In the system using ultrafiltration membrane, the production rate was 1.6 times higher than that of the reaction of the batch reaction using the purified enzymes. In the system using the ultrafiltration membrane, the produced CI4 was separated from the enzyme,

which would reduce the progress of hydrolysis and coupling reactions by the CI4Tases, contributing the increase of CI4 production rate. As a future perspective, a continuous reaction combining the CI4 separation using ultrafiltration membrane and addition of substrate would lead to the establishment of an efficient manufacturing process for CI4.

In terms of industrial production, the price of the starting material is also important. In this study, α-1,6 glucan was prepared by the action of 6GT on liquefied starch, followed by the action of MtCI4Tase to produce CI4 (Table 3-5). These results suggest a possibility that CI4 can be produced from starch, which is a raw material more inexpensive than dextran. The CI4 production rate from the α-1,6 glucan prepared by this method was low at 6.2% (24-h reaction + digestion) and 4.8% (72-h reaction + digestion) (Table 3-5). Even when the reaction time was extended from 24 to 72 h, there was almost no decrease in the amount of substrate above DP4, suggesting that the isomaltooligosaccharide structure above DP6 that is necessary for CI4 production, was not present at the non-reducing ends of the substrate at 24 h. As a future prospect, the preparation of substrates for the CI4Tases using DDase, which can prepare α-1,6 glucans chain longer than 6GT, would increase the CI4 production rate from starch.

In this study, CI4Tases were discovered and CI4 was produced from dextran using the CI4Tases. CI4 was also produced from α-1,6-glucan prepared from the liquefied starch. The CI4Hases, which hydrolyze the α-(1→6)-glucosidic linkages in CI4, were found by draft genome analysis of CI4-producing bacteria. The discovery of both enzymes suggests that dextran-related enzymes as diverse as starch-related enzymes still exist in nature. These results would lead to the expansion of oligosaccharide production technology using raw materials, starch and dextran.

References

Adachi, M., Mikami, B., Katsube, T., & Utsumi, S. (1998). Crystal structure of recombinant soybean β-amylase complexed with β-cyclodextrin. *Journal of Biological Chemistry*, **273**(31), 19859–19865. doi:10.1074/jbc.273.31.19859

Aga, H., Higashiyama, T., Watanabe, H., Sonoda, T., Nishimoto, T., Kubota, M., Fukuda, S., Kurimoto, M., & Tsujisaka, Y. (2002). Production of cyclic tetrasaccharide from starch using a novel enzyme system from *Bacillus globisporus* C11. *Journal of Bioscience and Bioengineering*, **94**(4), 336–342. doi:10.1016/S1389-1723(02)80174-8

Aga, H., Maruta, K., Yamamoto, T., Kubota, M., Fukuda, S., Kurimoto, M., & Tsujisaka, Y. (2002). Cloning and sequencing of the genes encoding cyclic tetrasaccharide-synthesizing enzymes from *Bacillus globisporus* C11. *Bioscience, Biotechnology, and Biochemistry*, **66**(5), 1057–1068. doi:10.1271/bbb.66.1057

Almagro Armenteros, J. J., Tsirigos, K. D., Sønderby, C. K., Petersen, T. N., Winther, O., Brunak, S., von Heijne, G., & Nielsen, H. (2019). SignalP 5.0 improves signal peptide predictions using deep neural networks. *Nature Biotechnology*, **37**(4), 420–423. doi:10.1038/s41587-019-0036-z

AOAC international. (2016). Vitamines and other nutrients. In G. Latimer (Ed.), *Official Methods of Analysis of AOAC INTERNATIONAL* (20th edition., pp. 111–116).

Berlina, Y. Y., Petrovskaya, L. E., Kryukova, E. A., Shingarova, L. N., Gapizov, S. S., Kryukova, M. V, Rivkina, E. M., Kirpichnikov, M. P., & Dolgikh, D. A. (2021). Engineering of thermal stability in a cold-active oligo-1,6-glucosidase from *Exiguobacterium sibiricum* with unusual amino acid content. *Biomolecules*, **11**(8), 1229-1244. doi:10.3390/biom11081229

Bolger, A. M., Lohse, M., & Usadel, B. (2014). Trimmomatic: a flexible trimmer for Illumina sequence data. *Bioinformatics*, **30**(15), 2114–2120. doi:10.1093/bioinformatics/btu170

Bruno, I. J., Cole, J. C., Edgington, P. R., Kessler, M., Macrae, C. F., McCabe, P., Pearson, J., & Taylor, R. (2002). New software for searching the cambridge structural database and visualizing crystal structures. *Acta Crystallographica Section B*, **58**(3 Part 1), 389–397. doi:10.1107/S0108768102003324

Chiba, S., Kimura, A., & Matsui, H. (1983). Quantitative study of anomeric forms of glucose produced by α-glucosidases and glucoamylases. *Agricultural and Biological Chemistry*, **47**(8), 1741–1746. doi:10.1271/bbb1961.47.1741

Chun, J., Lee, J. H., Jung, Y., Kim, M., Kim, S., Kim, B. K., & Lim, Y. W. (2007). EzTaxon: a

web-based tool for the identification of prokaryotes based on 16S ribosomal RNA gene sequences. *International Journal of Systematic and Evolutionary Microbiology*, **57**(10), 2259–2261. doi:10.1099/ijs.0.64915-0

Ciucanu, I., & Kerek, F. (1984). A simple and rapid method for the permethylation of carbohydrates. *Carbohydrate Research*, **131**(2), 209–217. doi:10.1016/0008-6215(84)85242-8

Cordovez, V., Schop, S., Hordijk, K., Dupré de Boulois, H., Coppens, F., Hanssen, I., Raaijmakers, J. M., & Carrión, V. J. (2022). Priming of plant growth promotion by volatiles of root-associated *Microbacterium* spp. *Applied and Environmental Microbiology*, **84**(22), e01865-18. doi:10.1128/AEM.01865-18

Delcher, A. L., Bratke, K. A., Powers, E. C., & Salzberg, S. L. (2007). Identifying bacterial genes and endosymbiont DNA with Glimmer. *Bioinformatics*, **23**(6), 673–679. doi:10.1093/bioinformatics/btm009

Drula, E., Garron, M. L., Dogan, S., Lombard, V., Henrissat, B., & Terrapon, N. (2022). The carbohydrate-active enzyme database: functions and literature. *Nucleic Acids Research*, **50**(D1), D571–D577. doi:10.1093/nar/gkab1045

Duan, K. J., Sheu, D. C., & Lin, C. T. (1995). Transglucosylation of a fungal α-glucosidase. *Annals of the New York Academy of Sciences*, **750**(1), 325–328. doi:10.1111/j.1749-6632.1995.tb19974.x

Elvira, K., Petri, S., & Timo, K. (2005). Microbial dextran-hydrolyzing enzymes: fundamentals and applications. *Microbiology and Molecular Biology Reviews*, **69**(2), 306–325. doi:10.1128/MMBR.69.2.306-325.2005

Evtushenko, L. I., & Takeuchi, M. (2006). The family *Microbacteriaceae* BT - The *Prokaryotes*: Volume 3: *Archaea*. *Bacteria*: *Firmicutes*, *Actinomycetes* (M. Dworkin, S. Falkow, E. Rosenberg, K. H. Schleifer, & E. Stackebrandt (Eds.); pp. 1020–1098). Springer New York. doi:10.1007/0-387-30743-5_43

Funane, K., Terasawa, K., Mizuno, Y., Ono, H., Gibu, S., Tokashiki, T., Kawabata, Y., Kim, Y. M., Kimura, A., & Kobayashi, M. (2008). Isolation of *Bacillus* and *Paenibacillus* bacterial strains that produce large molecules of cyclic isomaltooligosaccharides. *Bioscience, Biotechnology, and Biochemistry*, **72**(12), 3277–3280. doi:10.1271/bbb.80384

Funane, K., Terasawa, K., Mizuno, Y., Ono, H., Miyagi, T., Gibu, S., Tokashiki, T., Kawabata, Y., Kim, Y. M., Kimura, A., & Kobayashi, M. (2007). A novel cyclic isomaltooligosaccharide (cycloisomaltodecaose, CI-10) produced by *Bacillus circulans* T-

3040 displays remarkable inclusion ability compared with cyclodextrins. *Journal of Biotechnology*, **130**(2), 188–192. doi:10.1016/j.jbiotec.2007.03.009

Hakomori, S. (1964). A rapid permethylation of glycolipid, and polysaccharide catalyzed by methylsulfinyl carbanion in dimethyl sulfoxide. *The Journal of Biochemistry*, **55**(2), 205–208. doi:10.1093/oxfordjournals.jbchem.a127869

Harada, T., Yokobayashi, K., & Misaki, A. (1968). Formation of isoamylase by *Pseudomonas*. *Applied Microbiology*, **16**(10), 1439–1444. doi:10.1128/am.16.10.1439-1444.1968

Ichinose, H., Suzuki, R., Miyazaki, T., Kimura, K., Momma, M., Suzuki, N., Fujimoto, Z., Kimura, A., & Funane, K. (2017). *Paenibacillus* sp. 598K 6-α-glucosyltransferase is essential for cycloisomaltooligosaccharide synthesis from α-(1→4)-glucan. *Applied Microbiology and Biotechnology*, **101**(10), 4115–4128. doi:10.1007/s00253-017-8174-z

Jönsson, A. S., & Trägårdh, G. (1990). Ultrafiltration applications. *Desalination*, **77**, 135–179. doi:10.1016/0011-9164(90)85024-5

Kajitani, R., Toshimoto, K., Noguchi, H., Toyoda, A., Ogura, Y., Okuno, M., Yabana, M., Harada, M., Nagayasu, E., Maruyama, H., Kohara, Y., Fujiyama, A., Hayashi, T., & Itoh, T. (2014). Efficient de novo assembly of highly heterozygous genomes from whole-genome shotgun short reads. *Genome Research*, **24**(8), 1384–1395. doi:10.1101/gr.170720.113

Kato, T., & Horikoshi, K. (1986). A new γ-cyclodextrin forming enzyme produced by *Bacillus subtilis* no. 313. *Journal of the Japanese Society of Starch Science*, **33**(2), 137–143. doi:10.5458/jag1972.33.137

Kim, Y. K., Kitaoka, M., Hayashi, K., Kim, C. H., & Côté, G. L. (2004). Purification and characterization of an intracellular cycloalternan-degrading enzyme from *Bacillus* sp. NRRL B-21195. *Carbohydrate Research*, **339**(6), 1179–1184. doi:10.1016/j.carres.2004.02.008

Kita, A., Matsui, H., Somoto, A., Kimura, A., Takata, M., & Chiba, S. (1991). Substrate specificity and subsite affinities of crystalline α-glucosidase from *Aspergillus niger*. *Agricultural and Biological Chemistry*, **55**(9), 2327–2335. doi:10.1080/00021369.1991.10870952

Kitahata, S., Tsuyama, N., & Okada, S. (1974). Purification and some properties of cyclodextrin glycosyltransferase from a strain of *Bacillus* species. *Agricultural and Biological Chemistry*, **38**(2), 387–393. doi:10.1080/00021369.1974.10861152

Kobayashi, M., Funane, K., & Oguma, T. (1995). Inhibition of dextran and mutan synthesis by

cycloisomaltooligosaccharides. *Bioscience, Biotechnology, and Biochemistry*, **59**(10), 1861–1865. doi:10.1271/bbb.59.1861

Kobayashi, M., Takagi, S., Shiota, M., Mitsuishi, Y., & Matsuda, K. (1983). An isomaltotriose-producing dextranase from *Flavobacterium* sp. M-73: Purification and properties. *Agricultural and Biological Chemistry*, **47**(11), 2585–2593. doi:10.1271/bbb1961.47.2585

Kobayashi, S., Kainuma, K., & Suzuki, S. (1978). Purification and some properties of *Bacillus macerans* cycloamylose (cyclodextrin) glucanotransferase. *Carbohydrate Research*, **61**(1), 229–238. doi:10.1016/S0008-6215(00)84484-5

Kohno, M., Arakawa, T., Ota, H., Mori, T., Nishimoto, T., & Fushinobu, S. (2018). Structural features of a bacterial cyclic α-maltosyl-(1→6)-maltose (CMM) hydrolase critical for CMM recognition and hydrolysis. *Journal of Biological Chemistry,* **293**(43), 16874–16888. doi:10.1074/jbc.RA118.004472

Light, S. H., Cahoon, L. A., Halavaty, A. S., Freitag, N. E., & Anderson, W. F. (2016). Structure to function of an α-glucan metabolic pathway that promotes *Listeria monocytogenes* pathogenesis. *Nature Microbiology*, **2**(2), 16202. doi:10.1038/nmicrobiol.2016.202

Macrae, C. F., Bruno, I. J., Chisholm, J. A., Edgington, P. R., McCabe, P., Pidcock, E., Rodriguez-Monge, L., Taylor, R., van de Streek, J., & Wood, P. A. (2008). Mercury CSD 2.0 new features for the visualization and investigation of crystal structures. *Journal of Applied Crystallography*, **41**(2), 466–470. doi:10.1107/S0021889807067908

Macrae, C. F., Edgington, P. R., McCabe, P., Pidcock, E., Shields, G. P., Taylor, R., Towler, M., & van de Streek, J. (2006). Mercury: visualization and analysis of crystal structures. *Journal of Applied Crystallography*, **39**(3), 453–457. doi:10.1107/S002188980600731X

Macrae, C. F., Sovago, I., Cottrell, S. J., Galek, P. T. A., McCabe, P., Pidcock, E., Platings, M., Shields, G. P., Stevens, J. S., Towler, M., & Wood, P. A. (2020). Mercury 4.0: from visualization to analysis, design and prediction. *Journal of Applied Crystallography*, **53**(1), 226–235. doi:10.1107/S1600576719014092

Manners, D. J. (1963). Enzymic synthesis and degradation of starch and glycogen. *Advances in Carbohydrate Chemistry*, **17**, 371–430. doi:10.1016/S0096-5332(08)60139-3

McCleary, B. V, Gibson, T. S., Sheehan, H., Casey, A., Horgan, L., & O'Flaherty, J. (1989). Purification, properties, and industrial significance of transglucosidase from *Aspergillus niger*. *Carbohydrate Research*, **185**(1), 147–162. doi:10.1016/0008-6215(89)84030-3

Mistry, J., Chuguransky, S., Williams, L., Qureshi, M., Salazar, G. A., Sonnhammer, E. L. L.,

Tosatto, S. C. E., Paladin, L., Raj, S., & Richardson, L. J. (2021). Pfam: The protein families database in 2021. *Nucleic Acids Research*, **49**(D1), D412–D419. doi: 10.1093/nar/gkaa913

Mitsuishi, Y., Kobayashi, M., & Matsuda, K. (1979). Dextran α-1,2 debranching enzyme from *Flavobacterium* sp. M-73: Its production and purification. *Agricultural and Biological Chemistry*, **43**(11), 2283–2290. doi:10.1271/bbb1961.43.2283

Mitsuishi, Y., Kobayashi, M., & Matsuda, K. (1980). Dextran α-(1→2)-debranching enzyme from *Flavobacterium* sp. M-73. Properties and mode of action. *Carbohydrate Research*, **83**(2), 303–313. doi:10.1016/S0008-6215(00)84542-5

Mizuno, T., Matsui, H., Ito, H., Mori, H., Kimura, A., Honma, M., & Chiba, S. (1996). Reinvestigation of isomaltotrio-dextranase from *Brevibaeterium fuscum* var. *dextranlyticum*. *Journal of Applied Glycoscience*, **43**(3), 347–353. doi:10.11541/jag1994.43.347

Mori, T., Nishimoto, T., Okura, T., Chaen, H., & Fukuda, S. (2008). Purification and characterization of cyclic maltosyl-(1→6)-maltose hydrolase and α-glucosidase from an *Arthrobacter globiformis* strain. *Bioscience, Biotechnology, and Biochemistry*, **72**(7), 1673–1681. doi:10.1271/bbb.70759

Mori, T., Nishimoto, T., Okura, T., Chaen, H., & Fukuda, S. (2011). Cloning, sequencing and expression of the genes encoding cyclic α-Maltosyl-(1→6)-maltose hydrolase and α-glucosidase from an *Arthrobacter globiformis* strain. *Journal of Applied Glycoscience*, **58**(2), 39–46. doi:10.5458/jag.jag.JAG-2010_011

Moris, L. D. (1948). Quantitative determination of carbohydrates with Dreywood's anthrone reagent. *Science*, **107**(2775), 254–255. doi:10.1126/science.107.2775.254

Mukai, K., Watanabe, H., Kubota, M., Chaen, H., Fukuda, S., & Kurimoto, M. (2006). Purification, characterization, and gene cloning of a novel maltosyltransferase from an *Arthrobacter globiformis* strain that produces an alternating α-1,4- and α-1,6-cyclic tetrasaccharide from starch. *Applied and Environmental Microbiology*, **72**(2), 1065–1071. doi:10.1128/AEM.72.2.1065-1071.2006

Mukai, K., Watanabe, H., Oku, K., Nishimoto, T., Kubota, M., Chaen, H., Fukuda, S., & Kurimoto, M. (2005). An enzymatically produced novel cyclic tetrasaccharide, *cyclo*-{→6)-α-D-Glc*p*-(1→4)-α-D-Glc*p*-(1→6)-α-D-Glc*p*-(1→4)-α-D-Glc*p*-(1→} (cyclic maltosyl-(1→6)-maltose), from starch. *Carbohydrate Research*, **340**(8), 1469–1474. doi:10.1016/j.carres.2005.03.010

Naessens, M., Cerdobbel, A., Soetaert, W., & Vandamme, E. J. (2005). *Leuconostoc* dextransucrase and dextran: production, properties and applications. *Journal of Chemical Technology & Biotechnology*, **80**(8), 845–860. doi:10.1002/jctb.1322

NCBI Resource Coordinators. (2018). Database resources of the National Center for Biotechnology Information. *Nucleic Acids Research*, **46**(D1), D8–D13. doi:10.1093/nar/gkx1095

Nishimoto, T., Aga, H., Kubota, M., Fukuda, S., Kurimoto, M., & Tsujisaka, Y. (2004). Production of cyclic tetrasaccharide with 6-α-glucosyltransferase and α-isomaltosyltransferase. *Journal of Applied Glycoscience*, **51**(2), 135–140. doi:10.5458/jag.51.135

Nishimoto, T., Aga, H., Mukai, K., Hashimoto, T., Watanabe, H., Kubota, M., Fukuda, S., Kurimoto, M., & Tsujisaka, Y. (2002). Purification and characterization of glucosyltransferase and glucanotransferase involved in the production of cyclic tetrasaccharide in *Bacillus globisporus* C11. *Bioscience, Biotechnology, and Biochemistry*, **66**(9), 1806–1818. doi:10.1271/bbb.66.1806

Nordstedt, N. P., Roman-Reyna, V., Jacobs, J. M., & Jones, M. L. (2021). Comparative genomic understanding of Gram-positive plant growth-promoting *Leifsonia*. *Phytobiomes Journal*, **5**(3), 263–274. doi:10.1094/PBIOMES-12-20-0092-SC

Oguma, T. (1997). Study on the production of oligosaccharides by using enzymes from *Bacillus* Genus. *Oyo Toshitsu Kagaku: Journal of Applied Glycoscience*, **44**(1), 61–67. doi:10.11541/jag1994.44.61

Oguma, T., Kitao, S., & Kobayashi, M. (2014). Purification and characterization of cycloisomaltooligosaccharide glucanotransferase and cloning of *cit* from *Bacillus circulans* U-155. *Journal of Applied Glycoscience*, **61**(4), 93–97. doi:10.5458/jag.jag.JAG-2013_017

Oguma, T., Tobe, K., & Kobayashi, M. (1994). Purification and properties of a novel enzyme from *Bacillus* spp. T-3040, which catalyses the conversion of dextran to cyclic isomaltooligosaccharides. *FEBS Letters*, **345**(2), 135–138. doi:10.1016/0014-5793(94)00418-8

Oslancová, A., & Janeček, Š. (2002). Oligo-1,6-glucosidase and neopullulanase enzyme subfamilies from the α-amylase family defined by the fifth conserved sequence region. *Cellular and Molecular Life Sciences*, **59**(11), 1945–1959. doi:10.1007/PL00012517

Parte, A. C., Sardà Carbasse, J., Meier-Kolthoff, J. P., Reimer, L. C., & Göker, M. (2020). List

of prokaryotic names with standing in nomenclature (LPSN) moves to the DSMZ. *International Journal of Systematic and Evolutionary Microbiology*, **70**(11), 5607–5612. doi:10.1099/ijsem.0.004332

Pereira, C. S., Kony, D., Baron, R., Müller, M., van Gunsteren, W. F., & Hünenberger, P. H. (2006). Conformational and dynamical properties of disaccharides in water: a molecular dynamics study. *Biophysical Journal*, **90**(12), 4337–4344. doi:10.1529/biophysj.106.081539

Rawat, S., & Jain, S. K. (2004). Solubility enhancement of celecoxib using β-cyclodextrin inclusion complexes. *European Journal of Pharmaceutics and Biopharmaceutics*, **57**(2), 263–267. doi:10.1016/j.ejpb.2003.10.020

Robyt, J. F. (2008). Starch: structure, properties, chemistry, and enzymology. In B. O. Fraser-Reid, K. Tatsuta, & J. Thiem (Eds.), *Glycoscience: Chemistry and Chemical Biology* (pp. 1437–1472). Springer Berlin Heidelberg. doi:10.1007/978-3-540-30429-6_35

Saburi, W., Rachi-Otsuka, H., Hondoh, H., Okuyama, M., Mori, H., & Kimura, A. (2015). Structural elements responsible for the glucosidic linkage-selectivity of a glycoside hydrolase family 13 *exo*-glucosidase. *FEBS Letters*, **589**(7), 865–869. doi:10.1016/j.febslet.2015.02.023

Sadahiro, J., Mori, H., Saburi, W., Okuyama, M., & Kimura, A. (2015). Extracellular and cell-associated forms of *Gluconobacter oxydans* dextran dextrinase change their localization depending on the cell growth. *Biochemical and Biophysical Research Communications*, **456**(1), 500–505. doi:10.1016/j.bbrc.2014.11.115

Sawai, T., Toriyama, K., & Yano, K. (1974). A bacterial dextranase releasing only isomaltose from dextrans. *The Journal of Biochemistry*, **75**(1), 105–112. doi:10.1093/oxfordjournals.jbchem.a130363

Sawai, T., Yamaki, T., & Ohya, T. (1976). Purification and some properties of *Arthrobacter globiformis exo*-1,6-α-glucosidase. *Agricultural and Biological Chemistry*, **40**(7), 1293–1299. doi:10.1271/bbb1961.40.1293

Sayers, E. W., Cavanaugh, M., Clark, K., Ostell, J., Pruitt, K. D., & Karsch-Mizrachi, I. (2020). GenBank. *Nucleic Acids Research*, **48**(D1), D84–D86. doi:10.1093/nar/gkz956

Shimwell, J. L. (1947). A study of ropiness in beer. *Journal of the Institute of Brewing*, **53**(6), 280–294. doi:10.1002/j.2050-0416.1947.tb01339.x

Sidebotham, R. L. (1974). Dextrans. *Advances in Carbohydrate Chemistry and Biochemistry*, **30**, 371–444. doi:10.1016/S0065-2318(08)60268-1

Singh, B., & Röhm, K. H. (2008). Characterization of a *Pseudomonas putida* ABC transporter (AatJMQP) required for acidic amino acid uptake: biochemical properties and regulation by the Aau two-component system. *Microbiology*, **154**(3), 797–809. doi:10.1099/mic.0.2007/013185-0

Suzuki, N., Fujimoto, Z., Kim, Y. M., Momma, M., Kishine, N., Suzuki, R., Suzuki, S., Kitamura, S., Kobayashi, M., Kimura, A., & Funane, K. (2014). Structural elucidation of the cyclization mechanism of α-1,6-glucan by *Bacillus circulans* T-3040 cycloisomaltooligosaccharide glucanotransferase. *Journal of Biological Chemistry*, **289**(17), 12040–12051. doi:10.1074/jbc.M114.547992

Suzuki, R., Terasawa, K., Kimura, K., Fujimoto, Z., Momma, M., Kobayashi, M., Kimura, A., & Funane, K. (2012). Biochemical characterization of a novel cycloisomaltooligosaccharide glucanotransferase from *Paenibacillus* sp. 598K. *Biochimica et Biophysica Acta - Proteins and Proteomics*, **1824**(7), 919–924. doi:10.1016/j.bbapap.2012.04.001

Tagami, T., Miyano, E., Sadahiro, J., Okuyama, M., Iwasaki, T., & Kimura, A. (2016). Two novel glycoside hydrolases responsible for the catabolism of cyclobis-(1→6)-α-nigerosyl. *Journal of Biological Chemistry*, **291**(32), 16438–16447. doi:10.1074/jbc.M116.727305

The Uniprot Consortium. (2021). UniProt: the universal protein knowledgebase in 2021. *Nucleic Acids Research*, **49**(D1), D480–D489. doi:10.1093/nar/gkaa1100

Tsusaki, K., Watanabe, H., Nishimoto, T., Yamamoto, T., Kubota, M., Chaen, H., & Fukuda, S. (2009). Structure of a novel highly branched α-glucan enzymatically produced from maltodextrin. *Carbohydrate Research*, **344**(16), 2151–2156. doi:10.1016/j.carres.2009.08.016

Tsusaki, K., Watanabe, H., Yamamoto, T., Nishimoto, T., Chaen, H., & Fukuda, S. (2012). Purification and characterization of highly branched α-glucan- producing enzymes from *Paenibacillus* sp. PP710. *Bioscience, Biotechnology, and Biochemistry*, **76**(4), 721–731. doi:10.1271/bbb.110855

Weill, C. E., Burch, R. J., & Van Dyk, J. W. (1954). An α-amyloglucosidase that produces β-glucose. *Cereal Chemistry*, **31**(2), 150–158. doi:030/003/030003430.php

Yamamoto, K., Yoshikawa, K., Kitahata, S., & Okada, S. (1992). Purification and some properties of dextrin dextranase from *Acetobacter capsulatus* ATCC 11894. *Bioscience, Biotechnology, and Biochemistry*, **56**(2), 169–173. doi:10.1271/bbb.56.169

Yamamoto, K., Yoshikawa, K., & Okada, S. (1993a). Structure of dextran synthesized by

dextrin dextranase from *Acetobacter capsulatus* ATCC 11894. *Bioscience, Biotechnology, and Biochemistry*, **57**(9), 1450–1453. doi:10.1271/bbb.57.1450

Yamamoto, K., Yoshikawa, K., & Okada, S. (1993b). Dextran synthesis from reduced maltooligosaccharides by dextrin dextranase from *Acetobacter capsulatus* ATCC 11894. *Bioscience, Biotechnology, and Biochemistry*, **57**(1), 136–137. doi:10.1271/bbb.57.136

Yokota, A., Takeuchi, M., & Weiss, N. (1993). Proposal of two new species in the genus *Microbacterium*: *Microbacterium dextranolyticum* sp. nov. and *Microbacterium aurum* sp. nov. *International Journal of Systematic and Evolutionary Microbiology*, **43**(3), 549–554. doi:10.1099/00207713-43-3-549

Zhang, Y., Ren, H., & Zhang, G. (2014). *Microbacterium hydrothermale* sp. nov., an *Actinobacterium* isolated from hydrothermal sediment. *International Journal of Systematic and Evolutionary Microbiology*, **64**(Pt_10), 3508–3512. doi:10.1099/ijs.0.061697-0

Acknowledgements

This thesis was completed under the guidance of Professor Haruhide Mori at Research Faculty of Agriculture, Hokkaido University. I wish to express my sincere thanks to him for kind guidance and encouragement throughout this study. I would like to heartily thank to Professor Masayuki Okuyama, Professor Satoru Fukiya and Associate Professor Wataru Saburi at Research Faculty of Agriculture, Hokkaido University for reviewing this thesis.

This study was accomplished in Research & Technology Division, HAYASHIBARA CO., LTD. I wish to express my gratitude to Representative Director/President Naoki Yasuba and Managing Executive Director Koryu Yamamoto at HAYASHIBARA CO., LTD. who gave me the chance to publish this thesis.

I am deeply grateful to Dr. Shimpei Ushio, Dr. Hajime Aga, Dr. Tomoyuki Nishimoto, Dr. Tetsuya Mori, Dr. Hikaru Watanabe, Mr. Akira Kawashima, Ms. Keiko Hino, Dr. Masaki Kohno, Mr. Noriaki Kitagawa, Mr. Takashi Suzuki, Mr. Hiroki Fujisawa, Dr. Yuuki Mitsukawa and Mr. Yuki Kawauchi at HAYASHIBARA CO., LTD. for their sincere cooperation, useful suggestions and encouragement through this study.

I wish to express my sincere thanks to Dr. Yuji Noguchi and Dr. Shuichi Hirose at NAGASE & CO. LTD., Dr. Hiromi Ota, Ms. Tsugumi Shiokawa and Professor Hiroko Tada at Okayama University, and Dr. Jun-ichi Kakimura and Professor Shin-ichi Tate at Hiroshima University.

Finally, I thank my parents, my wife and my daughters for their incessant understanding and encouragement.